

Anders Dahle Thorsen

Experimental Strength Analysis and Material Modelling of 3D Printed Parts

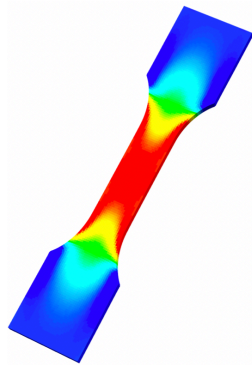
Master's thesis in Product and System Design

Supervisor: Henry Peter Piehl

June 2019

Anders Dahle Thorsen

Experimental Strength Analysis and Material Modelling of 3D Printed Parts



Master's thesis in Product and System Design
Supervisor: Henry Peter Piehl
June 2019

Norwegian University of Science and Technology
Faculty of Engineering
Department of Ocean Operations and Civil Engineering

 **NTNU**
Norwegian University of
Science and Technology

Abstract

The world of engineering is filled with solid knowledge of traditional strength analyzing methods going back decades. As the world moves forward, new things start to emerge from people trying new things, to see if it is possible to combine traditional methods and new technology to further our knowledge. The following master thesis is a deep dive into 3D printing and the assessment of the strength characteristic of a 3D printed material. More specifically, identifying the Young's modulus of 3D printed Polylactic Acid.

Combining traditional methods with new technology may detect new aspects that have not been seen before. The experimental tests are done using traditional tensile strength methods. Alongside the experimental test, Finite Element Method was used as the numerical analysis tool, supplied by Siemens NX. The numerical analysis was done to identify a stiffness coefficient ratio between the selected geometries.

The results from the tests have been statistically analyzed using MATLAB, and validated with results from other independent sources to conclude the feasibility of the method.

Sammendrag

Ingeniørens omfattende kunnskaper om styrkeanalyser er i all hovedsak basert på tradisjonell analysemetodikk fra langt tilbake i tid. Nå som verden beveger seg fremover, popper det stadig opp nye teknologier, produkter, krav og problemstillinger, hvor en kan undersøke mulighetene for å kombinere tradisjonelle metoder med ny teknologi, for å komme et kunnskapsmessig steg videre. Masteroppgaven er et dypdykk i 3D-printing og estimering av styrkekaraktistikken til et 3D-printet material. Nærmere bestemt, identifisere elastisitetsmodulen av 3D-printet Polylactic Acid.

Å kombinere tradisjonelle metoder med ny teknologi, kan føre til oppdagelse av aspekter som tidligere ikke er registrert. Forsøkstestene er gjort ved hjelp av tradisjonelle strekkfasthets-metoder. Ved siden av de eksperimentelle testene ble Finite Element Method brukt som numerisk analyseverktøy, levert av Siemens NX. Den numeriske analysen ble utført for å identifisere et stivhetskoeffisientforhold mellom de valgte geometriene.

Resultat fra testene er statistisk analysert ved hjelp av MATLAB og validert med resultater fra andre uavhengige kilder, for å konkludere metodens gjennomførbarhet.

Preface

This master thesis is written on behalf of the Department of Ocean and Civil Engineering at the Norwegian University of Science and Technology in Ålesund. It finalizes a 2-year master's degree in Product and System Design, and is the final result of work carried out during the spring semester of 2019. With all of the new technologies emerging throughout different sectors in the industry, I find 3D printing to be the most interesting. 3D printing in itself is not a new thing, but in terms of making 3D printed industry parts, it's relatively new. This thesis involves exploration of estimating the Young's modulus of 3D printed materials. For this thesis Polylactic Acid have been used. The thesis was presented by and written under the supervision of Associate Professor Henry Peter Piehl at NTNU Ålesund.

The reader is expected to have basic knowledge in engineering, but the thesis is hopefully written in a way that it is relatively easy to follow, if this is not the case. Working throughout the semester with this thesis, I have gained a lot of experience in organizing work, 3D printing, programming in MATLAB and experimental methods. When choosing the master thesis, I wanted to do something that had real-life physical experiments and something that involved 3D printing. In this thesis, I was fortunate enough to get both. The master thesis has been challenging and rewarding, and I am happy with my choice. I am grateful for the gained knowledge, and my personal development throughout the semester.

Acknowledgements

There are a lot of people that I need to express my gratitude towards. First of all, I owe my deepest gratitude to my supervisor, Associate Professor Henry Peter Piehl. Your guidance and knowledge have been invaluable for this thesis. You have learned me so much in the two years I have known you. You have always taken the time for me, even when you are busy, and I want to say thank you!

Furthermore, want to give a special thanks to André Tranvåg - Head Engineer at NTNU Ålesund. You were one of the first teacher I was introduced to at NTNU, and you have taught me so much. You are always there to help, and as expected you were eager to help me conduct the experiments in my research. Thank you!

I also want to thank Lars Petter Bryne, Assistant Professor at NTNU Ålesund. That is for your insight and knowledge in mechanical engineering, and that your office door is always open for any questions that I have had in all of the five years I have known you.

I want to thank NTNU Ålesund for the five years I have been a student here for providing the necessary tools, and work space for us students to excel as students. And also for the long lasting friendships I have gained throughout my time here.

Finally, I want to direct my gratitude towards my family and girlfriend.

Thank you all!
ADT

Table of Contents

Abstract	i
Sammendrag	iii
Preface	v
Acknowledgements	vii
Table of Contents	ix
List of Figures	xiii
List of Tables	xv
Nomenclature	xvii
1 Introduction	1
1.1 Problem	1
1.2 Motivation	3
1.3 Scope	4
1.4 Objective & Research Questions	5
1.5 Report Structure	6
2 Literature Review	7
2.1 3D Printing	7
2.2 Experimental Methods	18
2.3 Numerical Methods	23
2.4 Related Work	25
3 Methodology	27
3.1 Thesis Approach	27
3.2 Prototyping	28
3.2.1 Computer Aided Design	28
3.2.2 Computer Aided Manufacturing	30

3.2.3	3D Printing	31
3.2.4	Post Processing	33
3.3	Experimental Test - Tensile Test Setup	34
3.3.1	Experimental Test 1 - Specifics	34
3.3.2	Experimental Test 2 - Specifics	35
3.4	Statistical Analysis	36
3.4.1	Smoothing of Raw Data	36
3.4.2	Linear Region	38
3.5	Structural Analysis	41
3.5.1	Stiffness Coefficient Ratio	41
3.5.2	Mesh	43
3.5.3	Constraints	45
3.5.4	Load	46
3.5.5	Deformation	48
4	Results & Discussion	51
4.1	Experimental Tests Fracture Analysis	51
4.2	Young's Modulus of PLA	52
4.2.1	Initial Young's Modulus from Experimental Tests	52
4.2.2	Young's Modulus from Experimental Tests with Stiffness Ratio	55
5	Conclusion & Future Work	61
5.1	Conclusion	61
5.2	Future Work	62
	Bibliography	63
	Appendix	66
A	Test Specimens	67
A.1	Experimental Test 1 - Comparison Overview	68
A.1.1	Test 2.1 - Test 2.5, Printed at 0°	70
A.1.2	Test 3.1 - Test 3.5, Printed at 45°	75
A.1.3	Test 3.6 - Test 3.11, Printed at 90°	80
A.2	Experimental Test 2 - Comparison Overview	86
A.2.1	Test 4.1 - Test 4.5, Printed at 0°	88
A.2.2	Test 4.6 - Test 4.10, Printed at 45°	93
A.2.3	Test 4.11 - Test 4.15, Printed at 90°	98
B	Mesh Convergence Study	103
B.1	Mesh 0.5 mm element size	104
B.2	Mesh 1 mm element size	104

B.3	Mesh 2 mm element size	104
B.4	Mesh 4 mm element size	105
B.5	Mesh 8 mm element size	105
C	MATLAB Scripts	107
C.1	Main Script, example T3.1	108
C.2	Initial Young's Modulus Comparison	115
C.3	Young's Modulus Comparison	117
C.4	Mesh Convergence Study	121
D	Datasheets	123

List of Figures

1.1	Build direction - [1]	2
1.2	Strength failure - [3]	3
1.3	Scope	4
2.1	Classification of 3D Printing technologies - [5]	8
2.2	Material extrusion process - [6]	9
2.3	SLA Process - [7]	10
2.4	Powder Bed Fusion process - [8]	11
2.5	HP Jet Fusion Process - [10]	12
2.6	Additive Manufacturing - [12]	13
2.7	3D printing filament on drum - [14]	14
2.8	Layer orientation	15
2.9	Printed at 0°	15
2.10	Printed at 45°	15
2.11	Printed at 90°	15
2.12	Infill geometry - [15]	16
2.13	Tensile test specimen	19
2.14	Tensile test setup	19
2.15	Brittle and ductile- material curve	20
2.16	Steel stress-strain curve	21
2.17	Hooke's law - [18]	22
2.18	Visual representations of analysis steps - [21]	23
2.19	Element size and Von Mises stress - [23]	24
3.1	CAD model	28
3.2	Cura model	28
3.3	Finished model	28
3.4	Geometry 1	29
3.5	Geometry 2	29
3.6	Ultimaker Cura	30
3.7	Ultimaker2+ - [27]	31
3.8	Brim	33

3.9	Raw data curve of Test3.1	37
3.10	Raw data curve zoomed	37
3.11	Smoothed data zoomed	37
3.12	Smoothed raw data of Test3.1	37
3.13	Linear Region	38
3.14	Differentiated	38
3.15	Kernel distribution	39
3.16	Mean value of gradient	39
3.17	Calculated linear range	39
3.18	Range cropped force - elongation curve	39
3.19	Gauge Length example	41
3.20	Extensometer - [28]	41
3.21	Model range	42
3.22	Split CAD model of Model 4	43
3.23	Mesh of Model 4	43
3.24	Mesh Convergence	44
3.25	Coordinate system reference	45
3.26	Surface Constraint	46
3.27	Node Constraint	46
3.28	Applied Force	46
3.29	Model 4 FEM-ready	47
3.30	Stiffness k	48
4.1	Clean fracture along pattern	51
4.2	Diagonal fracture along pattern	51
4.3	Geometry 1 - Printed at 0°	52
4.4	Geometry 2 - Printed at 0°	52
4.5	Geometry 1 - Printed at 45°	53
4.6	Geometry 2 - Printed at 45°	53
4.7	Geometry 1 - Printed at 90°	53
4.8	Geometry 2 - Printed at 90°	53
4.9	Initial Young's Modulus	54
4.10	Young's Modulus	56
4.11	Separate Box Plot of Young's Modulus	57
4.12	Manufacturing of test specimens	58

List of Tables

2.1	Material Extrusion - Pros and cons	9
2.2	VAT Polymerization - Pros and cons	10
2.3	Powder Bed Fusion - Pros and cons	11
2.4	Multi Jet Fusion - Pros and cons	12
3.1	Ultimaker Cura Print Settings	30
3.2	Test Matrix	32
4.1	Independent sources	59

Nomenclature

Abbreviations

ABS Acrylonitrile Butadiene Styrene

ASTM American Society for Testing and Materials

CAD Computer Aided Design

CAE Computer Aided Engineering

CAM Computer Aided Manufacturing

DLP Direct Light Processing

FEA Finite Element Analysis

FEM Finite Element Method

FDM Fused Deposition Modelling

FFF Fused Filament Fabrication

ISO International Organization for Standardization

LS Laser Sintering

PDF Powder Bed Fusion

PLA Polyactic Acid

SLA Stereolithography

SLS Selective Laser Sintering

STL abbreviation of the word STereoLithography

Symbols

$^{\circ}$	Degree	<i>Angle</i>
δ	Elongation	<i>mm</i>
F	Force	<i>N</i>
L	Length	<i>mm</i>
μ	Micro	10^{-3}
k	Stiffness	<i>N/mm</i>
ϵ	Strain	$[-]$
σ	Stress	<i>N/mm²</i>
<i>E</i>	Young's Modulus	<i>MPa</i>

Chapter 1

Introduction

1.1 Problem

In today's engineering world, there are a lot of possibilities to explore new ways of producing products as a result of the 3D printing technologies that are available. Some of the products that are produced now were not possible before, due to the limitation of old manufacturing methods. The increasing use of 3D printing as a manufacturing method in today's industry, provides the need for a deeper understanding regarding the mechanical behavior of 3D printed parts. The way of thinking regarding producing new products needs to change as a result of the rapid rate of new manufacturing processes that are developing. Validation of the strength characteristics of 3D printed parts is problematic. In some cases, the manufacturer of 3D printed materials provides strength test results of the specific material they provide, but these results often vary between the manufacturers. Furthermore, its hard to know if these tests are done for a small batch or by the thousands.

3D printing technology is no new thing, but the implementation of industrial quality 3D printed parts is new, when for instance, comparing it to steel. Steel has an isotropic material property opposed to Polylactic Acid (PLA), which is an anisotropic material. An anisotropic material means the material properties in an object is not uniform in all directions, and thus more vulnerable for failure when a load is applied. This is amplified by the fact that the orientation the 3D printed parts are built at also has a large effect on the strength of the individual part, displayed in Figure 1.1. A steel wire and a steel cube have the same material properties, whereas a 3D printed wire and cube of PLA is different. Working with an anisotropic material is challenging, as well as potentially dangerous if not done correctly. Engineers up until today have used steel for centuries and have a solid experience of the behavior of the material, opposed to new 3D printing materials like PLA.

Due to the anisotropic properties of PLA, performing Finite Element Method(FEM)-

analysis is not a simple task. On top of that, how a 3D printed object is printed in terms of orientation influences the strength. Even though the Young's modulus of the material might be known, it may not fully represent the characteristics of the Young's modulus when performing test on different 3D printed objects.

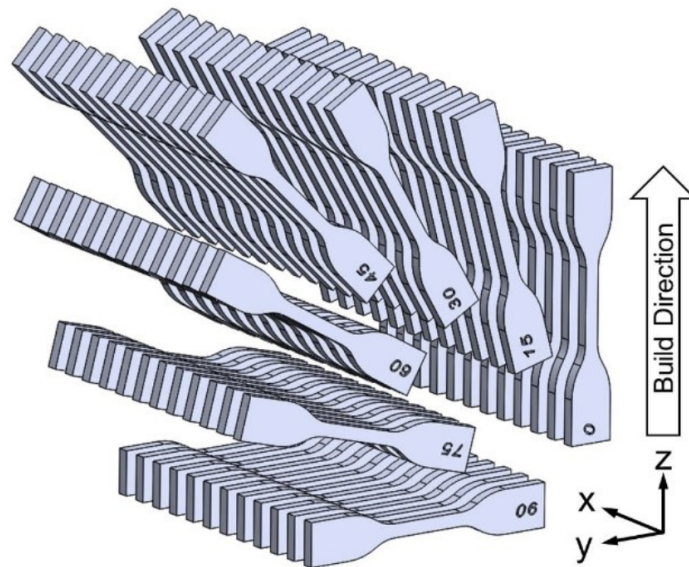


Figure 1.1: Build direction - [1]

1.2 Motivation

The motivation behind this research is to more precisely be able to make functional 3D printed components, thus look into their material properties. When producing components for costumers, as an engineer, you need to know how strong the material itself is, because this will influence the design of the component. If not, the components may need to be overly constructed, which counters the whole purpose of making specifically optimized 3D printed parts. To achieve this, a testing procedure is required to test incoming material and its performance. If successful, this will make the engineers job more efficient and precise. It will give the engineer faster and more accurate estimates to base their calculations of how thick or thin a given component shall, or can be constructed. Change in the material properties due to change in the way it is made can have huge consequences if not done correctly, visualized in Figure 1.2. There are a lot of companies involved, and a lot of activity revolving 3D printings industrial purpose, which makes this master thesis highly relevant [2].



Figure 1.2: Strength failure - [3]

1.3 Scope

The scope of this master thesis will mainly consist of three parts, displayed in Figure 1.3.

The 3D printing section will consist of making the test specimens that were experimentally tested in this research. This was done according to specific measurements presented later on in the thesis. The test specimens were made on Ultimaker 2+, which is a 3D printer supplied by Ultimaker. This printer uses Fused Deposition Method(FDM)- technology and the material that was used is called PLA.

The experimental methods section consists of the experimental tests done in this research. To identify the strength properties of the material, traditional tensile strength tests are used, located in the workshop at NTNU Ålesund. The tests are done using ISO guidelines and under the supervision of the Head Engineer, André Tranvåg at NTNU.

The numerical methods will be performed using the FEM Nastran solver in Siemens NX. The FEM analysis will be used to identify the stiffness coefficient ratio between the relevant geometries.

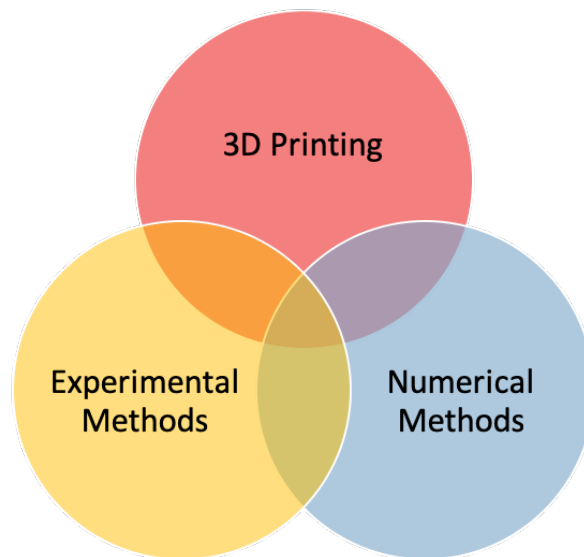


Figure 1.3: Scope

1.4 Objective & Research Questions

The main objective of this thesis is to look into the possibility of developing a test procedure to measure the material properties from 3D printed parts made from PLA. Validate the results derived from the thesis to independent sources.

The research questions this thesis is going to be based on, and worked towards are:

- RQ 1 : How to measure the strength of a 3D printed part made in PLA?
- RQ 2 : How is it possible to experimentally and numerically asses the strength properties of 3D printed parts made from PLA?
- RQ 3 : What are the procedures to experimentally and numerically asses correct strength evaluation?

1.5 Report Structure

This master thesis is divided into five chapters and contains the following:

Chapter 1 - Introduction:

- *In the first chapter the introduction containing the problem, motivation, scope, objective and research questions regarding this thesis is presented.*

Chapter 2 - Literature Review:

- *In the second chapter, the current start of the art on rapid prototyping, strength measurements and experimental analysis is presented.*

Chapter 3 - Methodology:

- *The third chapter contains the prototyping, experimental tests, statistical- and structural analysis.*

Chapter 4 - Results & Discussion:

Chapter 5 - Conclusion & Future Work:

Appendix:

- *Contains all of the individual experimental tests, mesh convergence study, MATLAB scripts and relevant datasheets.*

Chapter 2

Literature Review

2.1 3D Printing

3D printing is a manufacturing process where a part is build up layer by layer. 3D printing has many different variations to it and is now found in a lot of various industries with its individual benefits and limitations. They are used in industrial, medical, high tech, and commercial goods. Some are cheap, and some are extremely expensive. Materials can be in the range of plastic, resin, metal, paper, etc. 3D printing has evolved very rapidly the last 10-15 years from being more or less useless, to now be a highly valuable tool for many different manufacturers. Especially after the year 2009 when the patent for FDM-printing expired and made it available for everyone [4].

The demand for high-grade parts and easy to use machines are in constant development. Engineers in different sectors use it to create early design phase prototypes for the most part, but due to the increasing development of better and faster 3D printers, they have slowly been taking the engineering world to new possibilities. The most significant reasoning behind implementing 3D printing into the engineering industry is not to be limited by traditional manufacturing methods. As said before in the intro, there are parts that you can create using 3D printing that is not possible to produce while using traditional manufacturing methods. In 2015 the ISO/ASTM 52900 Standard was created to standardize all the terminology, as well as the classification of the different 3D printing process categories. There were established a total of seven technologies in this standard. All of them and their associated processes are described in Figure 2.1.

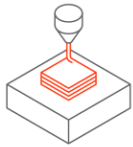
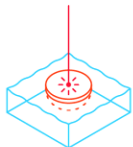
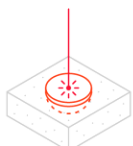
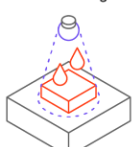

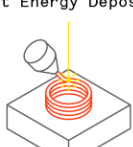
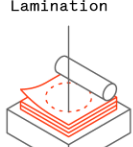
Process	Description	Technologies
<p>Material Extrusion</p> 	<p>Material is selectively dispensed through a nozzle or orifice.</p>	<p>Fused Filament Fabrication (FFF), more commonly referred to as Fused Deposition Modeling (FDM)</p>
<p>Vat Polymerization</p> 	<p>A liquid photopolymer in a vat is selectively cured by light-activated polymerization.</p>	<p>Stereolithography (SLA), Direct Light Processing (DLP)</p>
<p>Powder Bed Fusion</p> 	<p>Thermal energy selectively fuses regions of a powder bed.</p>	<p>Selective Laser Sintering (SLS), Direct Metal Laser Sintering (DMLS), Selective Laser Melting (SLM), Electron Beam Melting (EBM)</p>
<p>Material Jetting</p> 	<p>Droplets of material are selectively deposited and cured on a build plate.</p>	<p>Material Jetting (MJ), Drop On Demand (DOD)</p>
<p>Binder Jetting</p> 	<p>A liquid bonding agent selectively binds regions of a powder bed.</p>	<p>Binder Jetting (BJ)</p>
<p>Direct Energy Deposition</p> 	<p>Focused thermal energy is used to fuse materials by melting as they are being deposited.</p>	<p>Laser Engineering Net Shaping (LENS), Laser-Based Metal Deposition (LBMD)</p>
<p>Sheet Lamination</p> 	<p>Sheets of material are bonded to form a part.</p>	<p>Ultrasonic Additive Manufacturing (UAM), Laminated Object Manufacturing (LOM)</p>

Figure 2.1: Classification of 3D Printing technologies - [5]

Technologies

Material Extrusion

The most common material extrusion technology is Fused Filament Fabrication or FFF (generally referred to as Fused Deposition Modeling or FDM) [5]. FDM is a method where the material is loaded into the printer and heated up to its melting point and then extruded through a thin nozzle, visualized in Figure 2.2. The extrusion nozzle is attached to a 3-axis system that allows it to move in the X, Y and Z directions. This creates a string of material which is deposited layer-by-layer in predetermined locations, where it then cools and solidifies. FDM is a very common way of 3D printing as it is relatively cheap, but it has some limitations in which the strength characteristics are not properly stated. Thus, it has a way to go to being a solid manufacturing tool for industry graded parts as it stands now. The most essential pros and cons regarding this technology are displayed in Table 2.1.

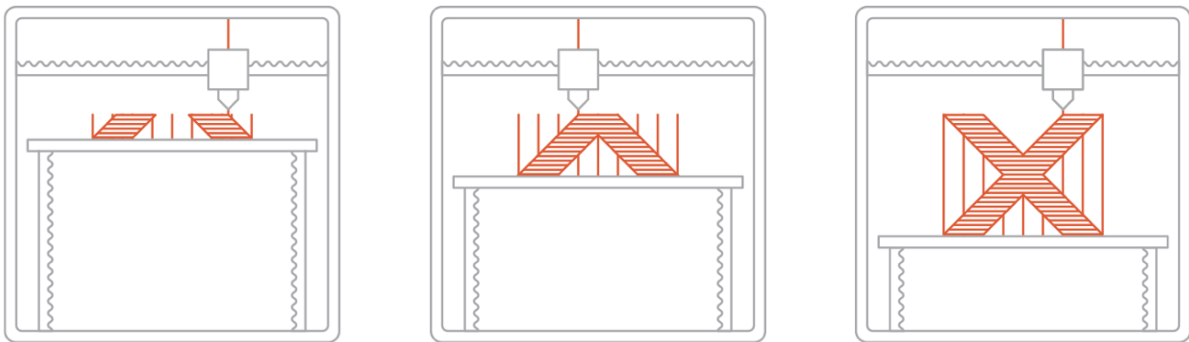


Figure 2.2: Material extrusion process - [6]

Table 2.1: Material Extrusion - Pros and cons

Material extrusion	
Pros	Cons
Cost effective	Time consuming
User friendly	Build limitations
High visual quality	Anisotropic

VAT Polymerization - SLA/DLP

This method the structure is made by selectively curing a polymer resin layer-by-layer. The materials used in Stereolithography(SLA) are photosensitive thermoset polymers that come in a liquid form. This is done using an ultraviolet laser beam. The SLA process is famous for being the first 3D-printing technology created back in 1986. SLA has many common characteristics with Direct Light Processing (DLP), another Vat Photopolymerization 3D printing technology. For simplicity, the two technologies can be treated as equals [7]. The SLA process in itself can be divided into bottom up and top down. This is just how the build plate is oriented which determines the objects way of getting printed. Using a human body as an example the top down technology will first print the feet and end up at the head, whereas bottom up will print the head first and lastly the feet. Due to this there are different attributes regarding their pros and cons displayed in Table 2.2.

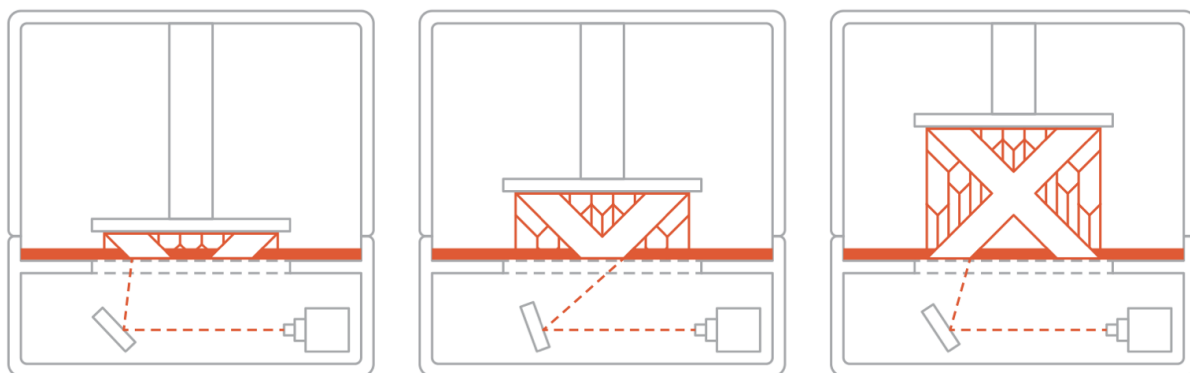


Figure 2.3: SLA Process - [7]

Table 2.2: VAT Polymerization - Pros and cons

VAT Polymerization			
Bottom up		Top down	
Pros	Cons	Pros	Cons
Cost	Build volume	Speed	Cost
Availability	Material range	Build volume	Special training
	Post processing due to support		Material switching creates waste due to tank removal

Powder Bed Fusion

Within the 3D printing industry, using Powder Bed Fusion(PBF)- technology with polymer powder to produce components is generally referred to as Selective Laser Sintering(SLS), or just Laser Sintering(LS) [5]. This technology uses high precision laser beams to melt and connect material grains to create a solid object, visualized in Figure 2.4. The material is spread out over a given build platform where the laser beam is beaming to the given layer pattern to form the object. As the object is created it is using all of its build space, which means there is a lot of excessive material. This excessive material is used as a support structure throughout the process. This excessive material is then later on removed to form the specific object. The most essential pros and cons regarding this technology is displayed in Table 2.3.

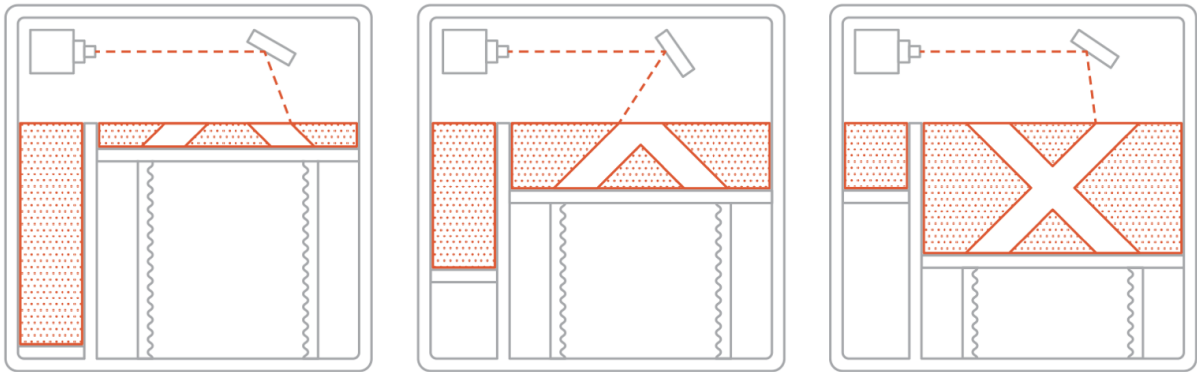


Figure 2.4: Powder Bed Fusion process - [8]

Table 2.3: Powder Bed Fusion - Pros and cons

Powder Bed Fusion	
Pros	Cons
High Accuracy	Expensive
Few build limitations	Not user friendly
Hard	Brittle

HP Multi Jet Fusion

This specific technology is added because of its position in the market. This specific technology is developed by HP. This goes under the same category as the SLS method, PBF- technology. This method is similar to a normal copying machine, visualized in Figure 2.5. Here is, opposed to ink, a binder which will work as an adhesive to connect the material grains to form the object. As the binder is placed, a heat source heats the binder to connect it to a solid layer by layer. After this is done all of the excessive material is removed and the solid part is put into a furnace to remove any internal and external stresses [9]. The pros and cons of this technology are displayed in Table 2.4.

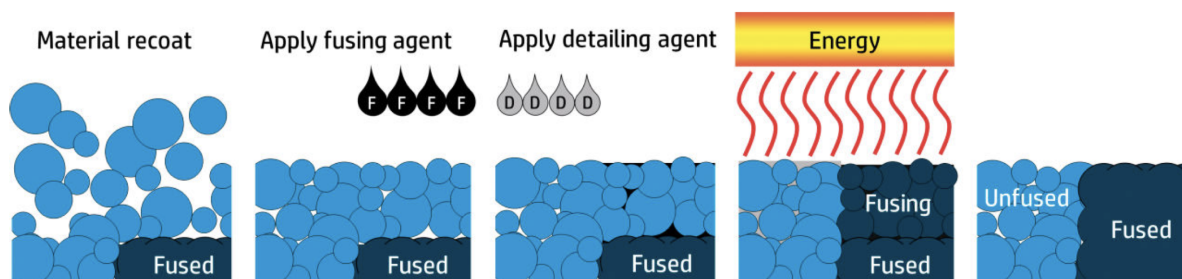


Figure 2.5: HP Jet Fusion Process - [10]

Table 2.4: Multi Jet Fusion - Pros and cons

HP Multi Jet Fusion	
Pros	Cons
High Accuracy	Expensive
Material strength	Not user friendly
Speed	Space

All of these technologies goes under the term 3D printing, but they also goes under the more broader term Additive Manufacturing. Additive manufacturing is often misinterpreted as 3D printing, but it is not the same thing [11]. In Figure 2.6 all the different manufacturing technologies which goes under the umbrella term additive manufacturing are displayed.

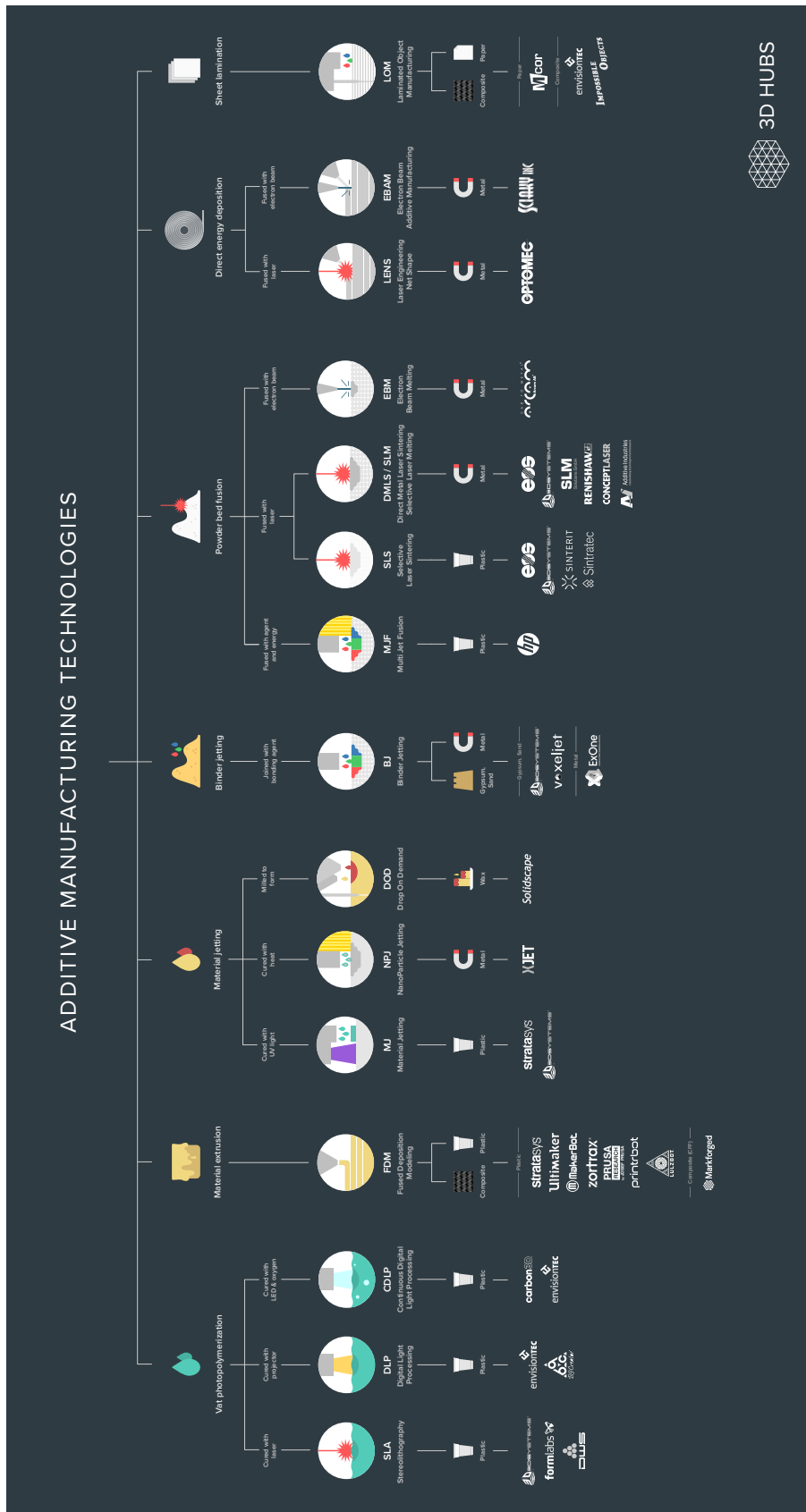


Figure 2.6: Additive Manufacturing - [12]

Material

PLA

The material that is going to be used in this research is PLA material, which is one of the most used 3D printing materials in the world. Its highly versatile and is easy to use, and also delivers good accuracy as well. Due to how its constructed there are numerous colors to choose from that has no measurable effect on its performance. Its cheap and also one of the most environmentally friendly materials on the market. PLA is derived from corn and sugarcane, which also makes the material renewable and biodegradable [13]. Having a material that is renewable by heating it back up to its melting point is a massive advantage and will make the excessive wastes to a minimum if done properly. As stated before in the earlier sections, the material is anisotropic and the material properties will have different values when exerted to a force. The material is for the most part delivered from manufacturers on small drums, displayed in Figure 2.7. The material that was used in is research is supplied by RS, and 3DNet.



Figure 2.7: 3D printing filament on drum - [14]

Orientation

The FDM technology uses, as stated before, a nozzle to extrude the material out and construct the part layer-by-layer. Due to this manufacturing method the part will have different strength properties as a consequence of what the orientation of the part was printed in. As the printed material is laid out layer-by-layer in a long string of material will make the strings of material act as material fibers strings. Having longitudinal fibers when exerted to a force along the fibers is much stronger, than having transverse fibers. As simplified method of showing this is displayed in Figure 2.8.

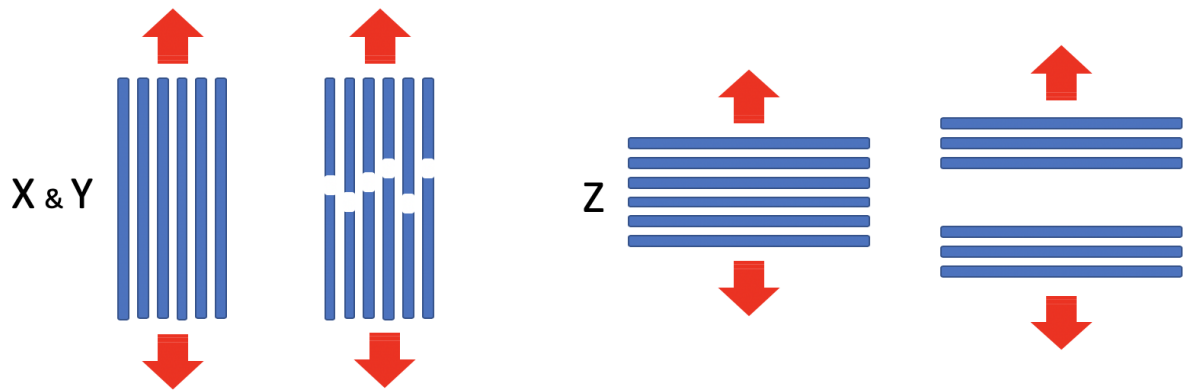
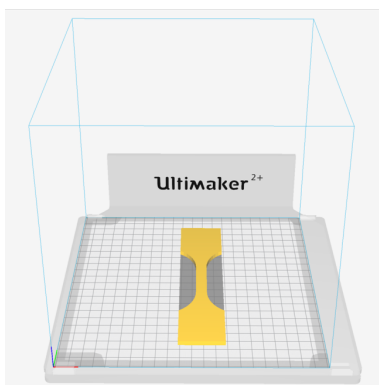
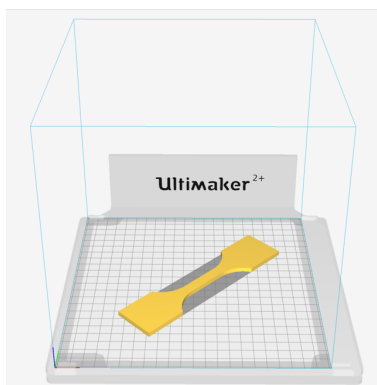
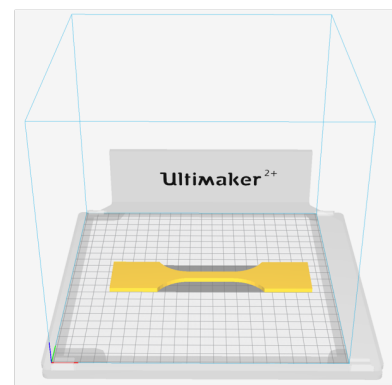


Figure 2.8: Layer orientation

Orientation Clarification

The different orientations that the test specimens are printed in are displayed in Figure 2.9 - Figure 2.11. Due to the way the 3D printer from Ultimaker 2+ lays the string of extruded material on the build plate, it will have an effect on how the test specimen is constructed. When the test specimen is printed at 0° and 90° , the printer applies the extruded material in a cross-pattern at an 45° angle. Whereas, when the test specimen is put at an 45° angle in the build plate this results in a longitudinal and transverse print pattern. This is done to identify the differences that may occur in strength due to the orientation of the printed matter. Later on when the experimental test will be presented, this method of explaining how the individual pieces are constructed will be used.

Figure 2.9: Printed at 0° Figure 2.10: Printed at 45° Figure 2.11: Printed at 90°

Infill

Infill is the pattern the 3D printer lays the material inside of the component itself. There are in most cases a lot of different geometries and percentage to choose from when printing a component. The infills percentage that is applied have a strong correlation to the strength and weight of the individual component. A component with a 90% infill will almost in every case be stronger than a component with an 20% infill, but it will also be heavier. It is here where the skill of the engineer and his/her understanding of the function of the final printed component is critical. A prototype where the form is the most important feature, the component can be printed with very low infill saving significantly cost, and time. Whereas, a bracket that will experience loading will need a higher infill percentage. In Figure 2.12 a selection of different infill geometries is visualized to get a better understanding of how 3D printed components can be on the inside.

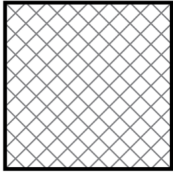
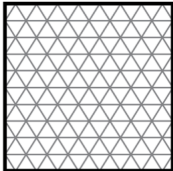

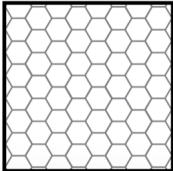
Infill geometry	Description
	Rectangular - Standard infill pattern for FDM prints. Has strength in all directions and is reasonably fast to print. Requires the printer to do the least amount of bridging across the infill pattern.
	Triangular or diagonal - Used when strength is needed in the direction of the walls. Triangles take a little longer to print.
	Wiggle - Allows the model to be soft, to twist, or to compress. Can be a good choice particularly with a soft rubbery material or softer nylon.
	Honeycomb - Popular infill. It is quick to print and is very strong, providing strength in all directions.

Figure 2.12: Infill geometry - [15]

Potential Problems

As this research will use FDM technology there are some potential problems that need to be addressed. The most common problems using FDM is for the most part layer adhesion of the model, and its potential for warping. As there are a lot of potential problem a list is made with a short explanation below.

- **Not sticking to print bed** - First layer does not stick to the bed, and the print fails.
- **Under Extrusion** - Printer does not extrude enough material, which leads to gaps in the model.
- **Over Extrusion** - Printer extrudes too much material making the model messy and dimensional incorrect.
- **Stringing** - Small strings of material that occur when the extruder head moves over different parts of the model.
- **Overheating** - Sections of the model gets too hot, making them melt and deform.
- **Layer Shifting** - Layers misaligned and shift due to error in file or mechanical failure.
- **Layer Separation** - Layers separates during printing, splitting up the model.
- **Jammed Extruder** - Extruder head is jammed and will not extrude material.
- **Curling** - Corners of the model tend to curl and deform as they are printed.
- **Small features not printed** - If the model have too small parts the printer may not print them. For instance, scaling down a big model- file may lead to this happening.
- **Warping** - Deformation of printed model due to inconsistent, and too high temperature while printing.
- **Dimensional Accuracy** - As a consequence of the way FDM technology uses a circular string of material to make the model, it will in many cases not fully represent its initial dimensions.

2.2 Experimental Methods

Method Approach

Designing any kind of parts or structures requires the engineer to understand the mechanical behavior of the material that is going to be used. A proven way of determining how the materials perform and behave when subjected to loads is through experiments. By doing this, the engineer can identify what the limitations and strengths of the material are, thus be more certain that the calculated results are similar to real life. To test materials there are developed international standards(ISO) for how these types of tests shall be performed. The ISO-standard that this research is going to be based on is the ISO 527:2012 [16]. The title of this standard is "Plastics - Determination of tensile properties." It is a standard that contains different methods to investigate the tensile behavior of the test specimens, and for determining the tensile strength, tensile modulus and other aspects of tensile stress/strain relationship under specific conditions. The specific geometry of the test specimens, temperature, pull speed of the machine, etc. This is done to ensure the results can be compared to earlier tests and also if needed, replicated. In Figure 2.13 and 2.14 the typical tensile test geometry and tensile test setup are displayed.

Performing the test, the test specimen displayed in Figure 2.13, is clamped between two grips and then loaded with tension. To identify how the specimen performs there are multiple measuring devices to see the deformation. Some devices are attached externally if the machine is not capable of doing it itself. The tensile test specimen is made in this way to ensure the failure in the specimen will occur inside of the light blue area. This will ensure the area is only subjected to pure tension in the longitudinal direction. Therefore, the outer parts where the grips will be clamped on to hold the specimen are made extra large, this is to ensure that they will not break at this region. The reason for this, is that in these outer areas the stress distribution is not uniform and will not provide correct results if it where to break at this area [17].

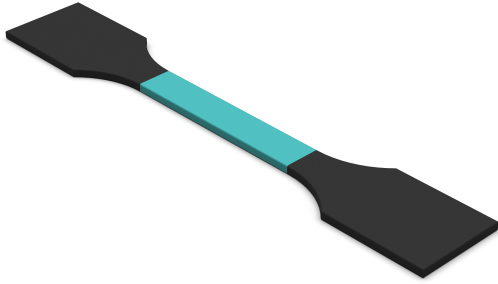


Figure 2.13: Tensile test specimen



Figure 2.14: Tensile test setup

Stress σ

The stress σ , acting on a structure can be calculated using equation 2.1. The stress is a measure of units of force per unit area. When a bar, cylinder, or any other kind of structure is stretched by a force F , the stresses are called tensile stresses. If it were to be compressed with a force F , the stresses obtained would be called compressing stresses. The equation however, is only valid if the stresses are uniformly distributed over the cross section area of the loaded part [17], displayed in Figure 2.13.

$$\sigma = \frac{F}{A} \quad (2.1)$$

Strain ϵ

The strain ϵ , an object is exposed to can be expressed by using equation 2.2. When a part is exerted to a force it will change its initial cross section. The elongation δ of a bar is the result of the stretching of all elements of the material throughout the volume of the bar, assuming the bar is made from one material. For instance, when a bar is exerted to a force axially, the length of the bar will either be stretched or compressed.

In general, the elongation δ of a segment is equal to its length divided by the total length L and multiplied by the total elongation δ . Therefore, a unit length of the bar will have an elongation equal to $1/L$ times δ . This quantity is called the elongation per unit length, or strain, and is denoted by the Greek letter ϵ (epsilon) [17].

$$\epsilon = \frac{\delta}{L} \quad (2.2)$$

The results extracted from the tests are based on the specific geometry of the test specimen in which it was performed. To make these results viable for any other geometries with the specific material, it is possible to convert these results to stress-strain diagrams. These diagrams can provide data revolving the materials behavior when exerted to a force. The material properties regarding the maximum tensile strength, yield point, Young's modulus, elastic limit and breaking point are properties that are possible to identify using stress-strain diagrams. And they will also show for instance if the material is brittle or ductile, visualized in Figure 2.15.

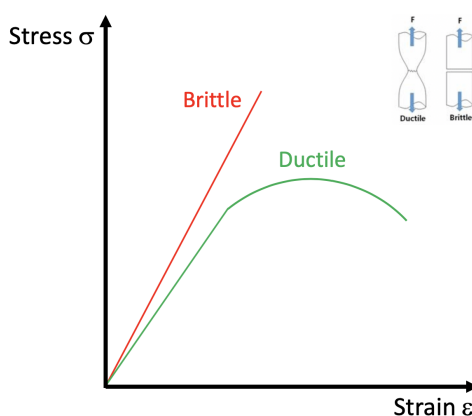


Figure 2.15: Brittle and ductile- material curve

Linear Elasticity

When the behavior of a material is acting elastic when exerted to load, and also displays a linear relationship between stress and strain, it goes under the term linearly elastic [17]. This is visualized in Figure 2.16. As an engineer this is very important to know when designing a new structure/product to avoid permanent deformation, as a result of yielding due to the specific material properties.

Beyond this point, the proportionality between stress and strain no longer exists; hence the stress at point is called the proportional limit. The slope of the straight line from origo to the proportional limit is called the modulus of elasticity or more commonly known as Young's Modulus E . Young's modulus is only valid in the range in which the stress is proportional to the strain, which means the material will return to its original dimensions when the exerted force is removed. In other words, in the linear elastic region. Surpassing this region the Young's modulus will in most cases not remain constant. The steeper the slope is, means the material is more resilient to elongation, hence have a greater stiffness. Because the linear slope has units of stress divided by strain, modulus of elasticity has the same units as stress i.e $\text{MPa} / [\text{N}/\text{mm}^2]$. In Figure 2.16 an example of a mild steel stress-strain curve is visualized.

1. Linear Elastic
2. Proportional Limit
3. Yield Stress
4. Ultimate Tensile Stress
5. Fracture

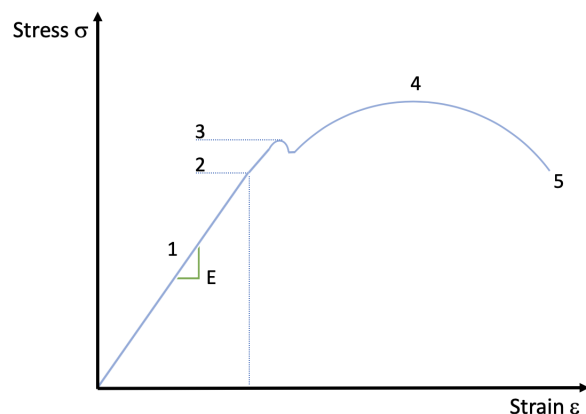


Figure 2.16: Steel stress-strain curve

Hooke's Law

The law is given by a direct proportionality between a spring's compression or elongation, and the restoring force which follows. This relationship is given by equation 2.3, where Δx is the distance a spring has been stretch due to the force F that has been exerted on the spring. k , is the spring constant which characterizes the elastic properties of the spring's material. This is visualized in Figure 2.17. This law is only valid within the elastic limit of a linear system. Looking at other materials it becomes clear that most materials act like springs when a forces is applied, where the force is proportional to the displacement. But as compared to springs, other materials possess an area in which must be accounted for which can be expressed by Equation 2.4. Rewriting the initial equation 2.3, replacing force with a measure of stress and displacement of strain, a combined equation is derived, displayed in equation 2.5. In which the σ is the axial stress, ϵ is the axial strain and E is the modulus of elasticity for the specific material [17]. These equations are crucial in this research.

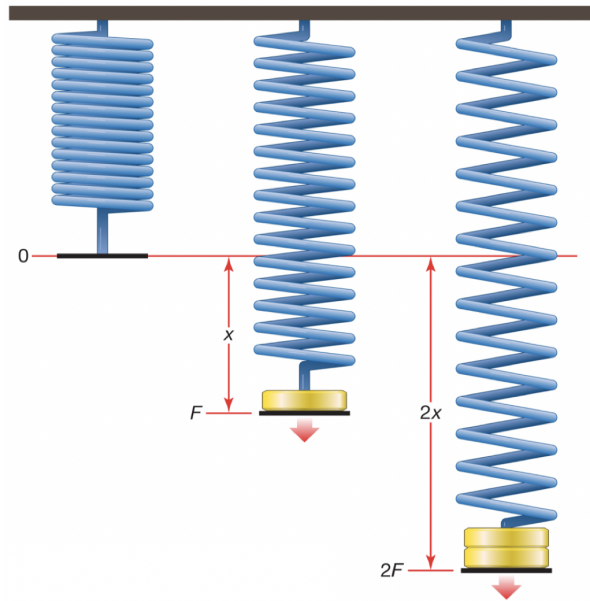


Figure 2.17: Hooke's law - [18]

$$F = -k \cdot \Delta x \quad (2.3)$$

$$k = \frac{EA}{L} \quad (2.4)$$

$$\sigma = E\epsilon \quad (2.5)$$

2.3 Numerical Methods

FEM is a numerical method which is used to solve complex, for the most part, engineering and physics problems. This is the mathematical basis behind the Finite Elements Analysis(FEA) which is more of the solver and practical application of the FEM. In this method the problem at hand is mathematically expressed in such a way it is possible to perform an analysis with all the data required to get an accurate virtual representation of the problem at hand. Engineers in today's industrial world use it to reduce the numbers of physical prototypes, numbers of experiments needed and also to optimize the components in the early design phase [19]. This is possible in many different Computer Aided Engineering(CAE)-software. Some of these are Nastran(Siemens NX), Autodesk Simulation, ANSYS to name a few.

Usually the process starts by making a Computer Aided Design(CAD)- component to perform analysis on. Based on this model a mesh is created to represent the CAD model by nodes and elements which will be used to run the analysis on [20]. An example of this is displayed in Figure 2.18 where the CAD, mesh and FEA model are represented.

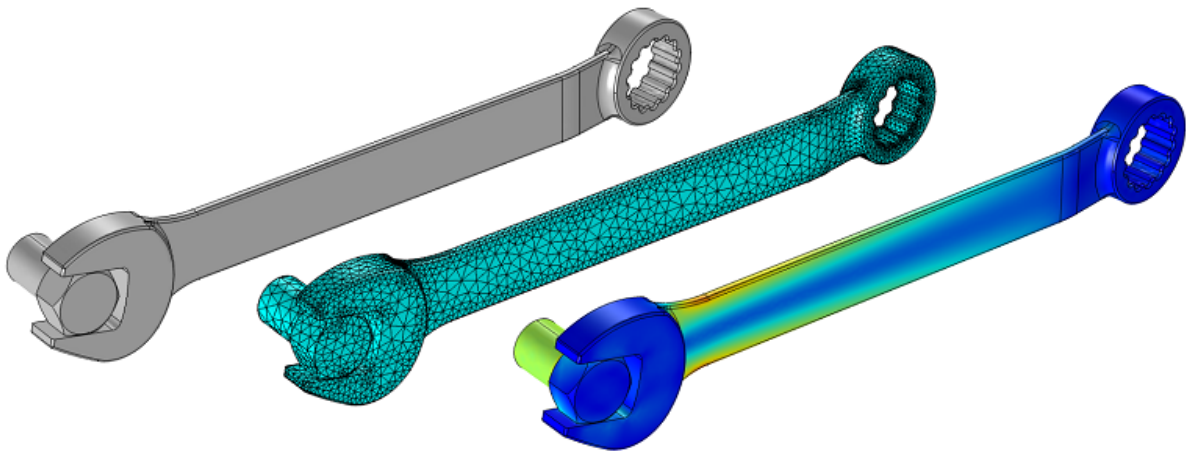


Figure 2.18: Visual representations of analysis steps - [21]

It is here the material and structural properties of the model is stated. Based on the complexity of the model the finite element mesh size can be different throughout the model. Specific areas which are subjected to specific loads and constraints may need a more refined mesh than other parts of the model. This is especially important around uniting parts and corners, if the CAD model is made properly. You could argue that using

a ultra fine mesh on the whole model would be beneficial, but then the computational power required to solve it would be enormous and take a huge amount of time to solve.

Another problem that possibly might occur is that the model would experience large stress concentrations, which is not representative of the actual stress in the affected area. This happens around, and with sharp angles and edges. The problem occurs when the CAD model with sharp internal corners/edges and point loads is that they are sources of numerical singularities. This means that these locations are incapable of predicting accurate results even with accurate input data and a very fine mesh. Reason for this is that numerically, finite element analysis calculates stress in corners based on the local element size, with smaller elements yielding higher stresses. As a consequence, increasing mesh refinement would only contribute to increase the stress without limitation [22]. A visualization of this is displayed in Figure 2.19.

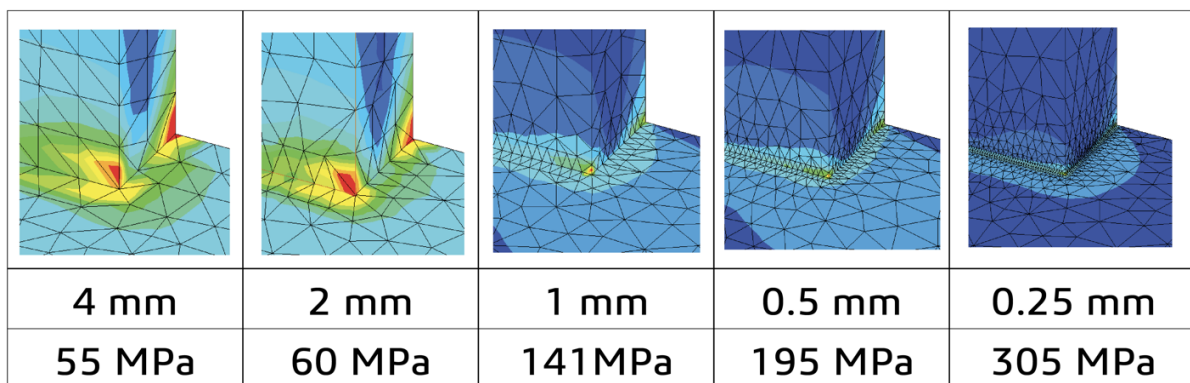


Figure 2.19: Element size and Von Mises stress - [23]

2.4 Related Work

One of the most interesting references found was an experiment where they were using FDM 3D printing to identify the material properties of ABS material. They used different standards to achieve their results and all is explained in a short and well organized manor. They were also looking into the orientation of the printed material and its effects it may cause. This is research paper which has 6 authors, so its an substantial amount of work done. The big missing part is an validation of the results in FEM and check if the values would give the same deflection results there, but this was not part of the study. They concluded however with this:

From the Design of Experiment for FDM ABS (P400), it was found that the air gap and raster orientation affect the tensile strength of an FDM part greatly. Bead width, model temperature, and color have little effect. The measured material properties showed that parts made by FDM have anisotropic characteristics. Measured tensile strengths of the typical Criss-cross raster [458/2458] and Cross raster [08/908] with 2 0.003 air gap were between 65 and 72 percent of the measured strength of injection molded FDM ABS. The compressive strength of FDM material was higher than the tensile strength and was not affected much by build direction. Because of the anisotropic behavior of the parts made by the FDM process, the strength of a local area in the part depends on the raster direction [24].

Another one, a master thesis with the title "Validation of material model for polypropylene". The thesis is written in 2012 at NTNU by Kjetil Vange. Due to the usage of, at the time, a new material was investigated if it was possible to derive a material model and validating it using FEM analysis. This thesis uses experimental methods of tensile strength and compression test to identify the material properties. From there, these values are used to validate the results using FEM. He concluded the research with this:

As a conclusion it can be stated that the material model has successfully managed to represent the polypropylene treated in this thesis. Even though the calibration procedure is fairly simple it has not stopped the material model from representing complex problems. A further enhancement would be to include the viscoelastic behaviour and a fracture criterion. By adding these properties can the material model represent an even wider range of problems. They should, however, be implemented in a way that does not complicate the calibration in any extent, thus conserving the simple yet complex nature of this material model [25].

Looking back at the research questions stated in the beginning. The measurements of strength of a 3D printed part is possible looking at the work done previously. But they used an other material which might make a difference as this is a big variable to change, however it shows that it is possible to generate data from 3D printed parts. The related work done and the theory behind gives a good platform to further explore the possibility to develop a functional test procedure.

Chapter 3

Methodology

3.1 Thesis Approach

The main objective is to derive a test procedure to measure the material properties, more specifically the Young's Modulus of 3D printed PLA. The preliminary step was to gather information and knowledge regarding different strength analysis methods and the basics of 3D printing. With this in mind, the manufacturing of the test specimens was conducted. How the experimental test should be performed was also an essential part of this research. A simple printed test specimen was tested to see if the intended experimental test procedure for this research would give any measurable results. As this was found to be accomplished, more specimens were printed with different geometries and printing orientations, which is further presented in this thesis. This was done to identify the importance of the manufacturing method and how a change in it may have a consequence on the results. All of the results were statistically analyzed using MATLAB.

Furthermore, alongside the experimental tests, strength analysis in FEM analysis was used to derive a stiffness coefficient ratio between the different geometries. This was done using Siemens NX Nastran solver to more accurately derive a Young's Modulus of the material.

3.2 Prototyping

The manufacturing of the 3D printed test specimens is made using the following procedure in this section. All the steps from CAD model to the final physical test specimen will be presented in this section. A visual representation of this procedure is visualized in Figure 3.1 - 3.3.

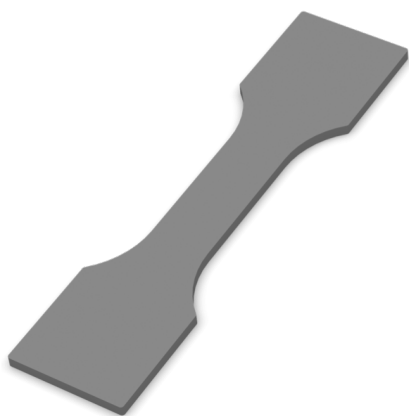


Figure 3.1: CAD model

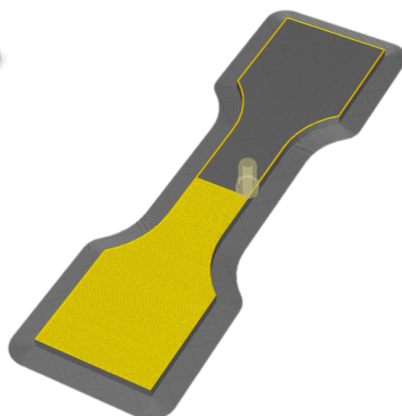


Figure 3.2: Cura model



Figure 3.3: Finished model

3.2.1 Computer Aided Design

The test specimens are created in Siemens NX, which is an advanced high-end CAE software, which is one of the software's that is available at NTNU Ålesund. Siemens NX also features, among other modes, a FEM analysis solver which will be used later on in the structural analysis section. The test specimens has taken inspiration from the ISO 527 standard previously presented. There is made two different geometries and they are visualized in Figure 3.4 and Figure 3.5. The geometry is based, as mentioned before, on the ISO standard but it needed some alteration due to the printer size. As explained in Section 2.2 they are made this way to ensure that the specimen subjected to pure tension in the smaller region, and that the fracture will most likely happen here.

After the geometry were set, they were exported as an STL file for further manufacturing. An STL file stores the geometry information of the exported CAD model. The format describes only the surface geometry of the CAD model without any representation of color, texture or other model features [26]. This is the file format which is used to slice the CAD model in the Computer Aided Manufacturing tool, Ultimaker Cura.

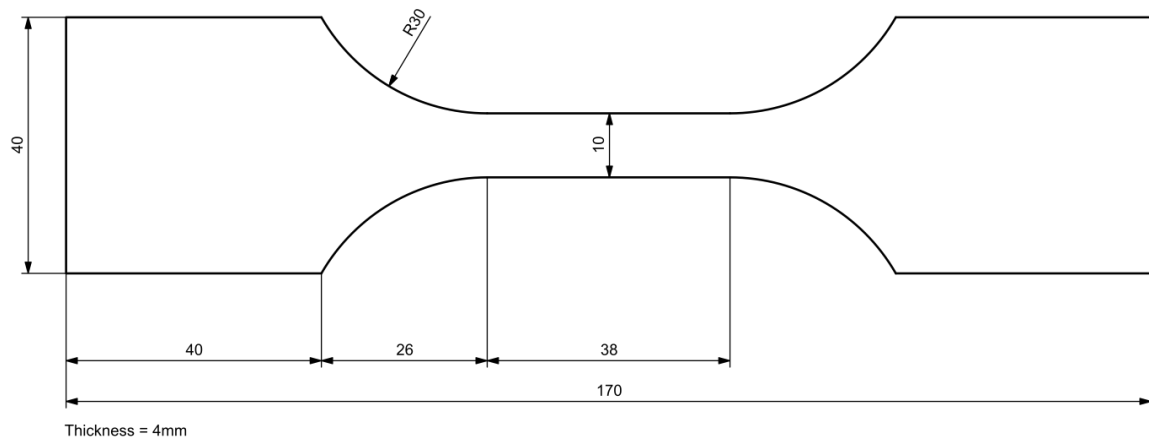


Figure 3.4: Geometry 1

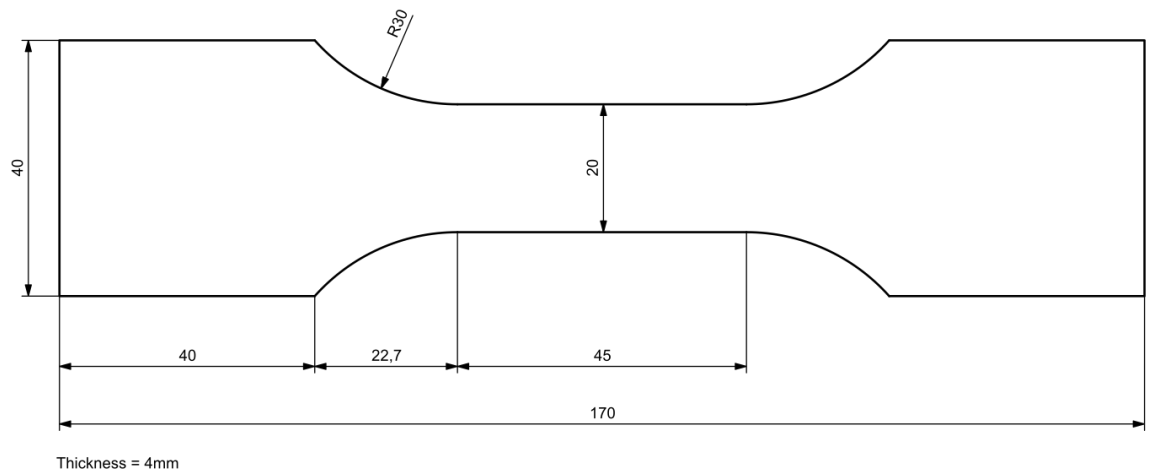


Figure 3.5: Geometry 2

3.2.2 Computer Aided Manufacturing

The exported STL files of the CAD models need to be further processed to eventually be 3D printed. The software used to read these files and set the 3D printing initial settings is called Ultimaker Cura. It is a free to download software that is relatively easy to use and has the 3D printer which will be used in its library, hence the name. Ultimaker Cura is used to take the STL file made, and slice the model into multiple layers, creating the 3D printer's extruding path. All of this information is then stored and exported using an g-code file format, which is automatically generated in Ultimaker Cura. G-code is one of the manufacturing languages that the 3D printers can understand. This code describes how a 3D printer should print a model layer-by-layer. It stores information in a text file where every task the 3D printer should do. All of the settings from how fast the printer should print, to at what temperature the nozzle should be, is stored in these files. 3D printing requires a large number of instructions for exact printing, which is why it separates the task into multiple layers.

There are a lot of different settings available in Ultimaker Cura, but all of the settings have a pop-up info window while hovering over the individual setting for a quick explanation. To have a little more control of the settings there were used the advanced mode where the different settings can be manually applied. The settings that are manually applied in Ultimaker Cura, and used on all of the printed test specimens are displayed in Table 3.1.

Table 3.1: Ultimaker Cura Print Settings

Generic PLA	
Filament diameter	2.85 mm
Layer Height	0.1 mm
Wall Thickness	0.4 mm
Top Thickness	0.8 mm
Bottom Thickness	0.8 mm
Infill Density	100%
Infill Pattern	Lines
Print Speed	50 mm/s
Build Plate	Brim

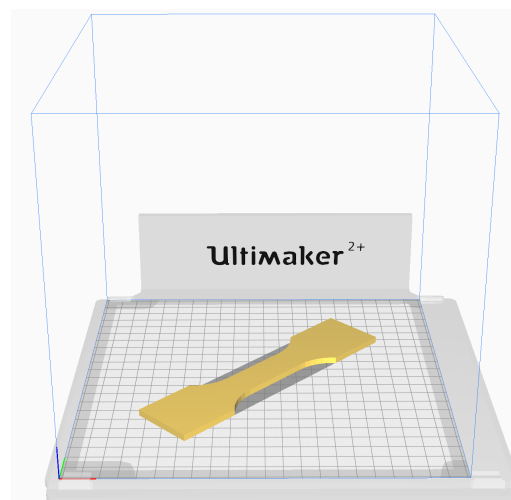


Figure 3.6: Ultimaker Cura

3.2.3 3D Printing

All of the 3D printed test specimens were printed on the same exact printer to make the manufacturing process as similar as possible, and avoid possible irregularities between multiple printers. The printer that is used throughout this project is an Ultimaker 2+, visualised in Figure 3.7. It is highly reliable, user friendly and creates, in most cases, good results. In Table 3.2 all of the tested test specimens individual 3D printer settings is visualized. The only difference in the printer settings that is notable, besides the section area of the test specimens and print orientation, is the bed temperature. Due to the length and width of the test specimen from T4.1 - T4.15, it became apparent that the size of the models made them experience warping. A solution for this was to turn down the temperature of the print bed with 8°C. This has negligible effect of the end results, but it reduces the chances of failed prints.

A part of the research is to identify the differences of how the 3D printed test specimens have been printed in terms of orientations, and its influence towards the strength. Displayed in Table 3.2 a total of 31 test specimens is shown with 10 printed at 0°, 10 printed at 45° and 11 printed at 90°. The reason for the odd number is that there was a hiccup at the first experimental test which made T3.6 fail, which is possible to see in the Appendix A.1. But fortunately one extra test specimen was made in the same batch and tested, labeled T3.11, which worked as a stand in for T3.6.



Figure 3.7: Ultimaker2+ - [27]

Table 3.2: Test Matrix

Name	Print Time Hours	Nozzle Size [mm]	Nozzle Temperature[°C]	Bed Temperature[°C]	Section Area [mm ²]	Print Orientation [°]
T2.1	7	0.4	205	60	40	0
T2.2	7	0.4	205	60	40	0
T2.3	7	0.4	205	60	40	0
T2.4	7	0.4	205	60	40	0
T2.5	7	0.4	205	60	40	0
T3.1	7	0.4	205	60	40	45
T3.2	7	0.4	205	60	40	45
T3.3	7	0.4	205	60	40	45
T3.4	7	0.4	205	60	40	45
T3.5	7	0.4	205	60	40	45
T3.6	7	0.4	205	60	40	90
T3.7	7	0.4	205	60	40	90
T3.8	7	0.4	205	60	40	90
T3.9	7	0.4	205	60	40	90
T3.10	7	0.4	205	60	40	90
T3.11	7	0.4	205	60	40	90
T4.1	8	0.4	205	52	80	0
T4.2	8	0.4	205	52	80	0
T4.3	8	0.4	205	52	80	0
T4.4	8	0.4	205	52	80	0
T4.5	8	0.4	205	52	80	0
T4.6	8	0.4	205	52	80	45
T4.7	8	0.4	205	52	80	45
T4.8	8	0.4	205	52	80	45
T4.9	8	0.4	205	52	80	45
T4.10	8	0.4	205	52	80	45
T4.11	8	0.4	205	52	80	90
T4.12	8	0.4	205	52	80	90
T4.13	8	0.4	205	52	80	90
T4.14	8	0.4	205	52	80	90
T4.15	8	0.4	205	52	80	90

3.2.4 Post Processing

After the test specimens were printed, there needed to be a little finishing touches, and a dimensional check. This is to ensure that all of the printed test specimens are free of excess material, and have the correct dimensions. On the printed specimens there was added a brim around the base layer of the model, visualized in Figure 3.8. This is done to ensure a good adhesion with the print bed, and reduce the potential of warping. This is just a very thin layer that is easily removed afterwards. Each individual test specimen was measured, and analysed to ensure that the initial geometry was on par with the rest of the batch with a very low deviation $\pm 0.5\%$. In addition, whenever a new specimen was finished, they were put and stored in the same box container with a moist reducer bag until they eventually were going to be tested.

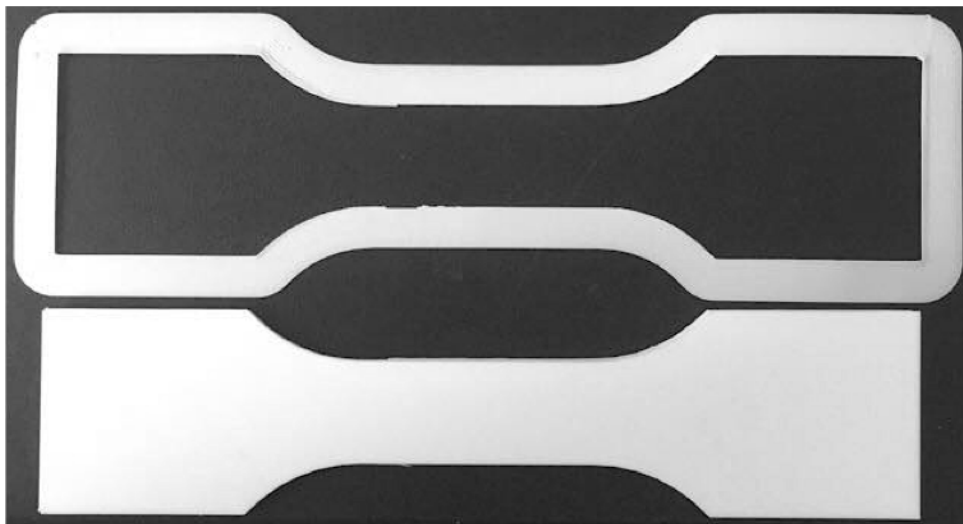


Figure 3.8: Brim

3.3 Experimental Test - Tensile Test Setup

The experimental test that was conducted to identify the material properties of PLA was the tensile strength test. How the test is specifically performed will not be addressed here, due to it all ready have been explained in Section 2.2. In the workshop at NTNU Ålesund, there is Galdabini Quasar 200 machine which were used to test the 3D printed test specimens. The machine has an maximum capacity of 200 kN, hens the name, and is suitable for metals, plastics, composites and other materials. A key feature of this specific machine is that in Galdabini's own words has an "extremely high resolution of load and stroke readings". The datasheet of the machine itself is added to Appendix D.

The experimental test of the different specimens was divided into two experiments. This was mostly due to the amount of hours it takes to print the specimens itself. As the printers are located at lab rooms, and the students have limited access of these rooms, the printing process itself were a bit more tedious than wanted. In addition, it was also done this way to have more control, and reduce the amount of time from the point where the specimens were printed, to the point where they were tested.

All of experimental tests have been done by, and under the supervision of:
André Tranvåg - Head Engineer at NTNU Ålesund.

3.3.1 Experimental Test 1 - Specifics

Tensile strength test of 15 test specimens with different orientations.

5 specimens with 45°diagonal print pattern printed at 0°.

5 specimens with longitudinal and transverse print pattern printed at 45°.

5 specimens with 45°diagonal print pattern printed at 90°.

Cross-section area of test specimen: 40 mm² - 10 mm wide and 4 mm thick

Print orientation of T2.1 - T2.5: 0°

Print orientation of T3.1 - T3.5: 45°

Print orientation of T3.6 - T3.11: 90°

Location: Workshop at NTNU Ålesund

Room temperature: 18-22° C

3.3.2 Experimental Test 2 - Specifics

Tensile strength test of 15 test specimens with different orientations

5 specimens with 45° diagonal print pattern printed at 0°

5 specimens with longitudinal and transverse print pattern printed at 45°.

5 specimens with 45° diagonal print pattern printed at 90°.

Cross-section area of test specimen: 80 mm² - 20 mm wide and 4 mm thick

Print orientation of T4.1 - T4.5: 0°

Print orientation of T4.6 - T4.10: 45°

Print orientation of T4.11 - T4.15: 90°

Location: Workshop at NTNU Ålesund

Room temperature: 18-22° C

Monitoring of the tests, and control of the initial results was done using Galdabini's own integrated software, Graphwork. The program features a graph where it is possible to have an initial peak at the force - deformation curve. As the test are being conducted the program plots simple force - deformation curves on top of each other. This is very useful as it is easy to very quickly identify how the test have performed, and also see if there are any initial irregularities between the tests. The only initial setting that was required to set before testing was setting the width of the test specimens, as presented in Section 3.2.1, these were 10- and 20 mm. The stroke speed used on all of the tests performed in this thesis were set at rate of 4 mm/min. After the individual tests were done the data was exported into Excel files, which would later be processed in MATLAB for the statistical analysis in Section 3.4.

3.4 Statistical Analysis

3.4.1 Smoothing of Raw Data

Exporting the data from Graphwork is first done to Excel-files. From Graphwork, it is possible to decide what data you want to export, to some extent. It all depends on the test. However, for this research the important data from the experimental test were the force and deformation rate from each individual test. These data, in addition to the cross head stroke of the machine itself were exported. On average the exported data consisted of approx 30,000 rows of raw data which needed to be analysed. The way of handling and analysis of the data is done using MATLAB. A script is made to directly import the Excel-files for further analysing, which is attached in the Appendix C.1. Keep in mind that all of the further coding is based on the force - deformation data from each test.

As said before there were a lot of data to process, initially the force - deformation looked like Figure 3.9. The red dots in Figure 3.10 represent the logged data output from the machine and Graphwork software, and is the same picture as Figure 3.9, only zoomed in to see the multiple entries of the force. The plot of the initial raw data shows that the data needs smoothing to better represent the force - elongation values. Interpretation of the initial data is that there are a lot of force data points on the same exact elongation level. A direct smoothing function does not work for these initial data points, because there are too many force data points on the same elongation level. Each red dot is indicating one measurement point. A solution to this, was for each multiple entries, a mean value is calculated and is represented by the green colored dots, visualized in Figure 3.11. Through the new green dots, it is applied a strong smoothing function that its represented by the blue colored line in Figure 3.11, and fully visualized in Figure 3.12. To show this, and the process, it is used the data of Test3.1 as an example, which is added to Appendix A.1, alongside all of the other tests.

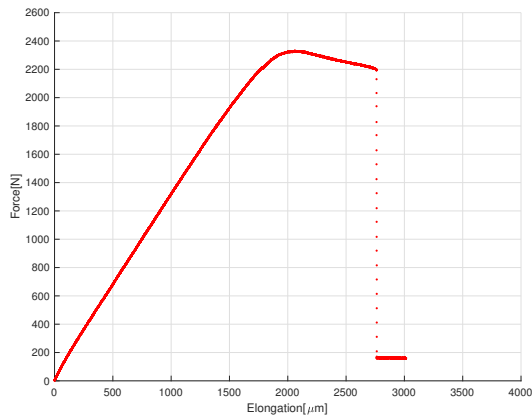


Figure 3.9: Raw data curve of Test3.1

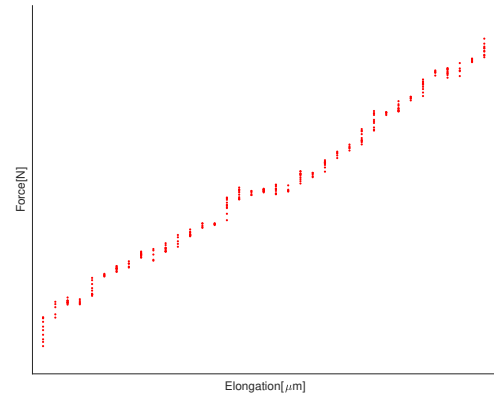


Figure 3.10: Raw data curve zoomed

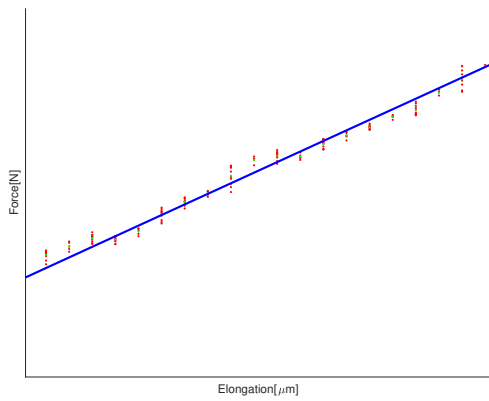


Figure 3.11: Smoothed data zoomed

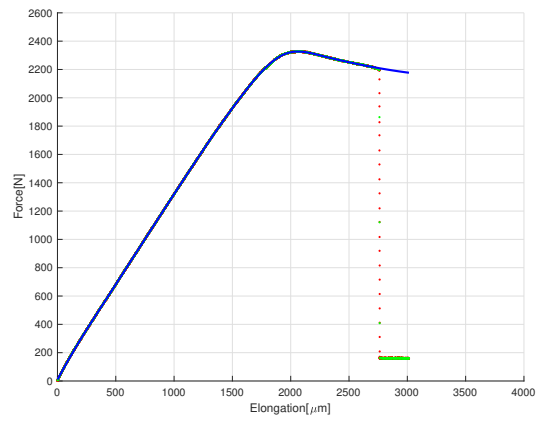


Figure 3.12: Smoothed raw data of Test3.1

- It is visible that the smoothing does not fully represent the raw data when the fracture occur visualized in Figure 3.12. As this research will base itself on the elastic region and this will not have an effect further on, other than on the pictures.

3.4.2 Linear Region

Now that the initial raw data have been cleaned up it is time to make use of them. The Young's modulus can be derived from the elastic area from the force - elongation curve. By only measuring by hand it is possible to derive it, but it would not be very accurate, and also as we will see later not fully represent the Young's modulus due to geometry of the test specimens. However, from the all of the tests it is possible to derive a procedure to eventually derive an initial Young's modulus. To derive the initial Young's modulus as accurate as possible, it was needed to find where the region in which the force - elongation curve behaves most linear. From the experiments and looking at the curves it was clear that there were a nonlinear region at the start of the curve, and obviously near the yield point of the curve. This required that the region had to be somewhere in between, exemplified by the red square in Figure 3.13. To find the gradient of the slope the force - elongation curve was differentiated, which makes it look like Figure 3.14. The horizontal part of curve in Figure 3.14 represent the range in which the gradient of the force - elongations curve is most constant, hens most linear, which is in this case somewhere around 1.25 when only looking at the curve in Figure 3.14.

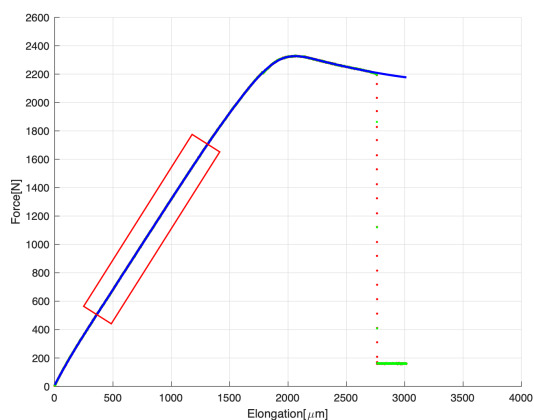


Figure 3.13: Linear Region

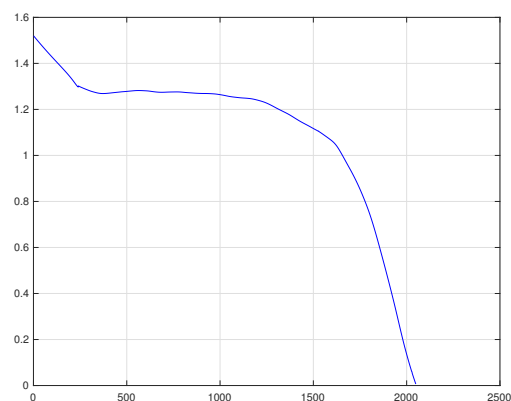


Figure 3.14: Differentiated

To have a better control of the range in which the gradient of the curve is derived, a kernel distribution of the values is used. This takes all of the data from the differentiated curve and distribute it accordingly visualized in Figure 3.15. From the kernel distribution a mean value of 1.2658 is found, from all of the initial data which will be used as a baseline for the linear region of T3.1, visualized in Figure 3.16. The mean value is then used to make a interval range in which is the gradient of the curve is constant to an optional certainty. The mean value in this case is multiplied with a deviation of $\pm 5\%$, and visualized in Figure 3.17. The pink line represent an increase of 5%, and the red line represent a decrease of 5%. The for loop in the script logs automatically when the blue

line passes, from left to right, under the pink line and again when it goes under the red line. Using the range inside of the pink and red line in which the gradient is "constant", a cropped curve of the force elongation curve is made, this is visualized in Figure 3.18. This represent a new cropped force - elongation curve in which the Young's modulus will be extracted from.

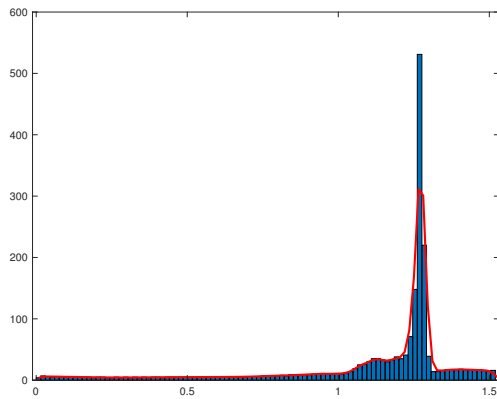


Figure 3.15: Kernel distribution

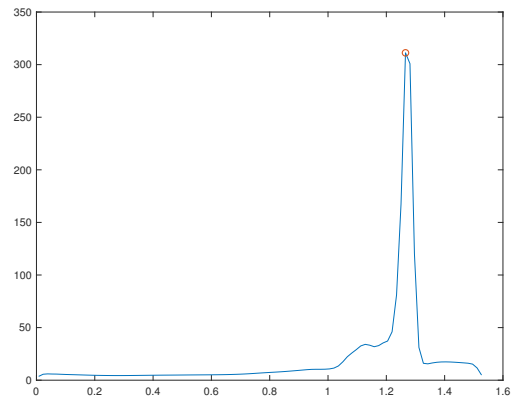


Figure 3.16: Mean value of gradient

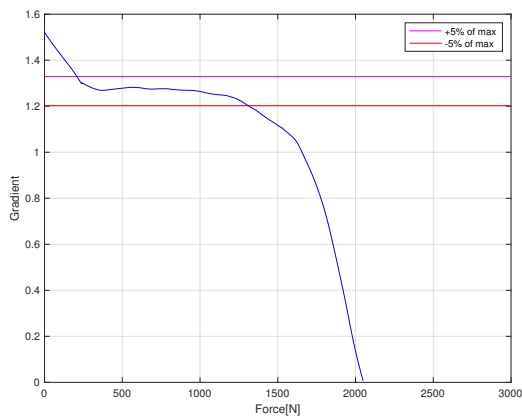


Figure 3.17: Calculated linear range

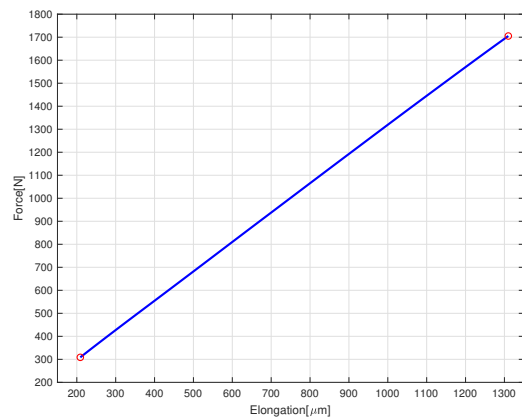


Figure 3.18: Range cropped force - elongation curve

The script will also log the start and end of the cropped force and elongation curve, which will obviously be different for every test, visualized in Figure 3.18. For T3.1, the elongation starts from 209 and goes up to 1310 μm , as the force goes from 309 and up until 1705 N. With these values and the geometry of the test specimen, it is possible to derive the initial Young's modulus visualized in equation 3.1.

Where the geometry of T3.1:

$$L = 170 \text{ mm}$$

$$A = 40 \text{ mm}^2$$

$$E = \frac{\sigma}{\epsilon} = \frac{\frac{F}{A}}{\frac{\delta}{L}} = \frac{\frac{(1703-309)N}{40\text{mm}^2}}{\frac{(1310-209)\mu m}{170 \cdot 10^3 \mu m}} \approx 5390 \text{ MPa} \quad (3.1)$$

From all of the steps now presented it is clear that this method can derive a Young's modulus, but it comes apparent that this Young's modulus do not fully represent the material. This is due to the geometry of the test specimen, and will be further elaborated in Section 3.5.

3.5 Structural Analysis

3.5.1 Stiffness Coefficient Ratio

The motivation behind using FEM analysis is the need to extract the proper Young's modulus of PLA, by identify a stiffness coefficient ratio. When performing a tensile strength test, the part itself is exerted to a force in which it is stretched. Normally to measure this stretch the test specimen have a specific gauge length, visualized as an example i Figure 3.19. This length is predetermined. To measure how far the gauge length stretches from its original length while the specimen is exerted to a force an extensometer is attached, visualized in Figure 3.20. This device is used to ensure that the tensile test specifically logs the strain in this smaller gauge length section of the part. The length is then only experiences pure tension from the force. By doing this the overall geometry is not taken into account which could ultimately effect the end result, which is the way of doing it according to ISO- standards. This is important to grasp, because it is not only the gauge length that is stretched under the influence of the force, but the whole test specimen.

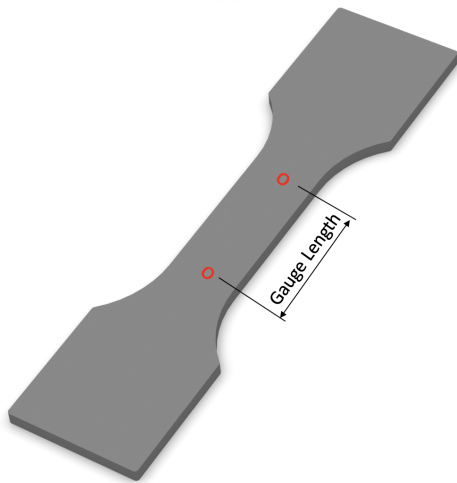


Figure 3.19: Gauge Length example



Figure 3.20: Extensometer - [28]

However, this research have explored an alternative way of taking the geometry of the test specimen into account, so that is is not required to use these types of devices to ensure that the Young's modulus is derived in well manor. This basis itself on using the elasticity theory and using the material behaviors similarity of steel in the linear region of the force - elongation curve to determine the Young's modulus of the material. A stiffness coefficient ratio between a flat bar and the test specimens have been made to determine the proper Young's modulus of the material.

This is done by comparing a flat bar and FEM analysis of the test specimens geometries and comparing the elongation between them. These different models are visualized in Figure 3.21. By doing this it is possible to determine the scaling effect of the geometry of the specific test specimen. The motivation behind this is that the tested specimens does not have a constant cross section that the force have been loaded onto and this needs to be accounted for. On all of the different models, it is possible to derive a stiffness coefficient ratio, but due to stress concentrations that are bound to happen in Model 2, this model will not be further tested. It is here the need for a more smooth section between the part in which the test specimens will clamped to, and the slimmer section in the middle. Model 1 works as the base and the others are cutout models of the original Model 1. This means that the measurements of the Model 1 is the same as the outer geometry of the test specimens in Section 3.2.1. With a length of 170 mm, width of 40 mm and a thickness of 4 mm. The geometry of Model 3 and 4 are the same as the test specimens in Figure 3.4 and 3.5, where Model 3 is Geometry 1, and Model 4 is Geometry 2.

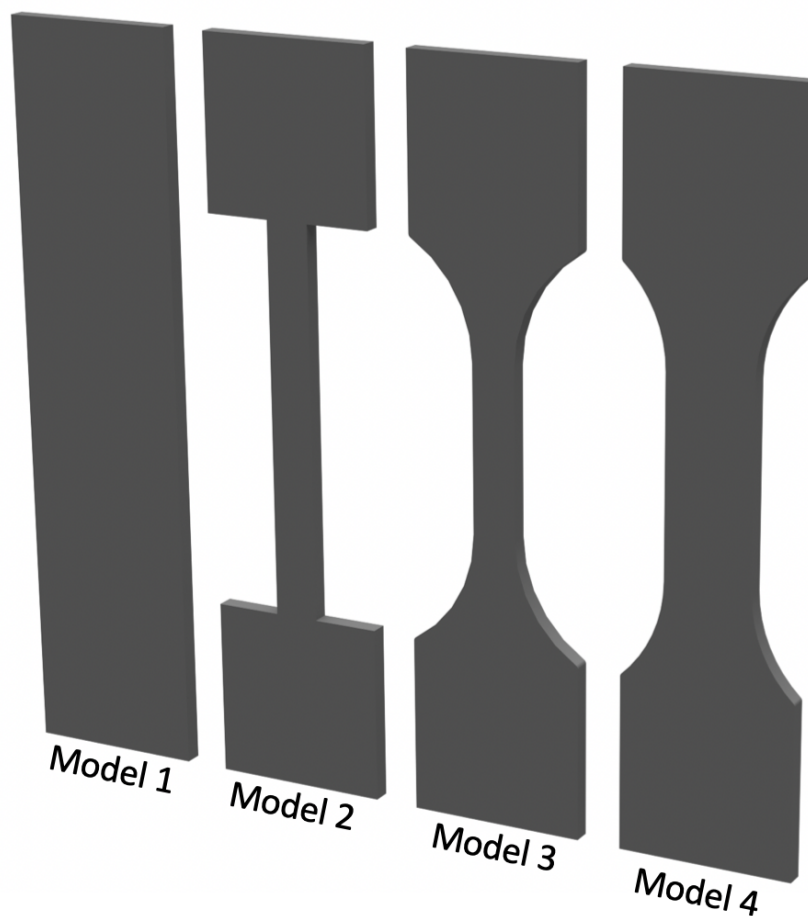


Figure 3.21: Model range

3.5.2 Mesh

Now that the geometry has been set, the mesh of the specimens can be made. The mesh that have been used on all of the specimens are the 3D Swept Mesh. This creates a mesh of 8- or 20-noded hexahedral elements on a solid. This is done by sweeping the mesh from a source face through the solid and creating the mesh. To make the bonding of the meshes nicer, the specimens have been divided up into smaller sections, visualised in Figure 3.22. For this thesis it was used the 8-noded hexahedral elements to perform the analysis. The base mesh of Model 4 is visualized in Figure 3.23.

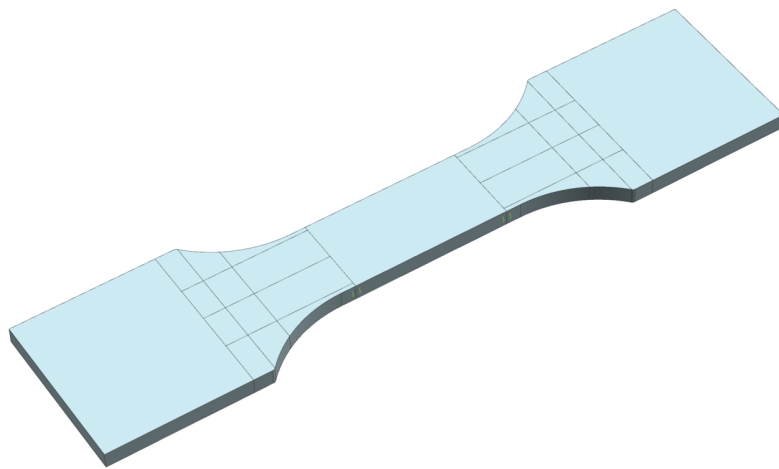


Figure 3.22: Split CAD model of Model 4

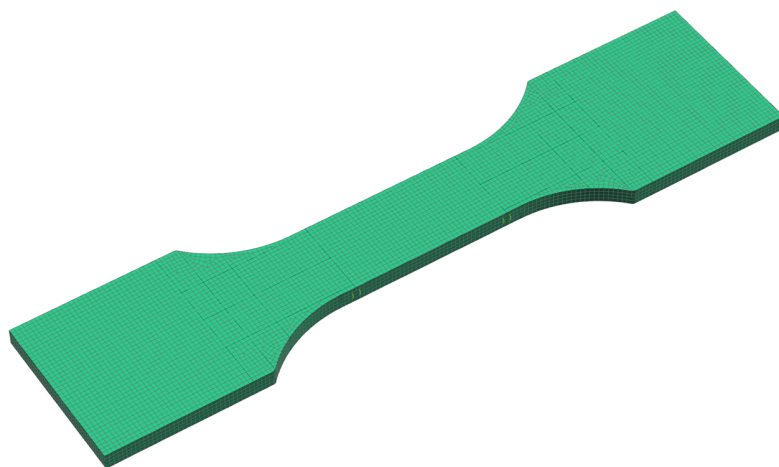


Figure 3.23: Mesh of Model 4

Mesh Convergence Study

When using any type of dimensional tool, to get the most accurate result the best thing to do, is doing a lot of tests. The mesh convergence study is used to find the optimal mesh element size for a given construction. This is used on the final models, and is nothing that is required in a early phase of a FEM analysis. Having a mesh with too large mesh element size may lead to inaccurate results, whereas too small mesh element size would be more accurate, but it would also lead to unnecessary use of time and computational power. It could also lead to the possibility of singularity in parts of the model, as explained in Section 2.3.

The word optimal is a good representation of this test because you want to find the mesh element size which is the best in terms of time and accuracy for your specific model. The models in this research is not big in any case, but they are required to be accurate. When doing a mesh convergence study it is required to follow a specific ratio. The element size in this study is reduced with $1/2$, for each step. The values that this study achieved is visualized in Figure 3.24. Ideally the curve would flatten out, and you would choose a suitable element size. Looking at Figure 3.24, it is clear that the deformation does not converge properly for this case. This means it is required to choose the element size another way. Based on experience and the size of the components, an element size of 1 mm was chosen.

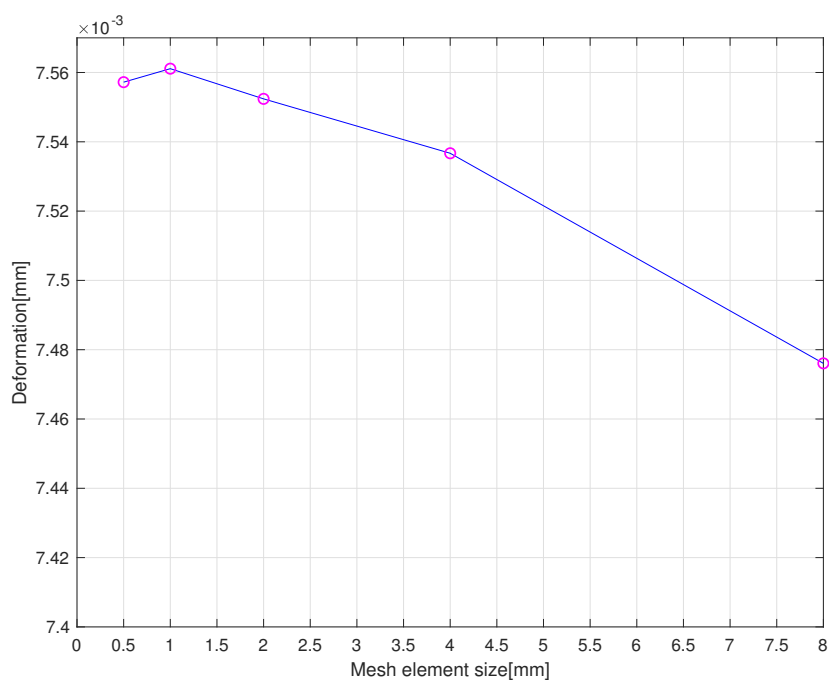


Figure 3.24: Mesh Convergence

Material

To perform the FEM analysis it is required to clarify the property of the mesh. As described earlier this FEM analysis basis itself on PLA's materials mechanical similarity in the linear region of the force - elongation curve as steel. This material is chosen due to it being well known and have the required material data in the FEM solver. The Young's modulus of steel in the Nastran solver in Siemens NX is 206 940 MPa.

3.5.3 Constraints

Constraining the individual models were done using user defined constraints. This was done to ensure that each of the models would be constrained in the same way, and that the setup was correct. Further on, the constraints and loads will be put at a specific direction, to simplify for the reader a reference frame is made, visualized in Figure 3.25.

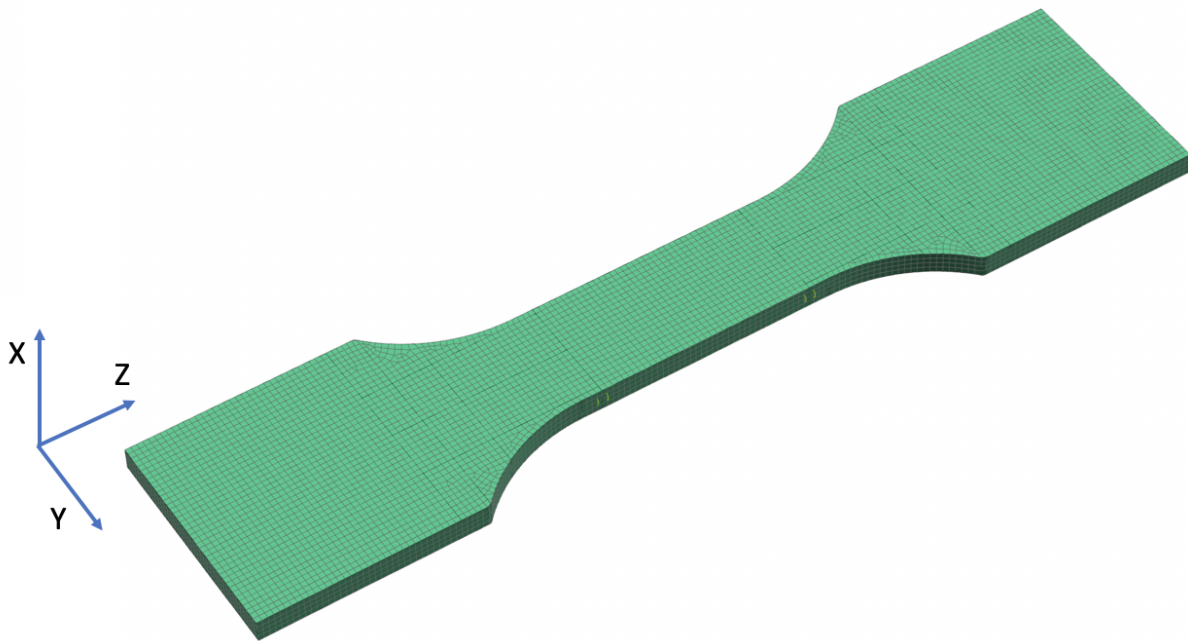


Figure 3.25: Coordinate system reference

The base surface of the models were fixed in Z - direction and free in all of other directions, visualized in Figure 3.26. To ensure that the model have the required wiggle room to deform and act similar to the experiments, the models is also required to be fixed in X and Y direction. This is done in the nodes of the mesh in the corner of the models, visualized in Figure 3.27. This prevents the model from shifting in these directions, but makes it possible for it to stretch and move in the longitudinal direction, also know as Z.

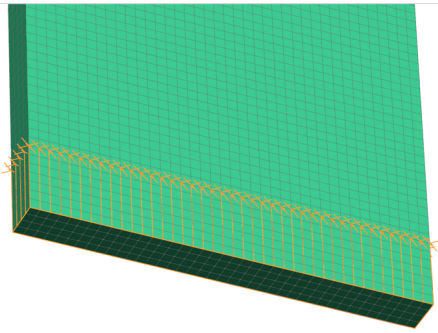


Figure 3.26: Surface Constraint

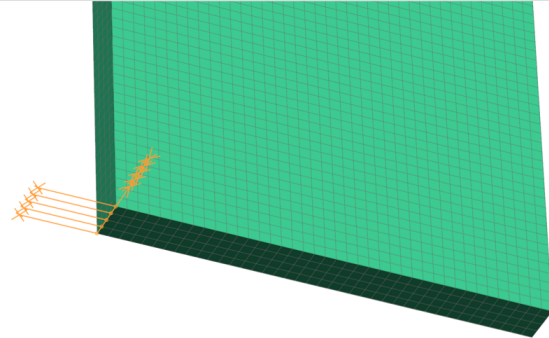


Figure 3.27: Node Constraint

3.5.4 Load

The load were distributed on the top plane of the models, visualized in Figure 3.28. The load for the tests were set at 1000 N in the longitudinal Z - direction and is called Force Load. This force will pull the model from the whole top surface with an combined force of 1000 N. A ready FEM model of Model 4 is visualized in Figure 3.29.

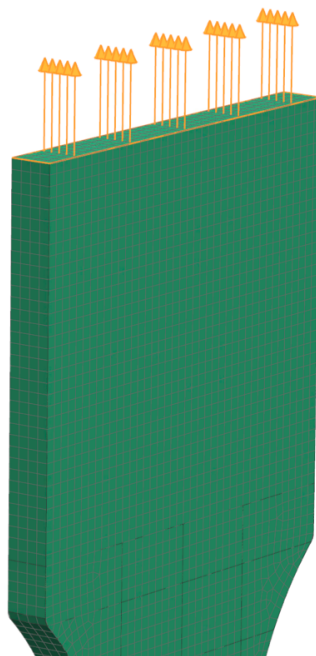


Figure 3.28: Applied Force

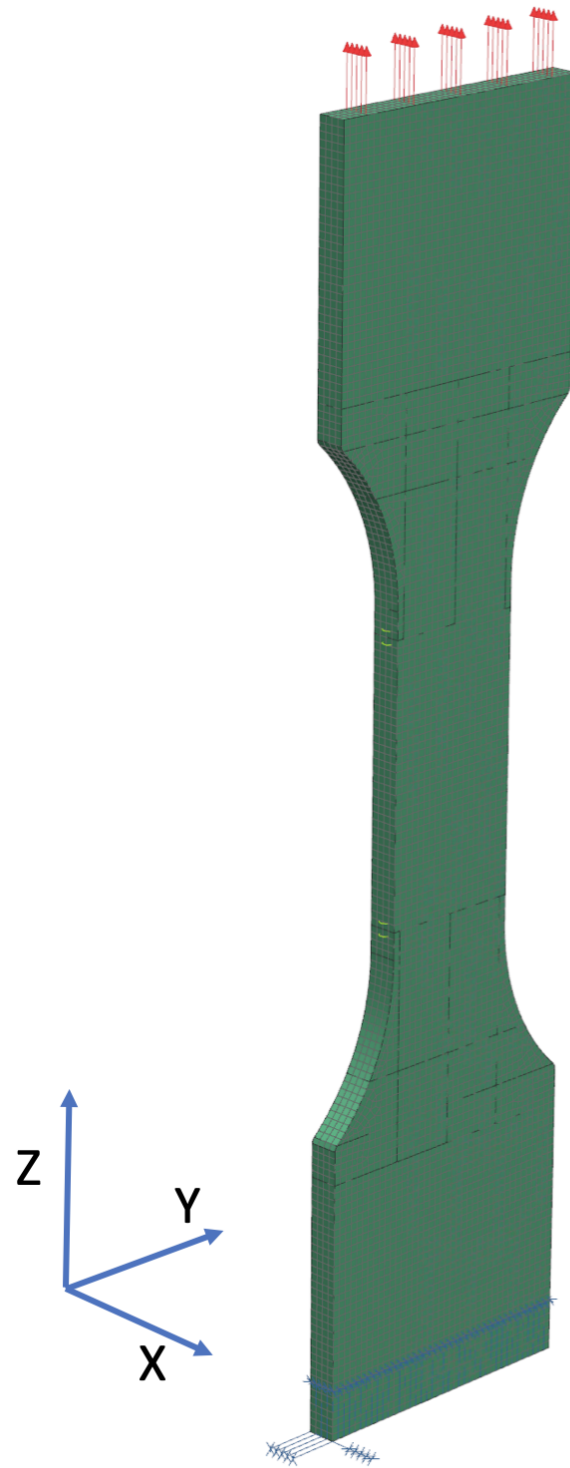


Figure 3.29: Model 4 FEM-ready

3.5.5 Deformation

After the mesh, material, constraints and force is applied the solver is ready to run. The structural analysis is done for the sole reason of finding a stiffness coefficient ratio between the geometries. Model 3 and 4 obviously experienced different deformations when the force were applied due to their different geometry. Model 1, which is used as the base model, can be defined in a different way, because of its geometry, apposed to Model 3 and 4. Stiffness is defined as to how much an object can withstand deformation when exerted to a load, and is dependent on the material and geometry. The geometries of Model 1, 3 and 4 are not the same, and will ultimately have different stiffness because of this, visualized in Figure 3.30.

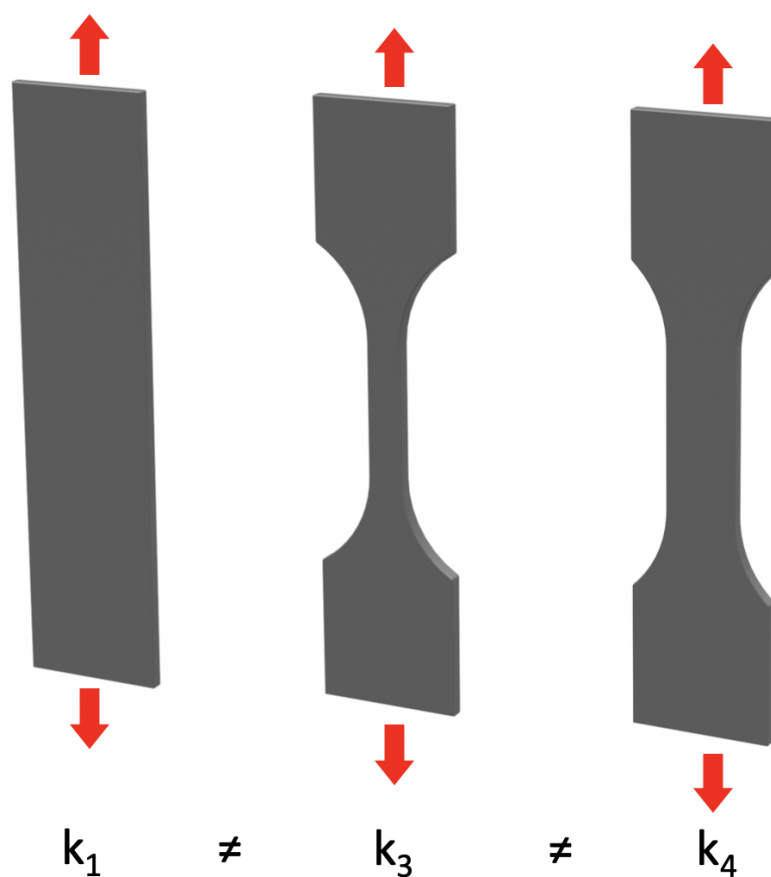


Figure 3.30: Stiffness k

Using the elasticity theory and the formulas from Section 2.3 it is possible to define a stiffness k for Model 1 based on its simple geometry. The Model 1 stiffness k_1 can be defined as equation 3.2. This is possible because of Model 1's solid and simple geometry. Whereas Model 3 and 4 stiffness, k_3 and k_4 , needs to be defined in another way using equation 3.3 and 3.4.

$$k_1 = \frac{E_{\text{FEMsteel}}A}{L} = \frac{206940 \text{ MPa} \cdot (40 \text{ mm} \cdot 4 \text{ mm})}{170 \text{ mm}} = 194767.06 \text{ N/mm} \quad (3.2)$$

$$k_3 = \frac{F}{\delta_{\text{FEM}}} = \frac{1000 \text{ N}}{0.0116004 \text{ mm}} = 86203.92 \text{ N/mm} \quad (3.3)$$

$$k_4 = \frac{F}{\delta_{\text{FEM}}} = \frac{1000 \text{ N}}{0.00755611 \text{ mm}} = 132343.23 \text{ N/mm} \quad (3.4)$$

Now that the stiffness k of the different geometries have been defined it is possible to derive a ratio between them which will be used on the values that have been acquired during the experimental tests. The stiffness coefficient ratio between the Model 1 and Model 3 is derived using equation 3.5, and the stiffness coefficient ratio between Model 1 and Model 4 is derived using equation 3.6.

$$\text{Ratio} = \frac{k_3}{k_1} = \frac{86203.92 \text{ N/mm}}{194767.06 \text{ N/mm}} = 0.4426 \approx 44\% \quad (3.5)$$

$$\text{Ratio} = \frac{k_4}{k_1} = \frac{132343.23 \text{ N/mm}}{194767.06 \text{ N/mm}} = 0.6795 \approx 68\% \quad (3.6)$$

This means in terms that according to the structural analysis and elasticity theory that the overall stiffness of Model 3 and 4 are 44% and 68% of the flat solid bar, Model 1. This stiffness coefficient ratio between the different geometries is used to identify the proper Young's modulus when they are applied to the experimental tests results and combined together.

Chapter 4

Results & Discussion

4.1 Experimental Tests Fracture Analysis

The experimental tests showed clear differences in how the different test specimens fractured. Almost all specimens showed a fracture in which was along the filament strings, independent of how they were printed. The ones that was printed at 0° and 90° showed more often than not a fracture which was much more stretched out apposed to the ones that was printed at 45° , visualized in Figure 4.1 and 4.2. This may be caused of the bonding between the outer wall of the printed specimen and the inner filament strings. These outer walls showed to be acting as a notch(kjerv) for the fracture itself. The diagrams of the different tests showed as well more of a ductile behavior on the specimens printed at 0° and 90° , apposed to the ones printed at 45° who acted more brittle.



Figure 4.1: Clean fracture along pattern



Figure 4.2: Diagonal fracture along pattern

4.2 Young's Modulus of PLA

4.2.1 Initial Young's Modulus from Experimental Tests

The stress-strain curves that the initial Young's modulus are derived from are visualized in Figure 4.3 - 4.8. They are divided into their respective geometry and print pattern to see how similar they are. From these plots it is also possible to see the difference and their individual behavior after the ultimate tensile stress to some extent. For simplicity and visualization purposes all of the plots of the stress-strain curves are set to the same scale. Due to it is most important what happens in the linear region before the ultimate tensile stress of the stress-strain curve, all of the plots are cut at 0.02 strain. As mentioned before, all of the individual tests with their respective results are available to see in Appendix A.1 and A.2.

As mentioned in Section 4.1, the ones that are printed at 45° shows more of a brittle behavior than the ones printed at 0° and 90°. These tend to break right after the ultimate tensile stress, whereas the ones printed at 0° and 90° are stretched much more before they break. Combining the initial Young's modulus that was found in the experiments and the stiffness coefficient ratio between the different models, makes it is possible to derive a proper Young's modulus that takes different geometries into account. In Figure 4.9, the initial Young's modulus from the experimental tests are visualized.

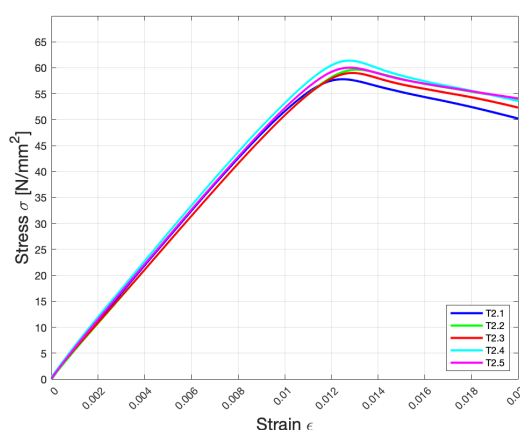


Figure 4.3: Geometry 1 - Printed at 0°

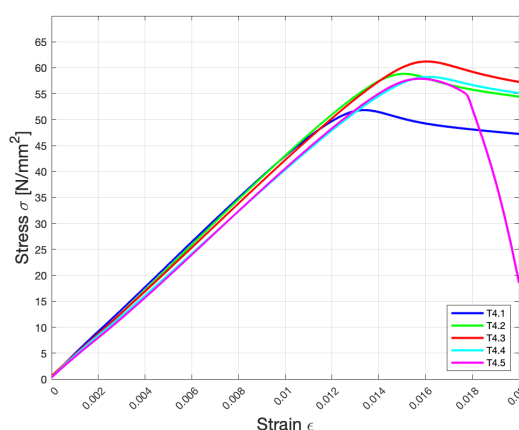


Figure 4.4: Geometry 2 - Printed at 0°

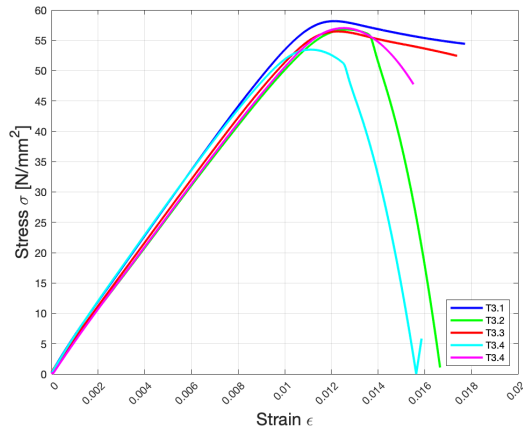


Figure 4.5: Geometry 1 - Printed at 45°

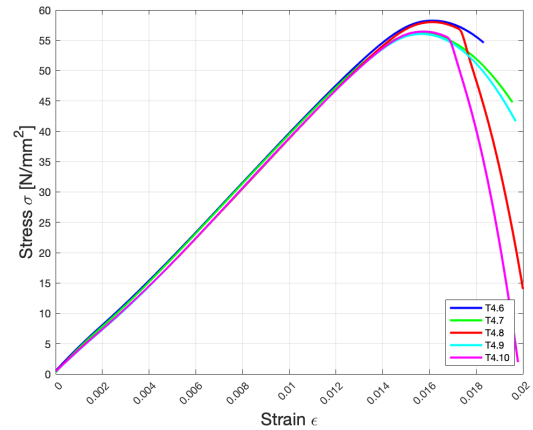


Figure 4.6: Geometry 2 - Printed at 45°

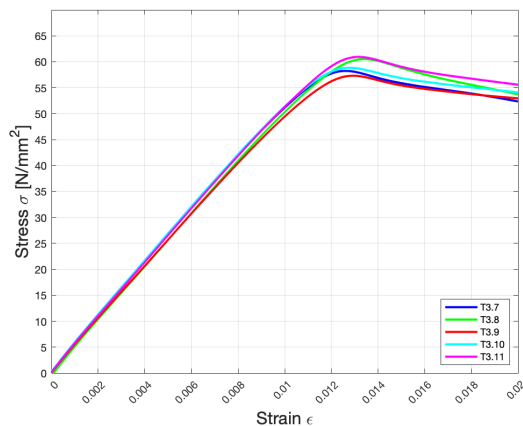


Figure 4.7: Geometry 1 - Printed at 90°

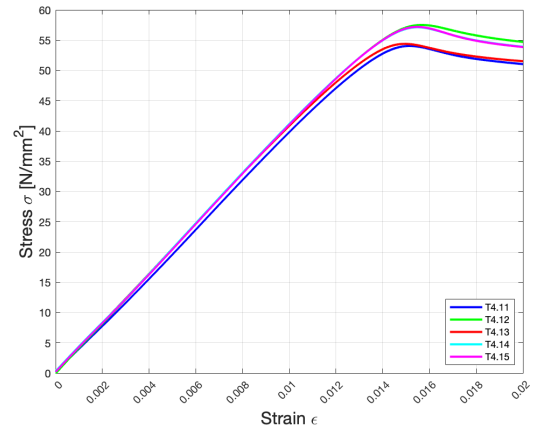


Figure 4.8: Geometry 2 - Printed at 90°

The results in Figure 4.9 have not taken the geometry into account and are consequently giving too high values for the Young's modulus of PLA. It is clear from Figure 4.9 that the specimens made according to Geometry 1 from Section 3.2.1 are the ones that give initially the highest Young's modulus, but also the ones that are most fluctuating. The maximum recorded Young's modulus with Geometry 1 was 5391 MPa, and the lowest one was 5002 MPa. The test specimens made according to Geometry 2 from Section 3.2.1, is sitting a bit lower with a maximum Young modulus of 4282 MPa and the lowest one at 3999 MPa. The different test specimens are described with colored squares.

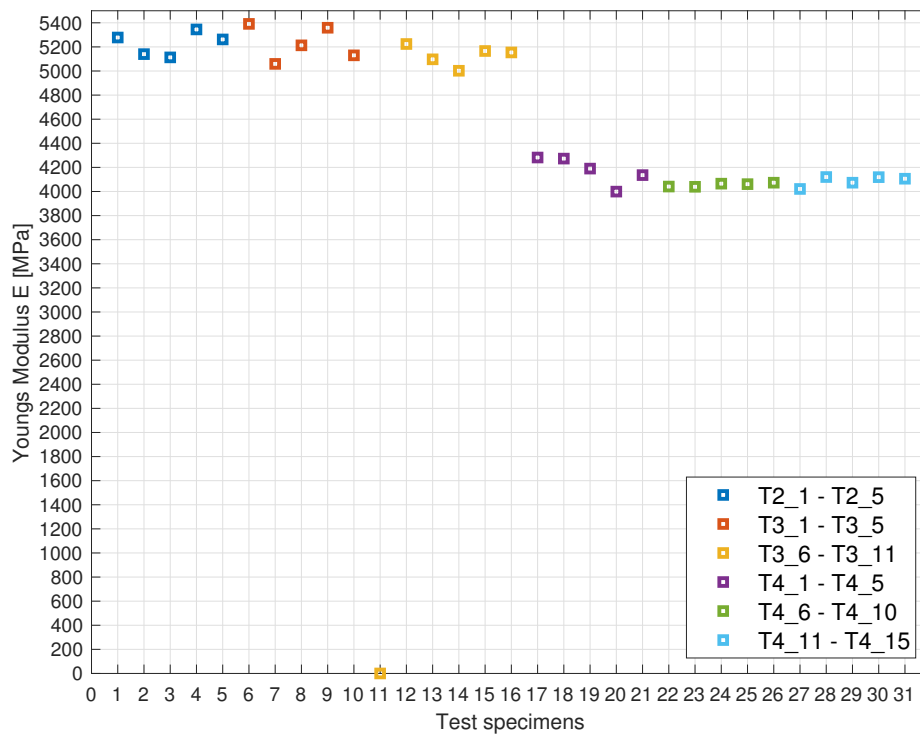


Figure 4.9: Initial Young's Modulus

- Specimen *T3.6* is added to show that through all of the experimental test, there were only one test was not able to provide results that could be further analysed, which gives an overall fail ratio of 3.23%.

4.2.2 Young's Modulus from Experimental Tests with Stiffness Ratio

Section 4.2.1 is added to see how the results could have been without taking the stiffness coefficient ratio into account when only looking at Figure 4.9 obviously. The proper Young's modulus can be derived using equation 4.1. For the ones that have a cross section area of 40 mm^2 in the middle, also known as Geometry 1 from Section 3.2.1, the Young's modulus is derived using equation 4.2. For the ones that have a cross section area of 80 mm^2 , known as Geometry 2 from Section 3.2.1, the Young's modulus is derived using equation 4.3.

This is done to all of the 30 tests that have been performed, and all of them are visualized in Figure 4.10. Not much has changed in regards to the deviation between the two geometries apposed to Figure 4.9, but the overall magnitude of the values has been decreased, and Geometry 2 is now displaying the highest Young's modulus as a consequence of the addition of the stiffness ratio. After the ratio is added the maximum recorded Young's modulus for Geometry 1 is 2386 MPa and the lowest one is 2214 MPa. For Geometry 2, the maximum Young's modulus is 2910 MPa and the lowest is 2717 MPa.

$$E = \frac{\sigma}{\epsilon} \cdot Ratio \quad (4.1)$$

$$E = \frac{\sigma}{\epsilon} \cdot \left(\frac{k3}{k1} \right) \quad (4.2)$$

$$E = \frac{\sigma}{\epsilon} \cdot \left(\frac{k4}{k1} \right) \quad (4.3)$$

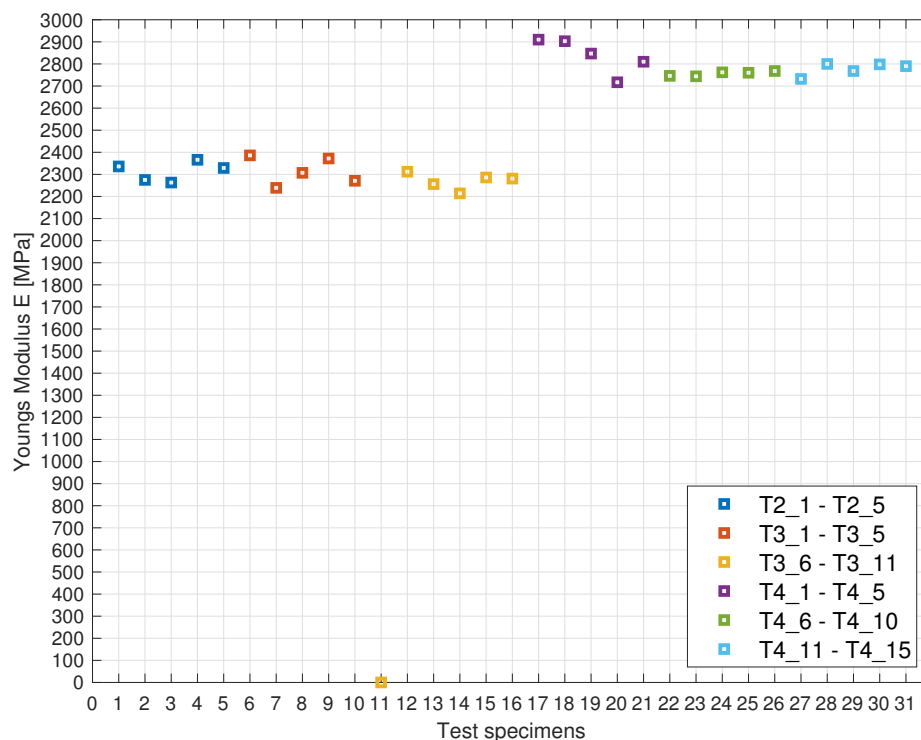


Figure 4.10: Young's Modulus

The values from the tests have been put into box plots in categories in which they were manufactured, visualized in Figure 4.11. These box plots give a better visual representation of the results, where it is more clear which of the manufacturing processes that are most consistent. The bottom and top edges of the box itself indicate the 25th and 75th percentiles of the values. The T-hat shows the range of the max- and minimum of what is recorded, and the red line shows the median. The black circle represents the mean value of the recorded values. From these box plots it is possible to see how the different orientations are performing overall, and to what extent they are consistent or not. The specimens printed at 0° with a Geometry 2 are most volatile of them all, whereas the one printed at 45° with Geometry 2 is the most consistent of them all.

The ones printed at 0° and 90° were more inconsistent, but not to a substantial amount. The biggest deviation between the biggest and lowest value is found in the Geometry 2 printed at 0°. This ranged from 2910 MPa to 2717 MPa, which gives an uncertainty range of 193 MPa.

Whereas;

Geometry 1 with 0° have a range of: 2366 MPa - 2263 MPa = 103 MPa

Geometry 1 with 45° have a range of: 2386 MPa - 2239 MPa = 147 MPa

Geometry 1 with 90° have a range of: 2312 MPa - 2214 MPa = 98 MPa

Geometry 2 with 45° have a range of: 2768 MPa - 2744 MPa = 24 MPa

Geometry 2 with 90° have a range of: 2800 MPa - 2732 MPa = 68 MPa

However, when looking at the mean value in between the two geometries they show pretty similar results independent of their print pattern. The mean Young's modulus of Geometry 1 is 2314 MPa, 2315 MPa and 2270 MPa for the 0°, 45° and 90° pattern. On Geometry 2 the mean value is 2837 MPa, 2756 MPa, and 2778 MPa in the same order. This shows that even though there is some fluctuation, the mean values within the individual geometries are consistent.

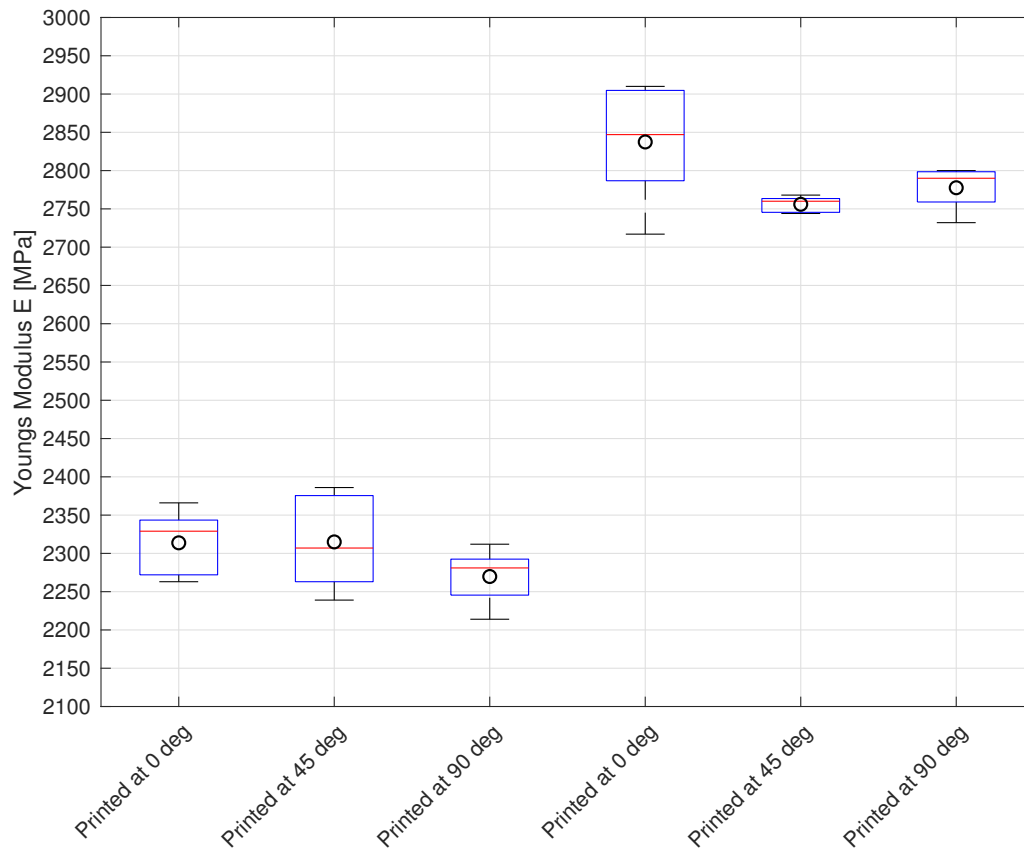


Figure 4.11: Separate Box Plot of Young's Modulus

Taking a step back, trying to find the root cause of the behavior is critical. As the cross section of the test specimen increase, it causes the Young's modulus to increase as well. Looking back to at Section 3.3 is interesting. As the test specimens are printed they are bound together by an outer wall that goes all around the specimen, visualized in Figure 4.12. In these pictures, the inner filament strings, outer wall, and the extruder head are visible. These walls are surrounding the test specimens, in both Geometry 1 and 2, they are 0.4 mm thick. In addition to work as a notch(kjerv), as mentioned earlier, they are not following the rest of the models' pattern when it is printed. In Figure 4.12 the path of the printer is visualized to state this more clearly. Here it is more clear that the inner material and the outer wall are separated in a way, because of the way it is printed. The inner material, independent of its pattern, is strong due to its volume and mass, compared to the outer wall that is very thin and weak. This can be directly applied to the data shown in Figure 4.11. As lower the ratio between the inner material and outer wall, the Young's modulus will be affected as a consequence.

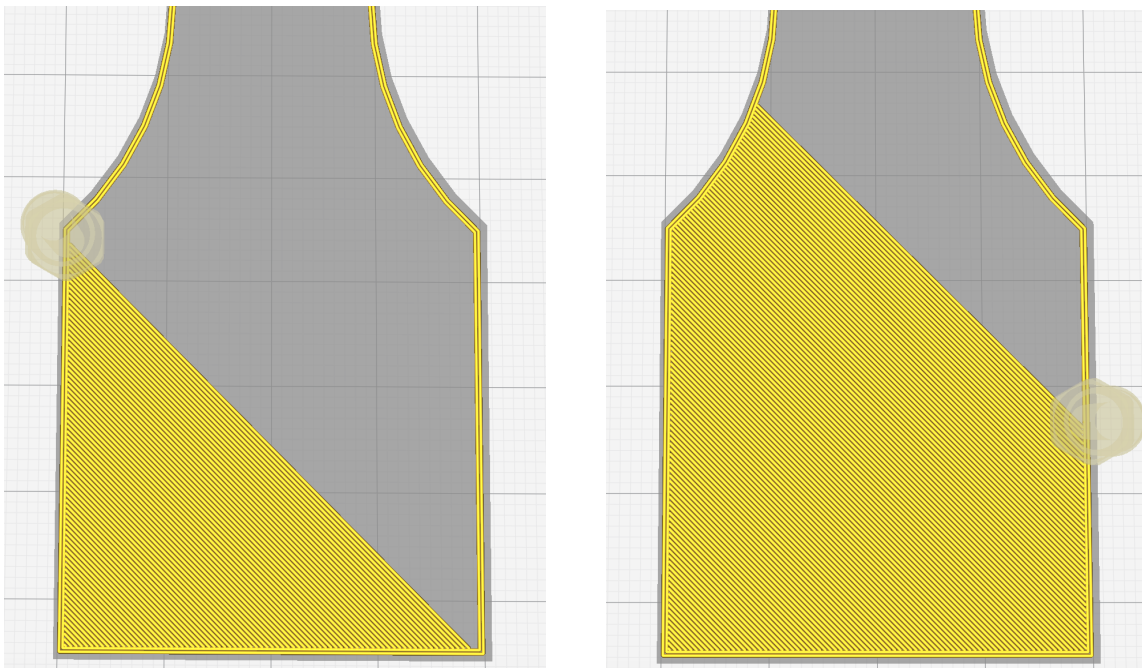


Figure 4.12: Manufacturing of test specimens

With the results in mind, it is interesting and critical to compare them to other sources. This is done to identify if there are any similarities or irregularities between this research results from multiple different sources of which have done other tests on PLA. These independent sources have used traditional ISO and ASTM standards to test the material. Specifically, the ISO 527- and the ASTM D638 standard. The majority of them have gotten Young's modulus of PLA that is on par with the Young's modulus found in this master thesis.

The independent sources are Ultimaker [29], Innofil [30], SD3D [31] and Polymaker [32]. Their stated Young's modulus from their different test methods is visualized in Table 4.1. As a note, the Innofil have stated an Young's modulus within a range of 2852+/-88 MPa, and Polymaker [32] is stating a Young's modulus within a range of 1879+/-109 MPa. Whereas the other two have stated a fixed value. These are related works to some extent as they provide an Young's modulus, but as they are not specifically using a non-standard method and are using ISO and ASTM - standards they were not necessary to be elaborate more in the research section.

Table 4.1: Independent sources

Sources	Test Method	Young's modulus [MPa]
Ultimater	ISO 527	2346
Innofil	ISO 527	2852
Polymaker	ASTM D638	1879
SD3D	ASTM D638	2300

It is clear that the Young's modulus of PLA that is found using the method in this research, is at least in the range of what other sources are providing. There are many different things when working with 3D printed objects that may affect the end results. All ranging from the manufacturing process of the material itself, 3D printer settings, test rig settings and quality of the equipment to name a few. This makes the comparison between the sources tricky, but it gives an indication of the test procedures accuracy and its credibility.

Chapter 5

Conclusion & Future Work

5.1 Conclusion

The main objective of this thesis was to look into the possibility of developing a test procedure for testing incoming 3D printed material, and validating them to other independent sources. Throughout the research, there are printed 31 specimens, which took a total amount of 258 hours. There was a total of 30 approved specimens that were tested, and then analyzed and validated.

The previous chapters have shown how the test procedure is developed, what it is based upon, and what kind of results it gave. The results have then been compared to other independent sources to validate the accuracy of the test procedure.

The research shows that measuring the strength of 3D printed parts by using a traditional tensile strength test is possible. In addition to finding a stiffness coefficient ratio using FEM analysis, it is possible to experimentally and numerically assess the strength properties of 3D printed PLA. The research identifies that the geometry of the specimens themselves have an effect on the Young's modulus. It shows that when working with PLA, the overall strength is dependent on the relationship between the inner and its outer core.

There are presented four independent sources that have tested PLA using the traditional ISO/ASTM standards, and they are getting a relatively broad range of differences between themselves. In addition to this, having the research results from this thesis of the material property of PLA in mind illustrates that the material is not an easy material to perform tests on. However, there are similarities between the results. And it is also worth noting that the PLA is likely to have come from different manufacturers, and they may have different manufacturing processes that could have a major influence on the initial material property.

Given the results found in this research are in the near region of the ones presented, that are tested using ISO and ASTM standards, give an indication on this test procedure overall feasibility. The results are consistent, but more extensive amount of experimental tests would even further validate the method.

Given the results presented, the test procedure developed in this master thesis showed potential as a method of testing the Young's modulus of incoming 3D printed materials.

5.2 Future Work

Taking the research a step further there are more things that can be done to develop this procedure further, and also the general knowledge regarding 3D printing materials.

- **Molded Test specimen:** It would be highly relevant to check a molded test specimen, created in the same way as the ones tested in this research, would perform in another way.
- **Different Geometries:** Test the method using multiple different geometries. Change the slim cross section area into different shapes and see if this has an effect(circular, hexagonal, triangle).
- **Test Different Materials:** Test multiple different materials that are 3D printed and also other standard materials to see if the procedure is still functioning.
- **Temperature:** Look at the effect the temperature has on these types of 3D printed materials, and to within what range the material is still steady.
- **Wet Substances** Look at the effect of water exposure over a period of time.
- **Usability:** Applications in which PLA can be suited to be used, other than early phase prototypes.

Bibliography

- [1] Veryst Engineering. *Anisotropy of 3D-Printed polymers*. URL: <https://www.veryst.com/project/Anisotropy-of-3D-Printed-Polymers>. (accessed: 11.03.2019).
- [2] 3Dhubs. *3D Printing Trends Q1 2019*. URL: https://downloads.3dhubs.com/3D_Printing_Trends_Q1_2019.pdf?utm_campaign=Gated%5C%20Content%5C%20Downloads&utm_source=hs_automation&utm_medium=email&utm_content=64642056&hsenc=p2ANqtz-_e41anMffz8Jx4midSbF1N0qbKz379mwke1AiMXGz9ul3B19V9_qIQFiP0YbZyjSOP64YGDNaWJjpKNDwaiPD8HzaJwNh49RMVThPsEoW36VHkcxY&hsmi=64642056. (accessed: 24.05.2019).
- [3] Formlabs. *Validating Isotropy in SLA 3D Printing*. URL: <https://formlabs.com/blog/isotropy-in-SLA-3D-printing/>. (accessed: 24.05.2019).
- [4] Hannah Bensoussan. *The History of 3D Printing: 3D Printing Technologies from the 80s to Today*. URL: <https://www.sculpteo.com/blog/2016/12/14/the-history-of-3d-printing-3d-printing-technologies-from-the-80s-to-today>. (accessed: 08.10.2018).
- [5] Garret Redwood Schoffer. *The 3D Printing Handbook*. Amsterdam, The Netherlands: Coers & Roest, 2017. ISBN: 978-90-827485-0-5.
- [6] Alkaios Bournias Varotsis. *Introduction to FDM 3D printing*. URL: <https://www.3dhubs.com/knowledge-base/introduction-fdm-3d-printing>. (accessed: 06.03.2019).
- [7] Alkaios Bournias Varotsis. *Introduction to SLA 3D Printing*. URL: <https://www.3dhubs.com/knowledge-base/introduction-sla-3d-printing>. (accessed: 08.10.2018).
- [8] Alkaios Bournias Varotsis. *Introduction to SLS 3D printing*. URL: <https://www.3dhubs.com/knowledge-base/introduction-sls-3d-printing>. (accessed: 06.03.2019).
- [9] Hewlett-Packard. *Kraftige HP Voxel starter 3D-skriverrevolusjonen*. URL: <https://www8.hp.com/no/no/printers/3d-printers.html>. (accessed: 05.11.2018).
- [10] Hewlett-Packard. *HP Jet Fusion 3D 4200, 4210 Printing Solution User Guide*. URL: <http://h10032.www1.hp.com/ctg/Manual/c05358991>. (accessed: 25.05.2019).

- [11] GE. *What is Additive Manufacturing?* URL: <https://www.ge.com/additive/additive-manufacturing>. (accessed: 20.11.2018).
- [12] 3DHubs. *Additive Manufacturing Technologies: An Overview*. URL: <https://www.3dhubs.com/knowledge-base/additive-manufacturing-technologies-overview>. (accessed: 25.05.2019).
- [13] Simplify3D. *PLA overview*. URL: <https://www.simplify3d.com/support/materials-guide/pla/>. (accessed: 25.11.2018).
- [14] RS Pro. *RS PRO 2.85mm White PLA 3D Printer Filament, 1kg*. URL: <http://rcduniya.com/product/wanhao-white-abs-175-mm-1-kg-filament-for-3d-printer-premium-quality>. (accessed: 25.05.2019).
- [15] 3DHubs. *Selecting the optimal shell and infill parameters for FDM 3D Printing*. URL: <https://www.3dhubs.com/knowledge-base/selecting-optimal-shell-and-infill-parameters-fdm-3d-printing>. (accessed: 26.05.2019).
- [16] ISO. *Additive manufacturing - General principles - Terminology*. URL: <https://www.iso.org/standard/69669.html>. (accessed: 20.11.2018).
- [17] James M. Gere. *Mechanics of Materials*. 6th ed. Belmont, Calif: Brooks/Cole, 2004. ISBN: 0534417930.
- [18] Britannica. *Hooke's Law*. URL: <https://www.britannica.com/science/Hookes-law/media/271336/153434>. (accessed: 06.05.2019).
- [19] Simscale. *What is FEA | Finite Element Analysis?* URL: <https://www.simscale.com/docs/content/simwiki/fea/whatisfea.html>. (accessed: 26.11.2018).
- [20] Siemens. *Finite Element Analysis (FEA)*. URL: <https://www.plm.automation.siemens.com/global/en/our-story/glossary/finite-element-analysis-fea/13173>. (accessed: 23.11.2018).
- [21] Walter Frei. *Parameterizing the Dimensions of Imported CAD Files*. URL: <https://www.comsol.com/blogs/parameterizing-dimensions-imported-cad-files/>. (accessed: 27.04.2019).
- [22] Steven Hale. *Why Worry About Sharp Corners and Point Loads?* URL: <https://caeai.com/blog/why-worry-about-sharp-corners-and-point-loads>. (accessed: 26.11.2018).
- [23] SOLIDWORKS Tech Blog. *What is a stress singularity in SOLIDWORKS Simulation?* URL: <https://blogs.solidworks.com/tech/2018/07/what-is-a-stress-singularity-in-solidworks-simulation.html>. (accessed: 27.04.2019).
- [24] Sung-Hoon Ahn Michael Montero Dan Odell Shad Roundy and Paul K. Wright. "Anisotropic material properties of fused deposition modeling ABS". In: *Rapid Prototyping Journal* 8.4 (Dec. 2002). An optional note, pp. 248–257.

- [25] Kjetil Vange. “Validation of material model for polypropylene (PP)”. MA thesis. Trondheim: Norwegian University of Science and Technology, June 2012.
- [26] Dibya Chakravorty. *STL File Format (3D Printing) – Simply Explained*. URL: <https://all3dp.com/what-is-stl-file-format-extension-3d-printing/>. (accessed: 07.05.2019).
- [27] Ultimaker. *Ultimaker 2+*. URL: <https://ultimaker.com/en/products/ultimaker-2-plus>. (accessed: 08.05.2019).
- [28] GA Precision. *Extensometer*. URL: <https://www.gaprec.com/products/metal-testing-equipment/extensometer/>. (accessed: 21.05.2019).
- [29] Ultimaker. *Technical Data Sheet PLA*. URL: <https://ultimaker.com/download/74599/UM180821%5C%20TDS%5C%20PLA%5C%20RB%5C%20V10.pdf>. (accessed: 26.05.2019).
- [30] Innofil3D. *Technical Data Sheet PLA*. URL: <https://www.innofil3d.com/wp-content/uploads/2016/05/TDS-Innofil3D-PLA-160608.pdf>. (accessed: 20.11.2018).
- [31] SD3D. *Technical Data Sheet PLA*. URL: https://www.sd3d.com/wp-content/uploads/2017/06/MaterialTDS-PLA_01.pdf. (accessed: 27.05.2019).
- [32] Polymaker. *PolyMax™ PLA Technical Data Sheet*. URL: <https://eu.polymaker.com/product/polymax-pla/>. (accessed: 08.10.2018).

Appendix A

Test Specimens

This section consist of pictures and data from all the test specimens that have been tested in this thesis. This section will first show a overview of all the test specimens that have been tested, and then individual with its data.

A.1 Experimental Test 1 - Comparison Overview

This section consist of pictures and data from Experimental Test 1, which consist of sixteen test specimens printed at different orientation with identical measurements, visualized in Figure A.1 - A.3.

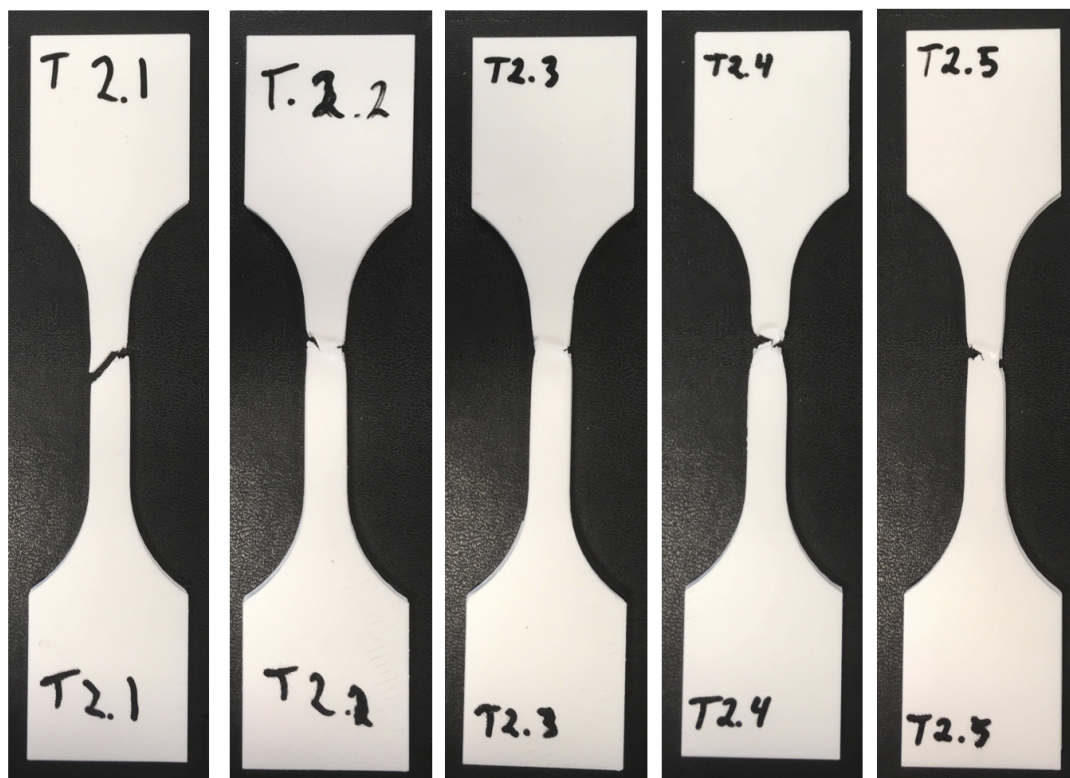


Figure A.1: Test 2.1 - 2.5

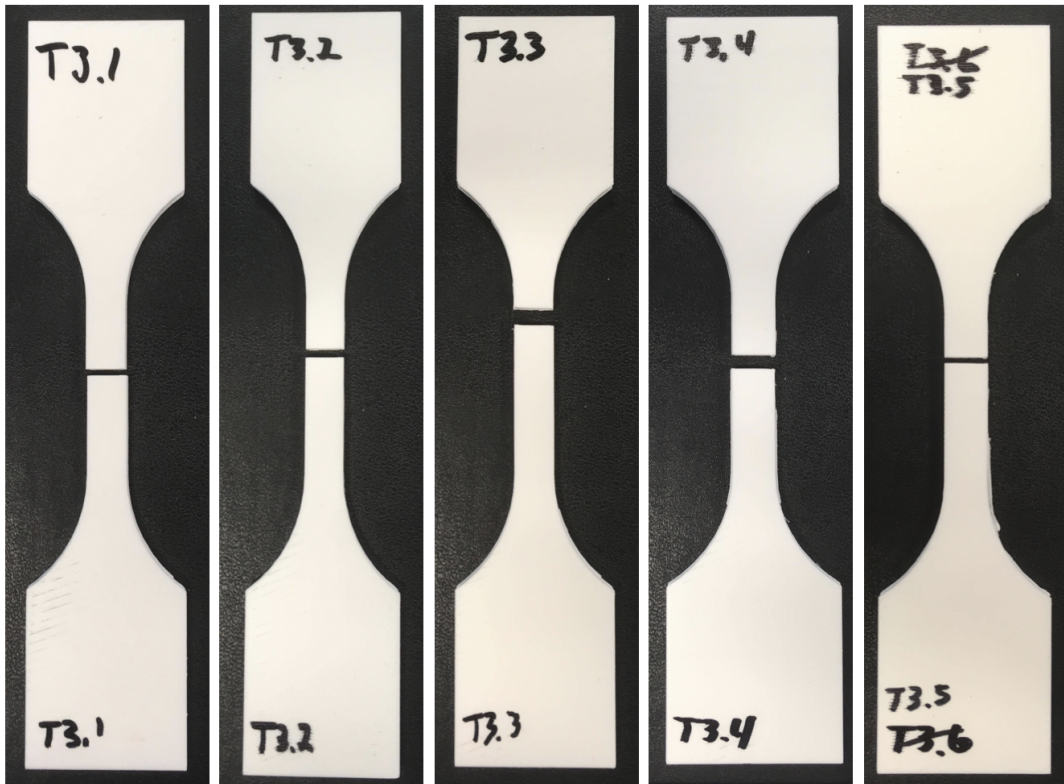


Figure A.2: Test 3.1 - 3.5

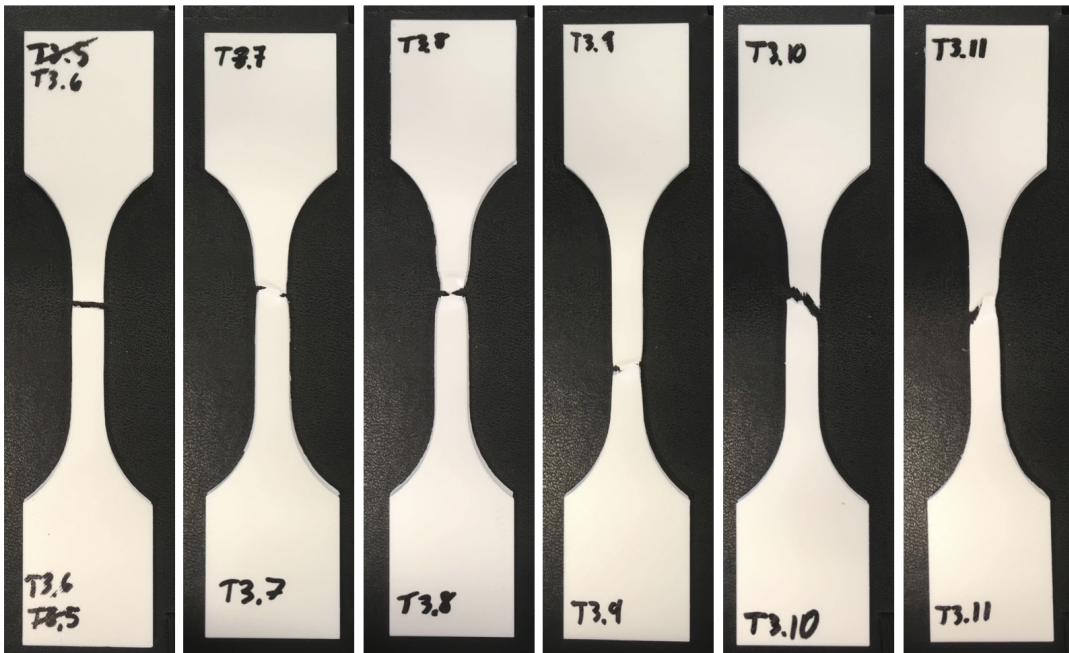


Figure A.3: Test 3.6 - 3.11

A.1.1 Test 2.1 - Test 2.5, Printed at 0°

Test 2.1



Figure A.4:
Test 2.1 Specimen

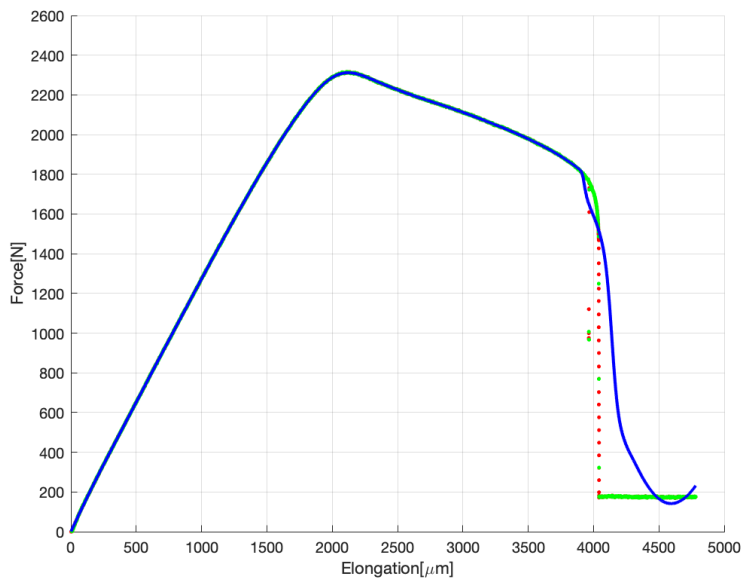


Figure A.5: Test 2.1 Force - Elongation curve

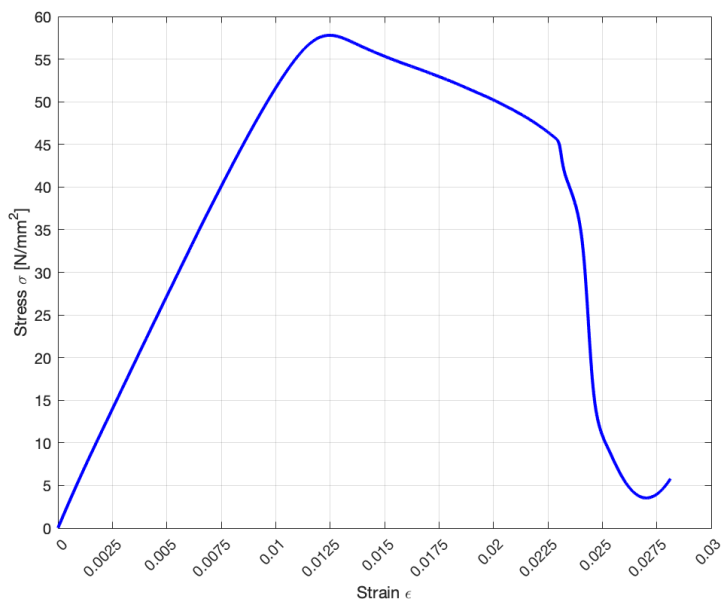


Figure A.6: Test 2.1 Stress - Strain curve

Print Duration [Hours]	Ultimate Tensile Stress [MPa]	Young's Modulus [MPa]	Cross Section Area [mm ²]	Print Orientation [°]
7	57.79	2336	40	0

Test 2.2



Figure A.7:
Test 2.2 Specimen

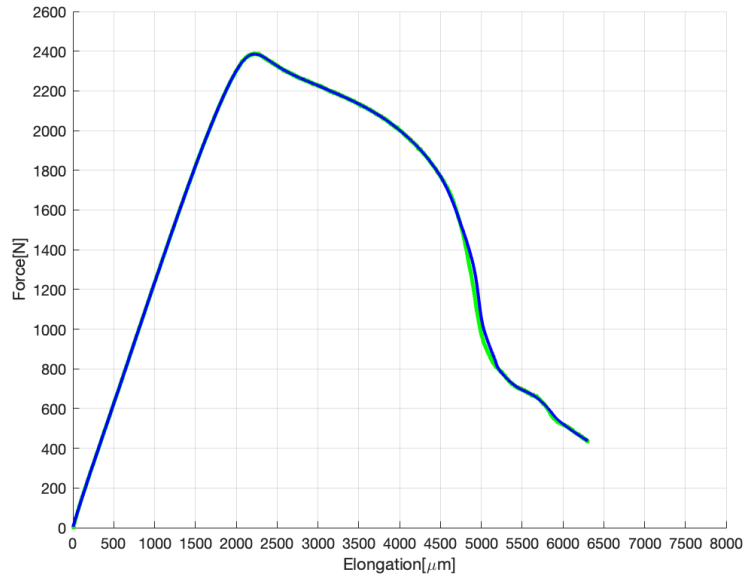


Figure A.8: Test 2.2 Force - Elongation curve

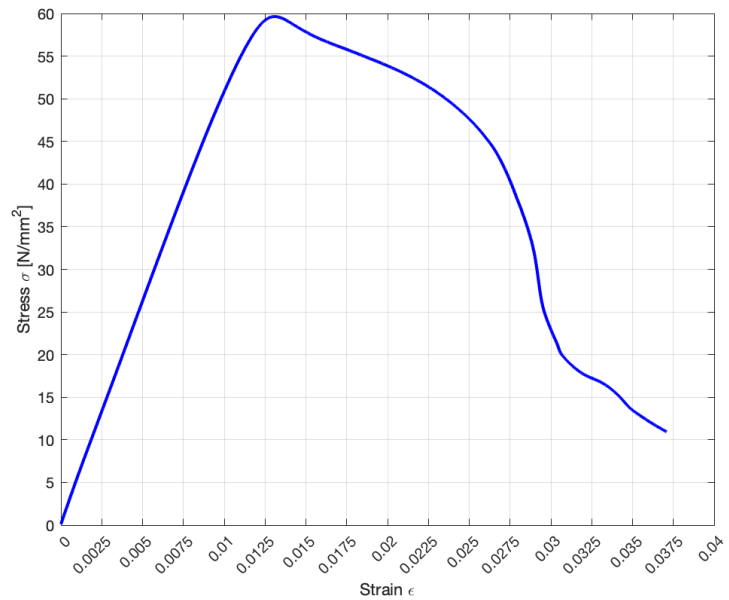


Figure A.9: Test 2.2 Stress - Strain curve

Print Duration [Hours]	Ultimate Tensile Stress [MPa]	Young's Modulus [MPa]	Cross Section Area [mm ²]	Print Orientation [°]
7	59.64	2275	40	0

Test 2.3



Figure A.10:
Test 2.3 Specimen

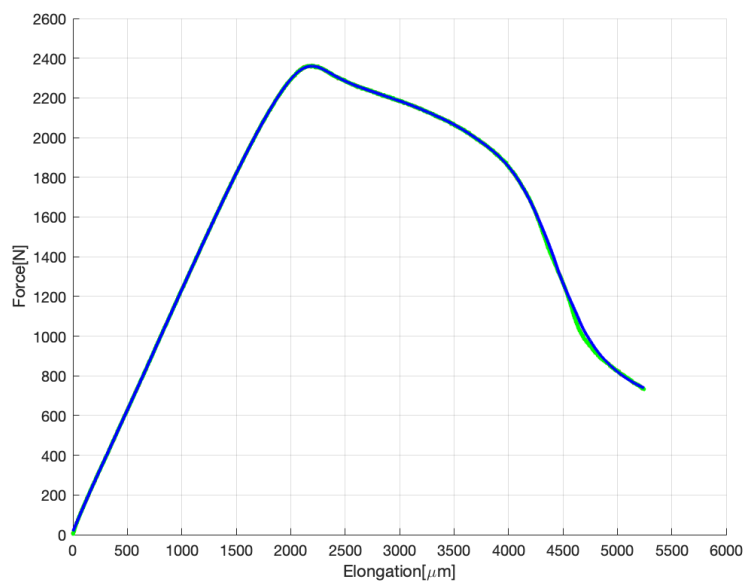


Figure A.11: Test 2.3 Force - Elongation curve

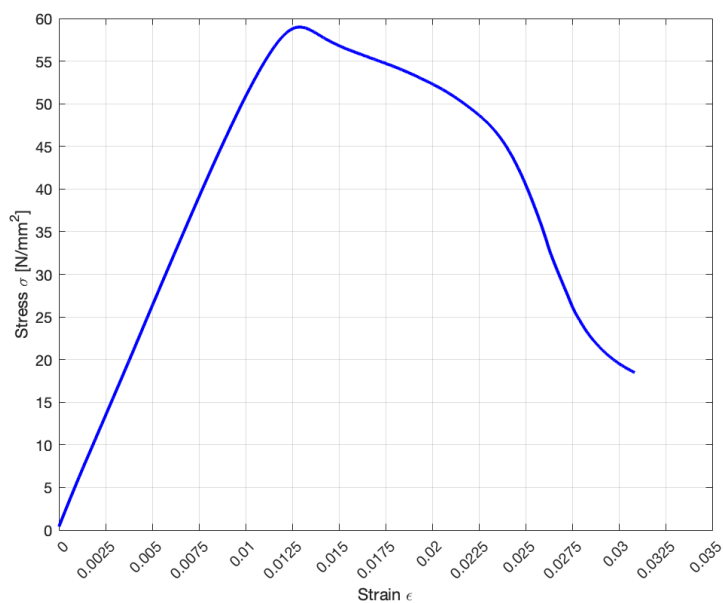


Figure A.12: Test 2.3 Stress - Strain curve

Print Duration [Hours]	Ultimate Tensile Stress [MPa]	Young's Modulus [MPa]	Cross Section Area [mm ²]	Print Orientation [°]
7	58.99	2263	40	0

Test 2.4



Figure A.13:
Test 2.4 Specimen

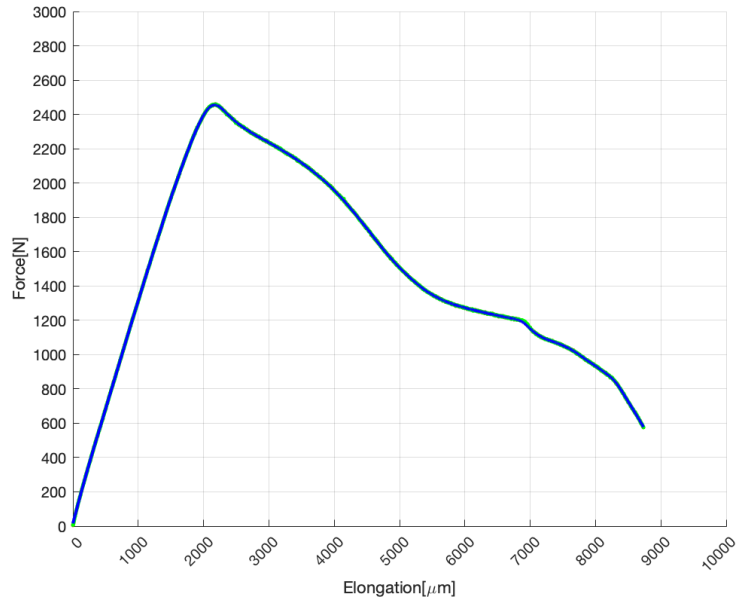


Figure A.14: Test 2.4 Force - Elongation curve

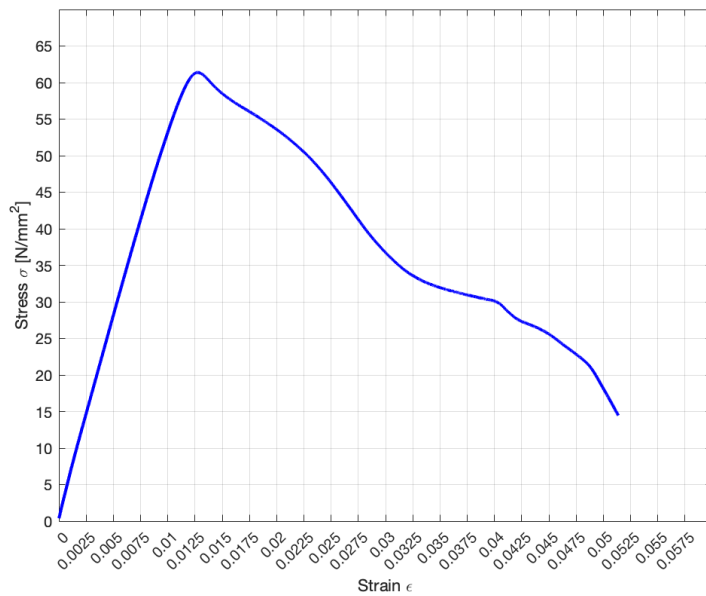


Figure A.15: Test 2.4 Stress - Strain curve

Print Duration [Hours]	Ultimate Tensile Stress [MPa]	Young's Modulus [MPa]	Cross Section Area [mm ²]	Print Orientation [°]
7	61.38	2366	40	0

Test 2.5



Figure A.16:
Test 2.5 Specimen

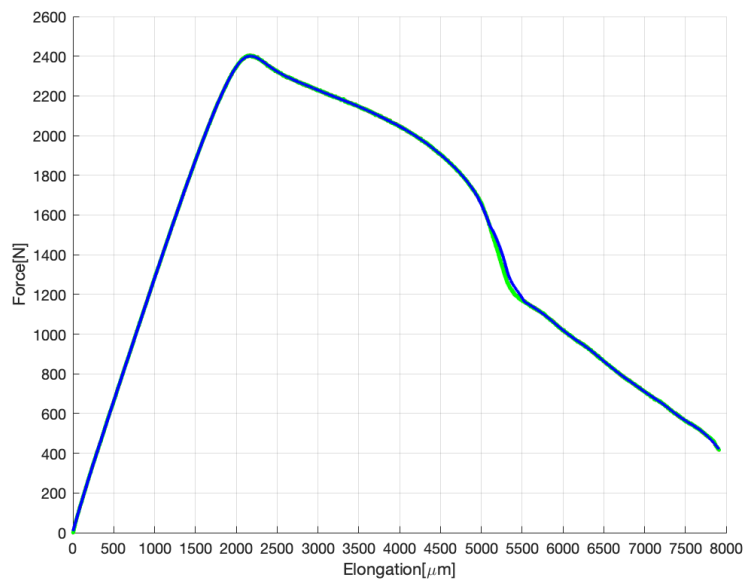


Figure A.17: Test 2.5 Force - Elongation curve

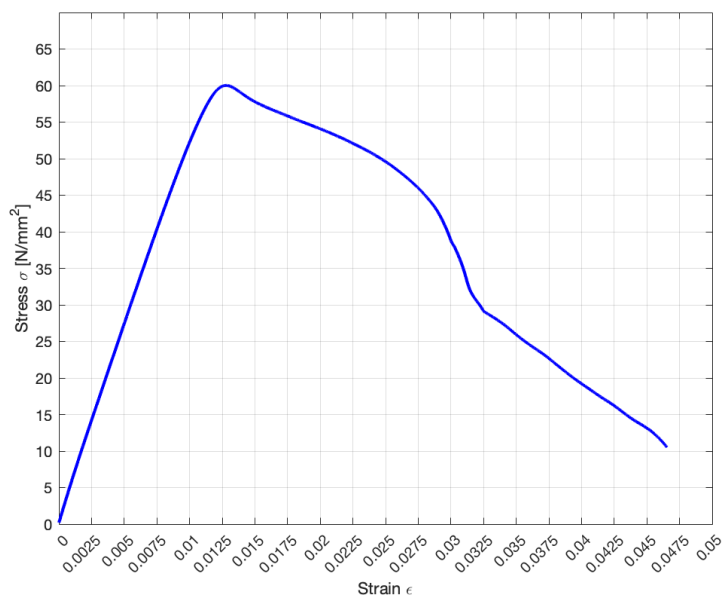


Figure A.18: Test 2.5 Stress - Strain curve

Print Duration [Hours]	Ultimate Tensile Stress [MPa]	Young's Modulus [MPa]	Cross Section Area [mm ²]	Print Orientation [°]
7	60.02	2329	40	0

A.1.2 Test 3.1 - Test 3.5, Printed at 45°

Test 3.1

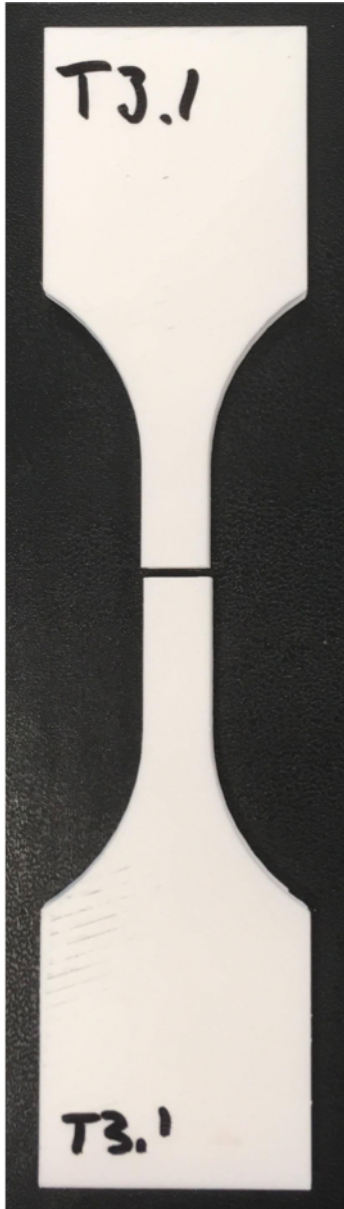


Figure A.19:
Test 3.1 Specimen

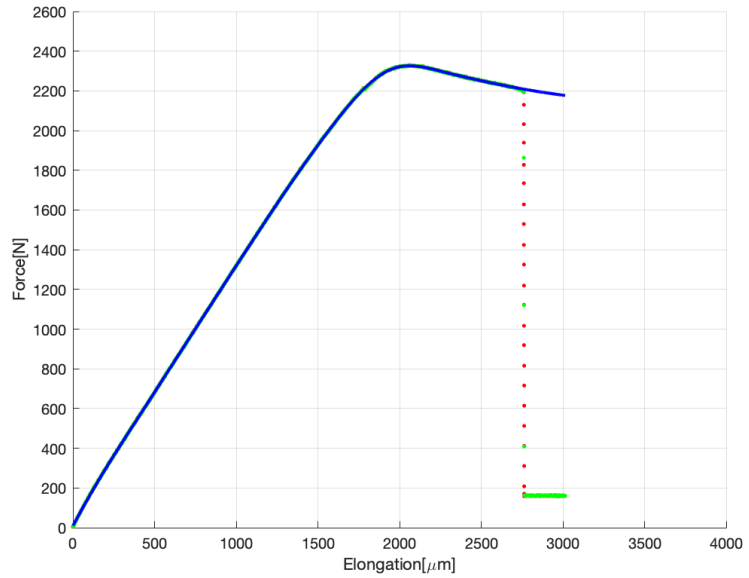


Figure A.20: Test 3.1 Force - Elongation curve

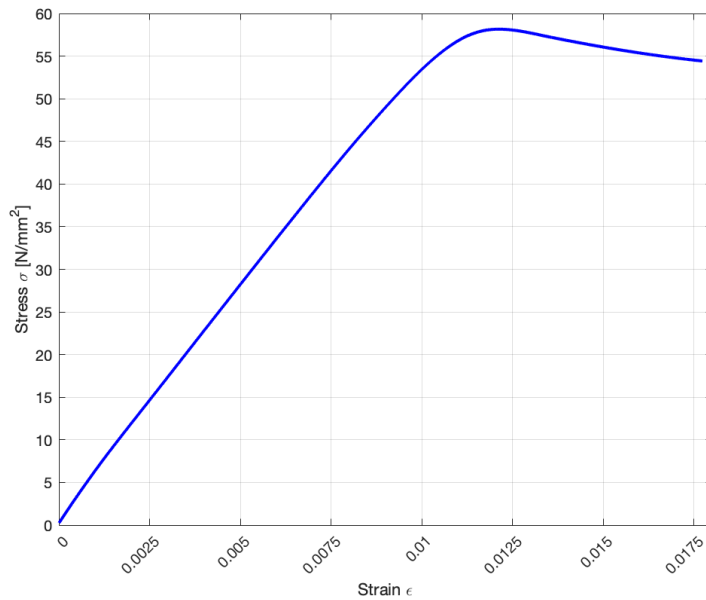


Figure A.21: Test 3.1 Stress - Strain curve

Print Duration [Hours]	Ultimate Tensile Stress [MPa]	Young's Modulus [MPa]	Cross Section Area [mm^2]	Print Orientation [$^\circ$]
7	58.16	2386	40	45

Test 3.2



Figure A.22:
Test 3.2 Specimen

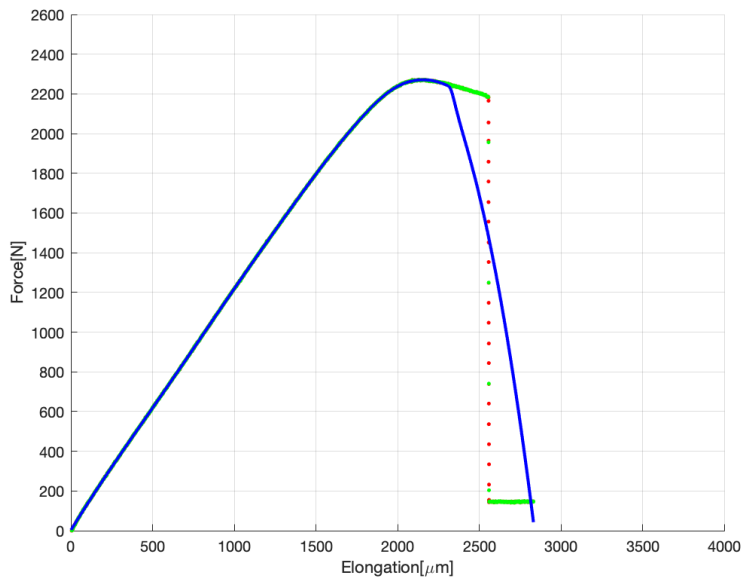


Figure A.23: Test 3.2 Force - Elongation curve

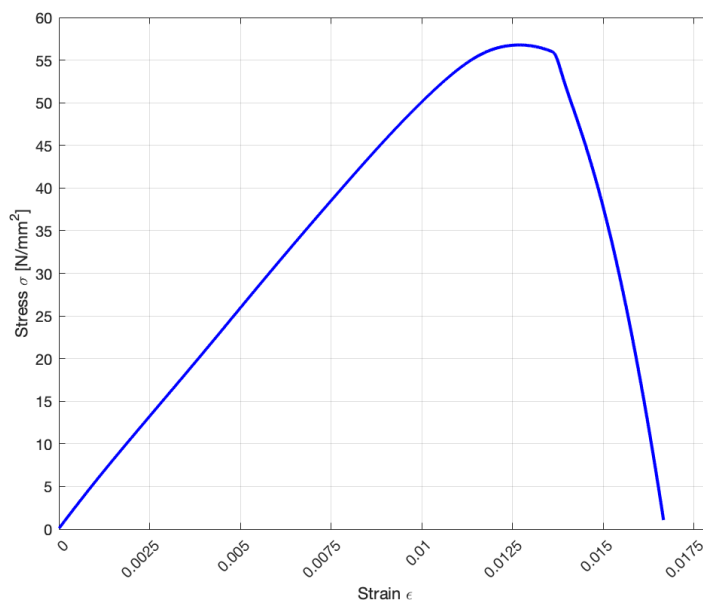


Figure A.24: Test 3.2 Stress - Strain curve

Print Duration [Hours]	Ultimate Tensile Stress [MPa]	Young's Modulus [MPa]	Cross Section Area [mm ²]	Print Orientation [°]
7	56.77	2239	40	45

Test 3.3



Figure A.25:
Test 3.3 Specimen

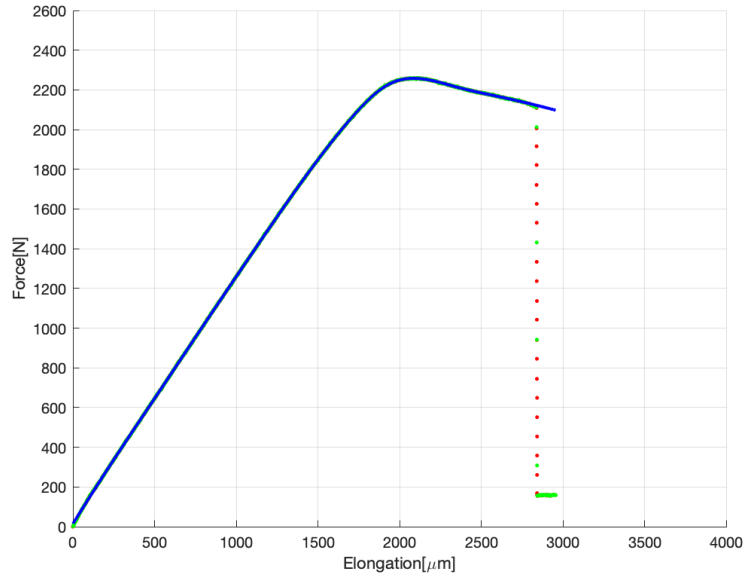


Figure A.26: Test 3.3 Force - Elongation curve

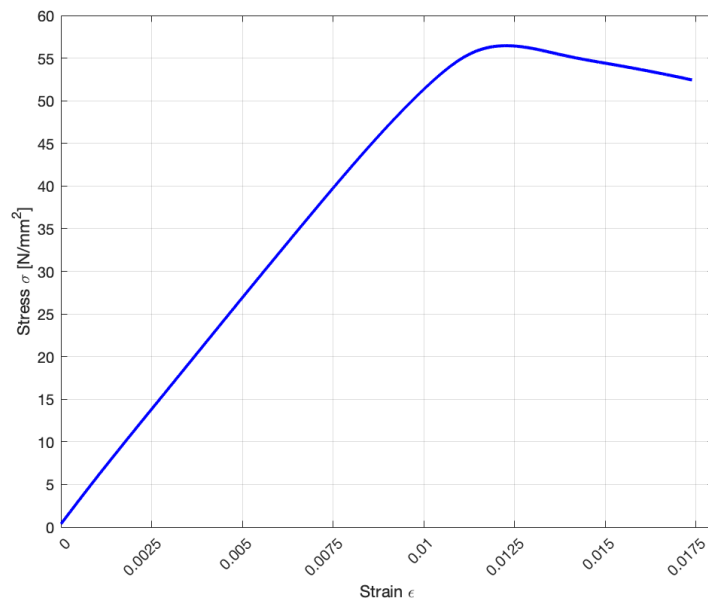


Figure A.27: Test 3.3 Stress - Strain curve

Print Duration [Hours]	Ultimate Tensile Stress [MPa]	Young's Modulus [MPa]	Cross Section Area [mm^2]	Print Orientation [$^\circ$]
7	56.45	2307	40	45

Test 3.4



Figure A.28:
Test 3.4 Specimen

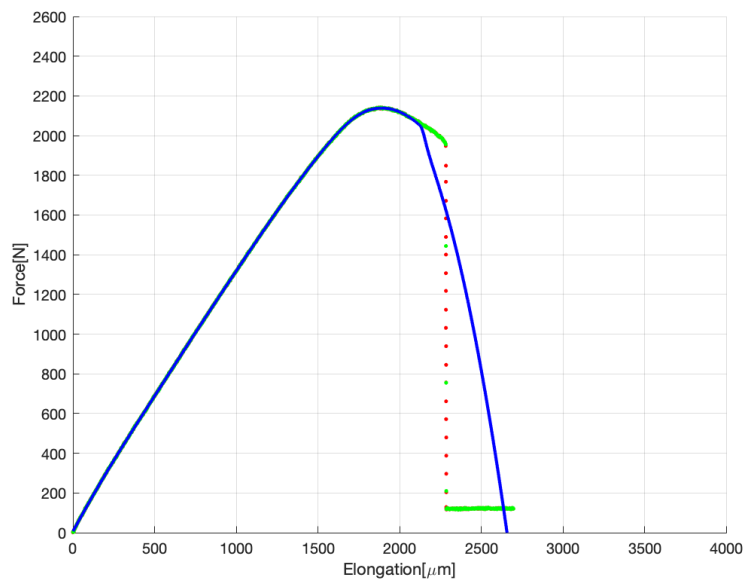


Figure A.29: Test 3.4 Force - Elongation curve

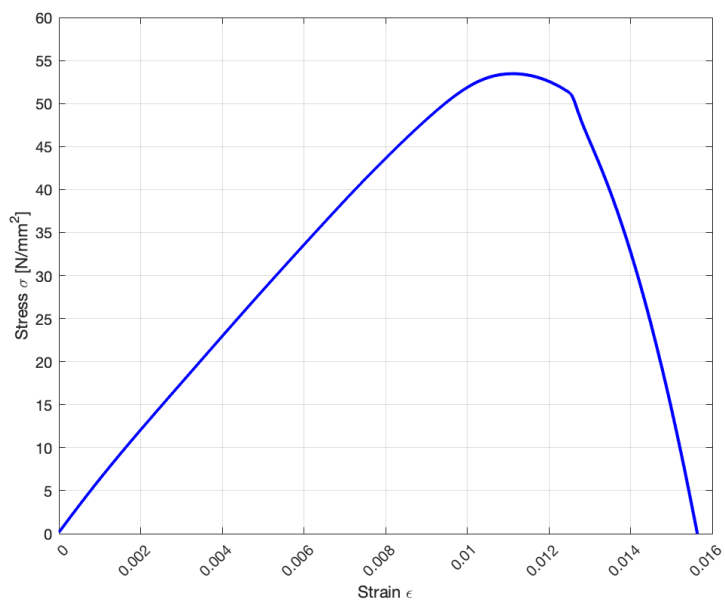


Figure A.30: Test 3.4 Stress - Strain curve

Print Duration [Hours]	Ultimate Tensile Stress [MPa]	Young's Modulus [MPa]	Cross Section Area [mm ²]	Print Orientation [°]
7	53.46	2372	40	45

Test 3.5



Figure A.31:
Test 3.5 Specimen

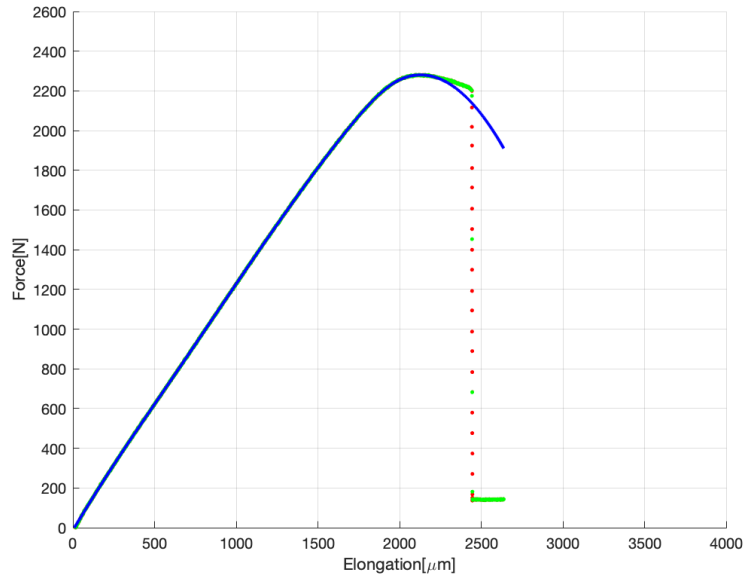


Figure A.32: Test 3.5 Force - Elongation curve

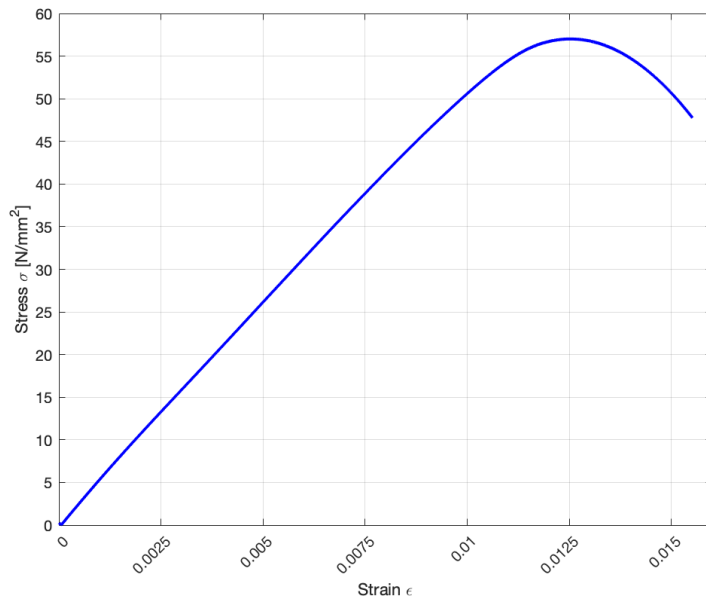


Figure A.33: Test 3.5 Stress - Strain curve

Print Duration [Hours]	Ultimate Tensile Stress [MPa]	Young's Modulus [MPa]	Cross Section Area [mm ²]	Print Orientation [°]
7	57.01	2271	40	45

A.1.3 Test 3.6 - Test 3.11, Printed at 90°

Test 3.6 - Failed



Figure A.34:
Test 3.6 Specimen

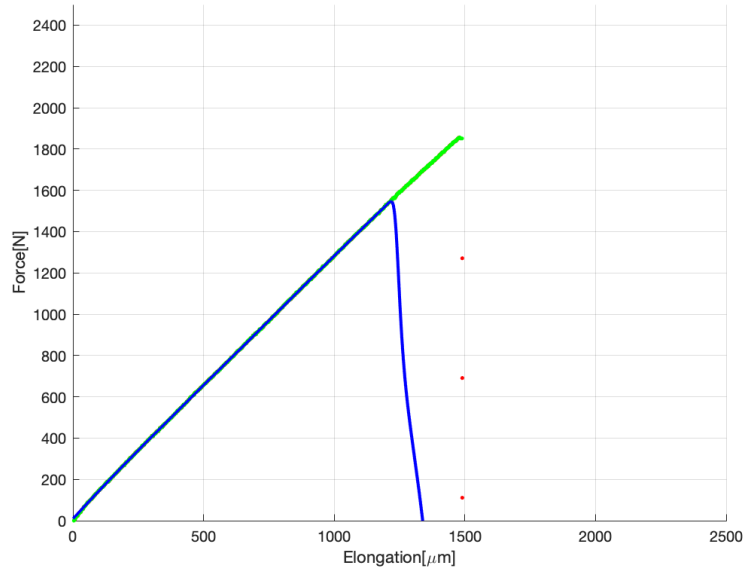


Figure A.35: Test 3.6 Force - Elongation curve

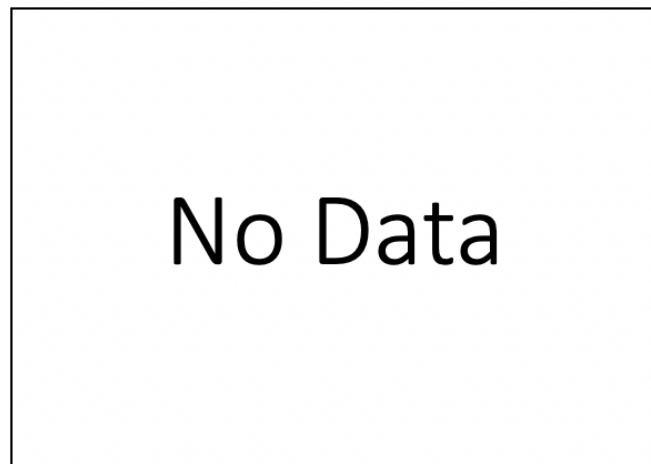


Figure A.36: Test 3.6 Stress - Strain curve

Print Duration [Hours]	Ultimate Tensile Stress [MPa]	Young's Modulus [MPa]	Cross Section Area [mm ²]	Print Orientation [°]
7	-	-	40	90

Test 3.7



Figure A.37:
Test 3.7 Specimen

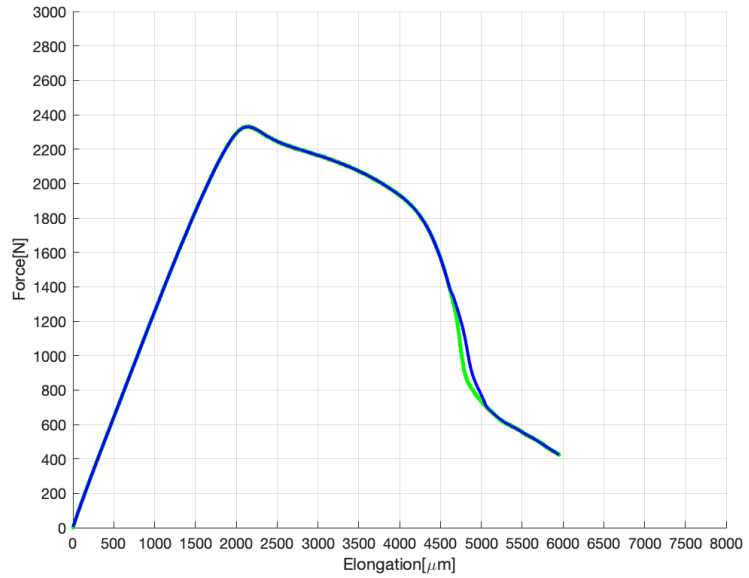


Figure A.38: Test 3.7 Force - Elongation curve

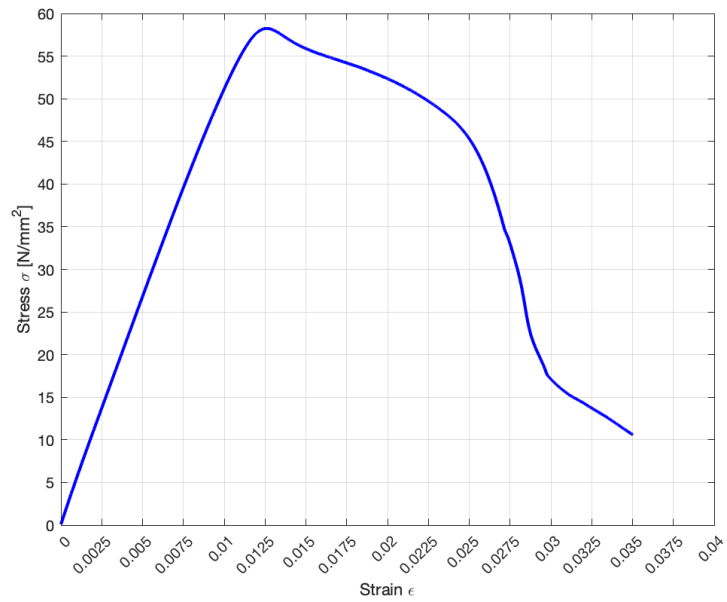


Figure A.39: Test 3.7 Stress - Strain curve

Print Duration [Hours]	Ultimate Tensile Stress [MPa]	Young's Modulus [MPa]	Cross Section Area [mm^2]	Print Orientation [$^\circ$]
7	58.24	2312	40	90

Test 3.8



Figure A.40:
Test 3.8 Specimen

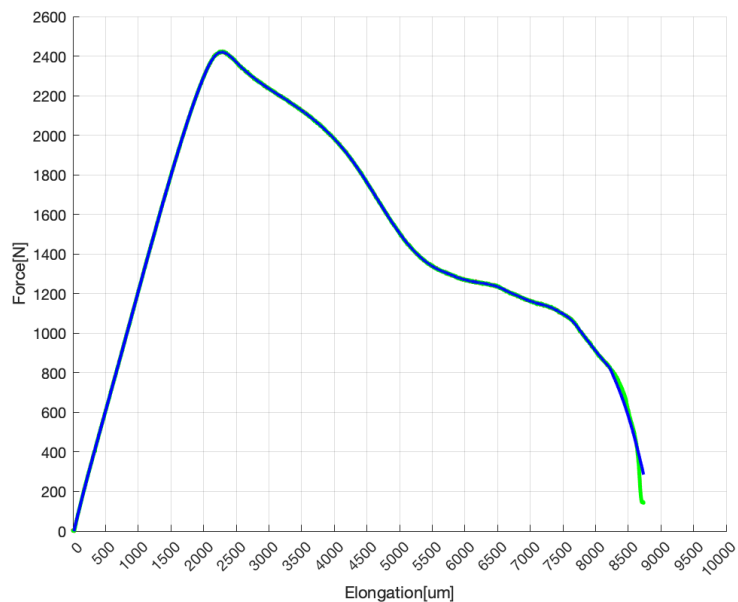


Figure A.41: Test 3.8 Force - Elongation curve

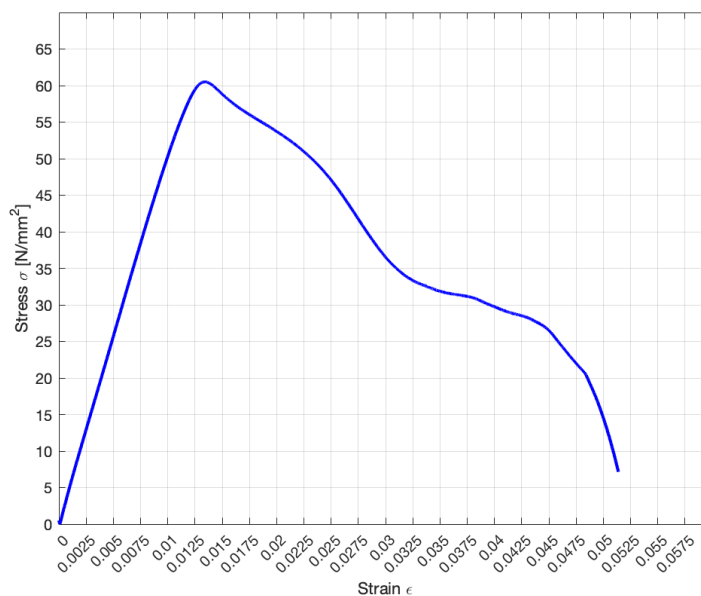


Figure A.42: Test 3.8 Stress - Strain curve

Print Duration [Hours]	Ultimate Tensile Stress [MPa]	Young's Modulus [MPa]	Cross Section Area [mm ²]	Print Orientation [°]
7	60.50	2256	40	90

Test 3.9



Figure A.43:
Test 3.9 Specimen

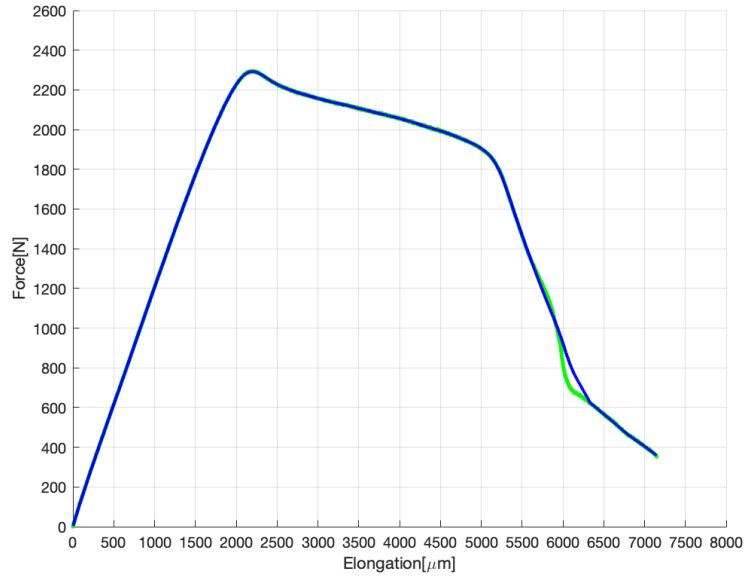


Figure A.44: Test 3.9 Force - Elongation curve

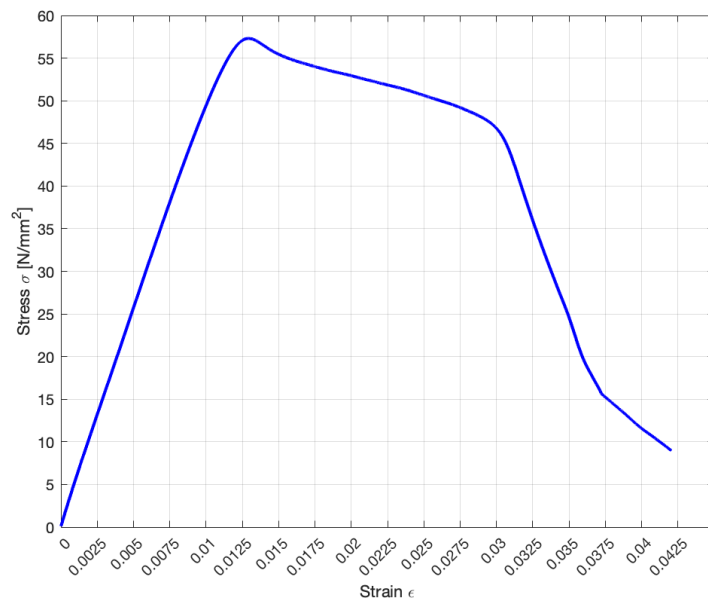


Figure A.45: Test 3.9 Stress - Strain curve

Print Duration [Hours]	Ultimate Tensile Stress [MPa]	Young's Modulus [MPa]	Cross Section Area [mm^2]	Print Orientation [$^\circ$]
7	57.31	2214	40	90

Test 3.10



Figure A.46:
Test 3.10 Specimen

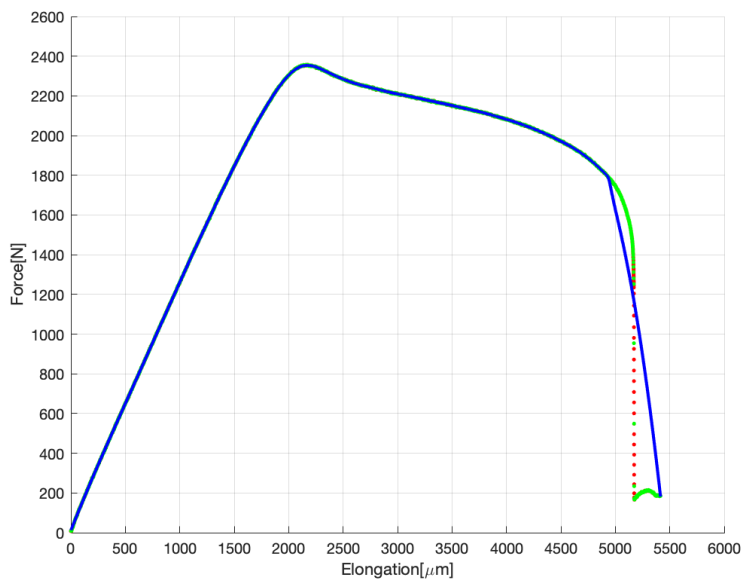


Figure A.47: Test 3.10 Force - Elongation curve

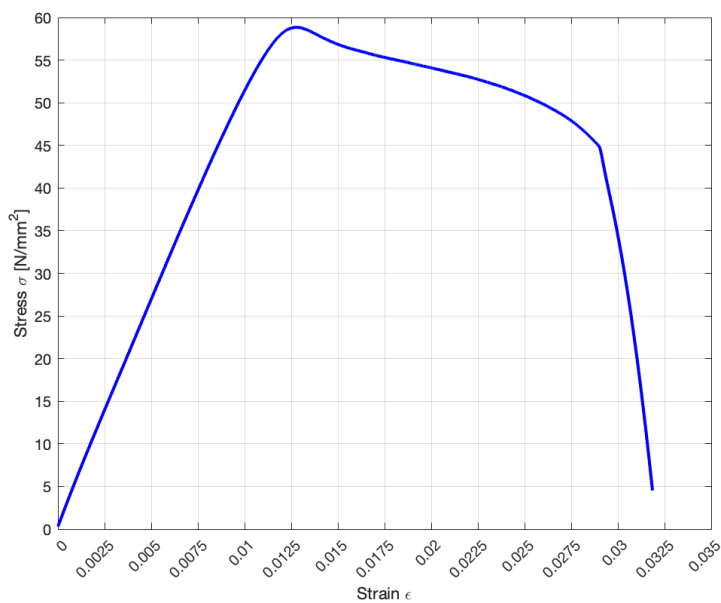


Figure A.48: Test 3.10 Stress - Strain curve

Print Duration [Hours]	Ultimate Tensile Stress [MPa]	Young's Modulus [MPa]	Cross Section Area [mm ²]	Print Orientation [°]
7	58.84	2286	40	90

Test 3.11



Figure A.49:
Test 3.11 Specimen

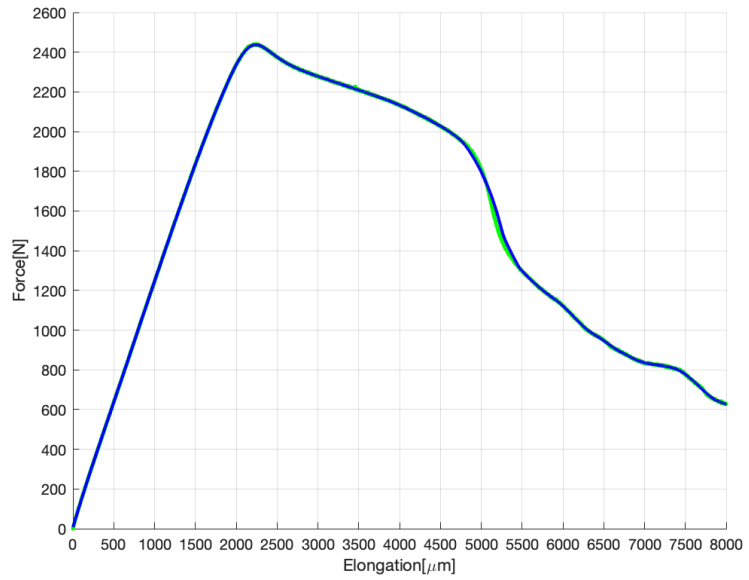


Figure A.50: Test 3.11 Force - Elongation curve

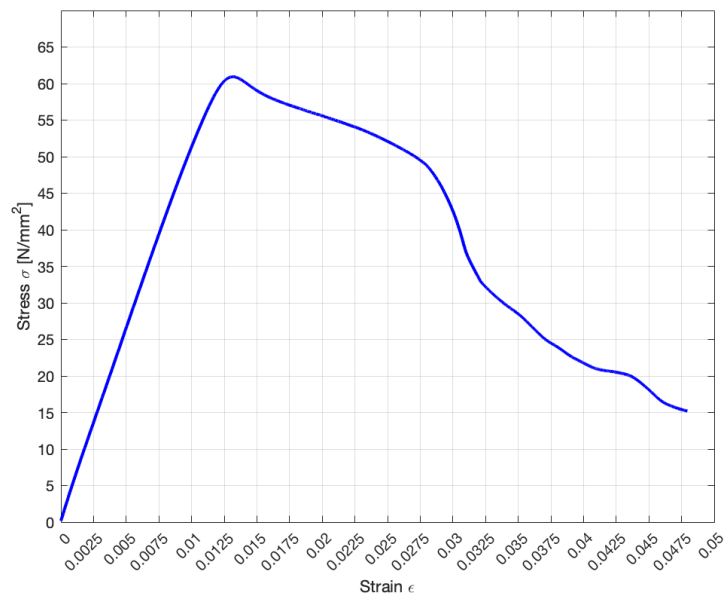


Figure A.51: Test 3.11 Stress - Strain curve

Print Duration [Hours]	Ultimate Tensile Stress [MPa]	Young's Modulus [MPa]	Cross Section Area [mm ²]	Print Orientation [°]
7	60.94	2281	40	90

A.2 Experimental Test 2 - Comparison Overview

This section consist of pictures and data from Experimental Test 2, which consist of fifteen test specimens printed at different orientation with identical measurements, visualized in Figure A.52 - A.54.

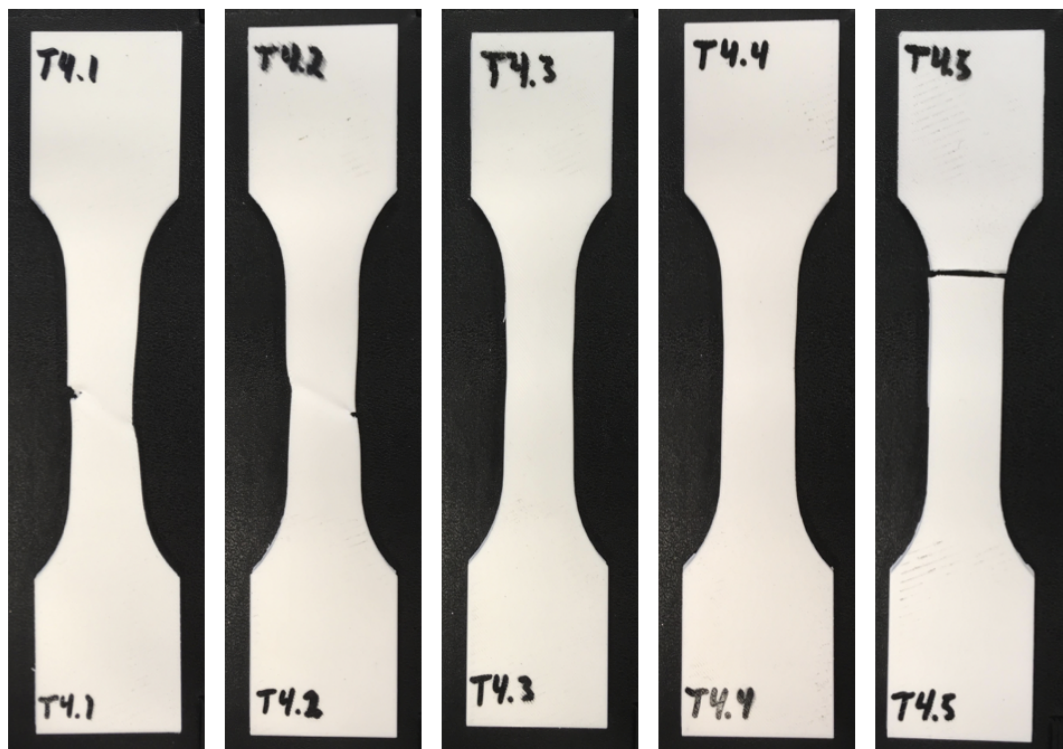


Figure A.52: Test 4.1 - 4.5



Figure A.53: Test 4.6 - 4.10

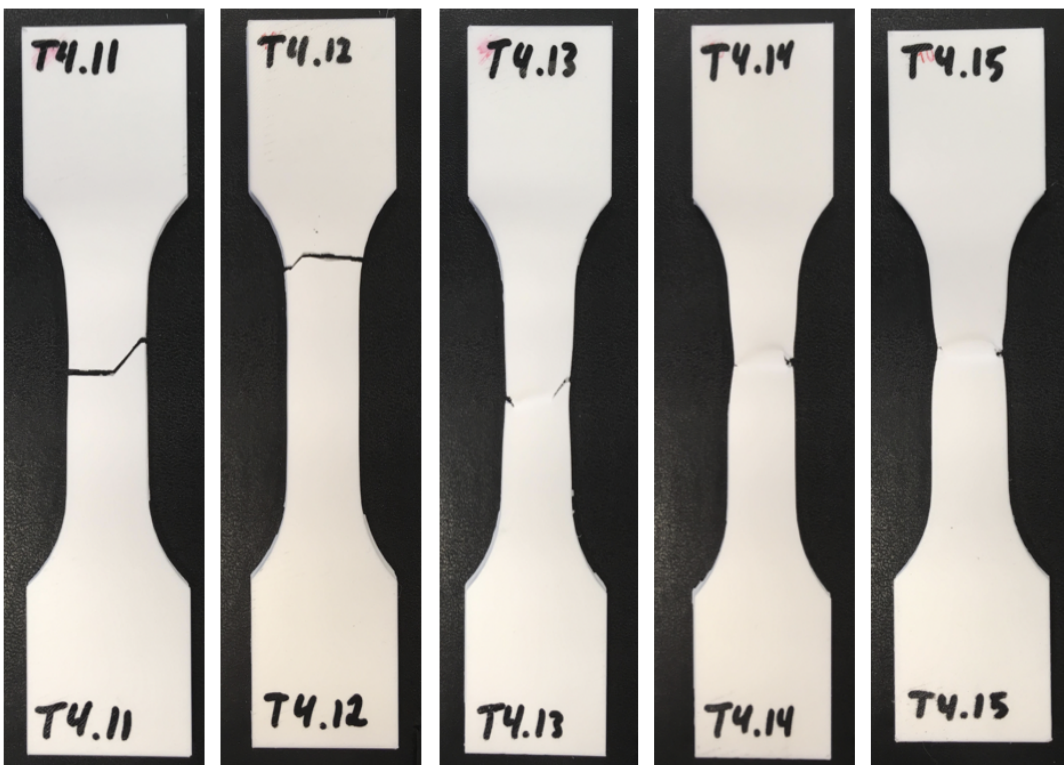


Figure A.54: Test 4.11 - 4.15

A.2.1 Test 4.1 - Test 4.5, Printed at 0°

Test 4.1



Figure A.55:
Test 4.1 Specimen

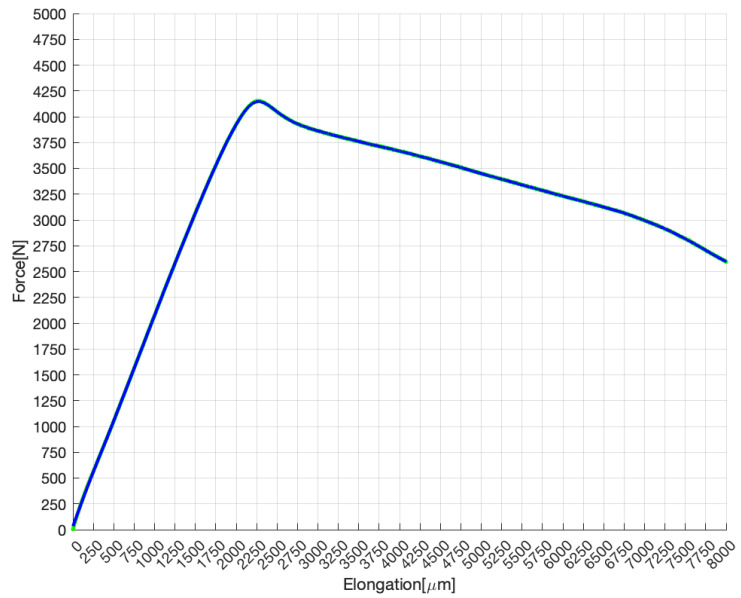


Figure A.56: Test 4.1 Force - Elongation curve

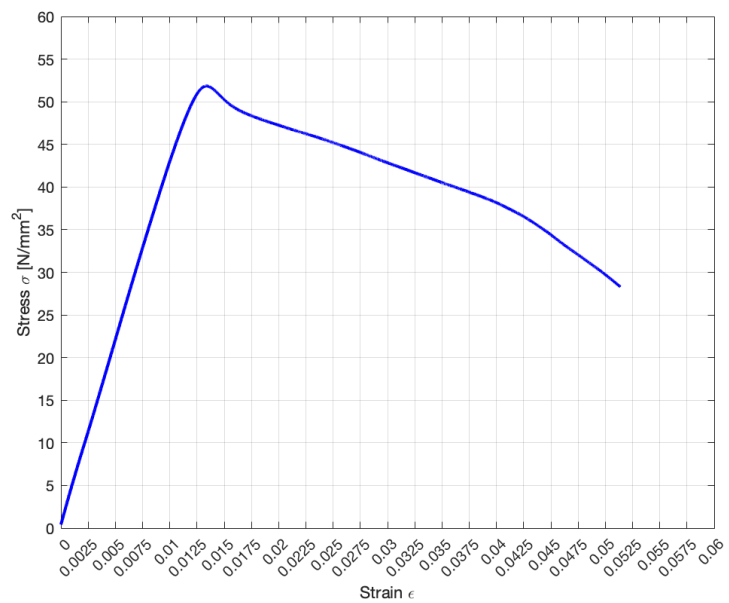


Figure A.57: Test 4.1 Stress - Strain curve

Print Duration [Hours]	Ultimate Tensile Stress [MPa]	Young's Modulus [MPa]	Cross Section Area [mm ²]	Print Orientation [°]
8	51.84	2910	80	0

Test 4.2



Figure A.58:
Test 4.2 Specimen

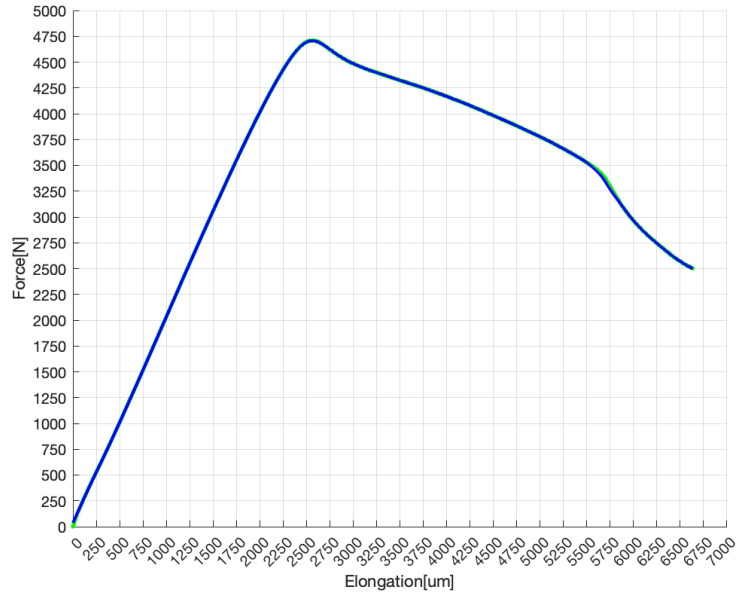


Figure A.59: Test 4.2 Force - Elongation curve

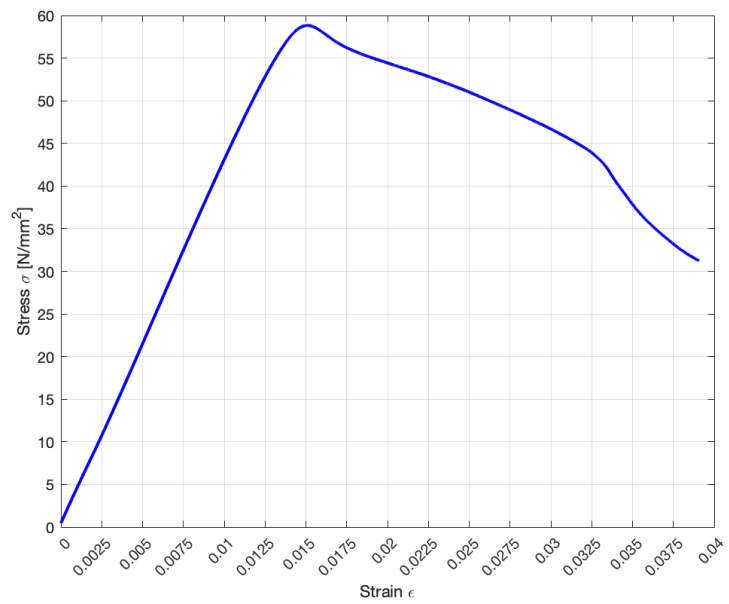


Figure A.60: Test 4.2 Stress - Strain curve

Print Duration [Hours]	Ultimate Tensile Stress [MPa]	Young's Modulus [MPa]	Cross Section Area [mm ²]	Print Orientation [°]
8	58.83	2903	80	0

Test 4.3



Figure A.61:
Test 4.3 Specimen

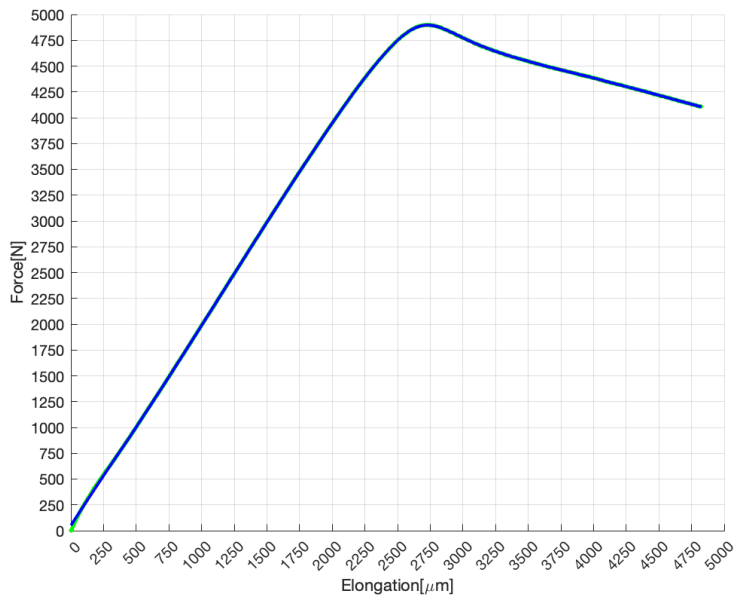


Figure A.62: Test 4.3 Force - Elongation curve

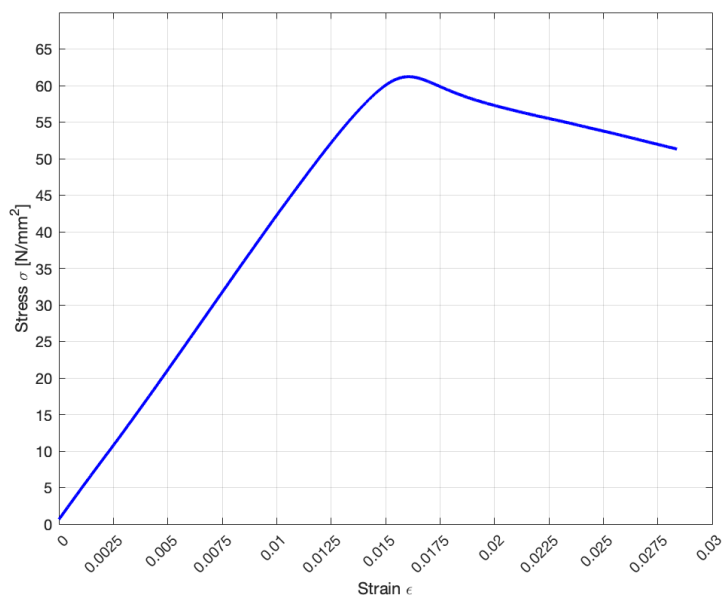


Figure A.63: Test 4.3 Stress - Strain curve

Print Duration [Hours]	Ultimate Tensile Stress [MPa]	Young's Modulus [MPa]	Cross Section Area [mm ²]	Print Orientation [°]
8	61.21	2847	80	0

Test 4.4



Figure A.64:
Test 4.4 Specimen

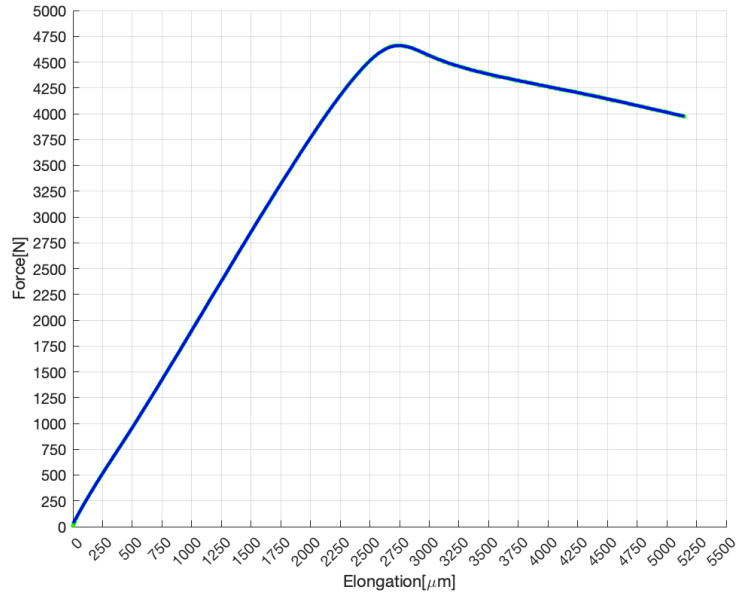


Figure A.65: Test 4.4 Force - Elongation curve

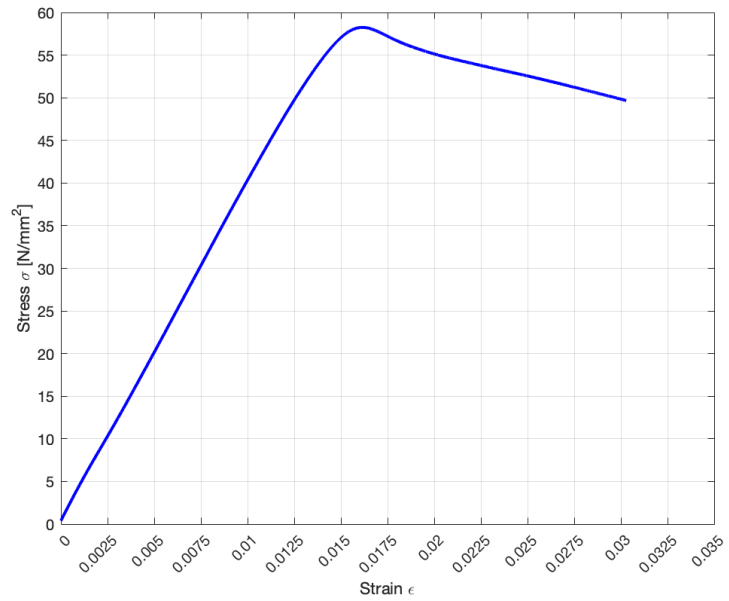


Figure A.66: Test 4.4 Stress - Strain curve

Print Duration [Hours]	Ultimate Tensile Stress [MPa]	Young's Modulus [MPa]	Cross Section Area [mm ²]	Print Orientation [°]
8	58.25	2717	80	0

Test 4.5



Figure A.67:
Test 4.5 Specimen

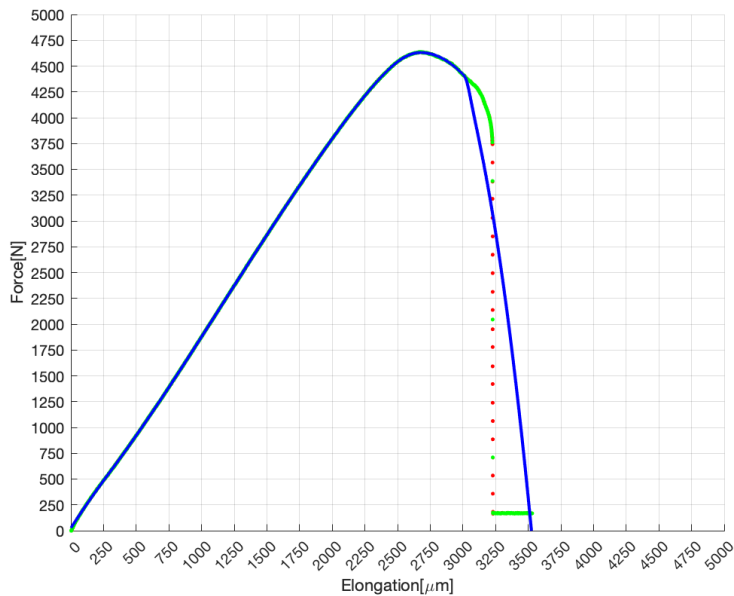


Figure A.68: Test 4.5 Force - Elongation curve

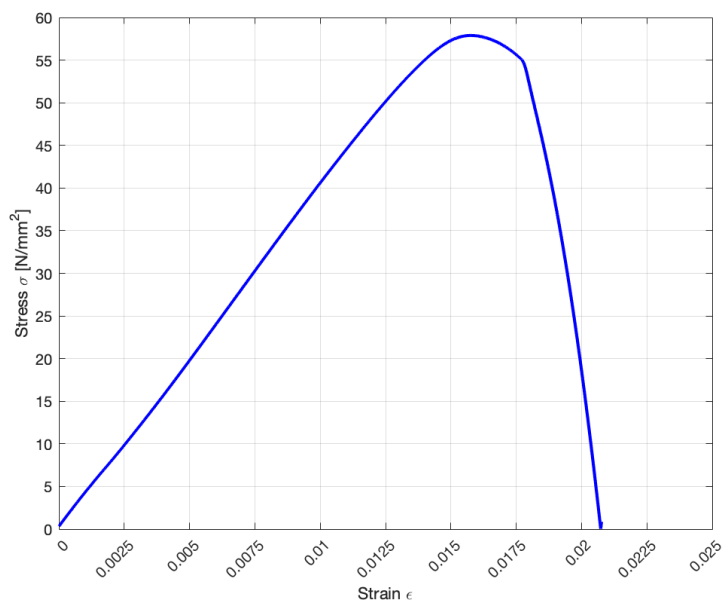


Figure A.69: Test 4.5 Stress - Strain curve

Print Duration [Hours]	Ultimate Tensile Stress [MPa]	Young's Modulus [MPa]	Cross Section Area [mm ²]	Print Orientation [°]
8	57.89	2810	80	0

A.2.2 Test 4.6 - Test 4.10, Printed at 45°

Test 4.6



Figure A.70:
Test 4.6 Specimen

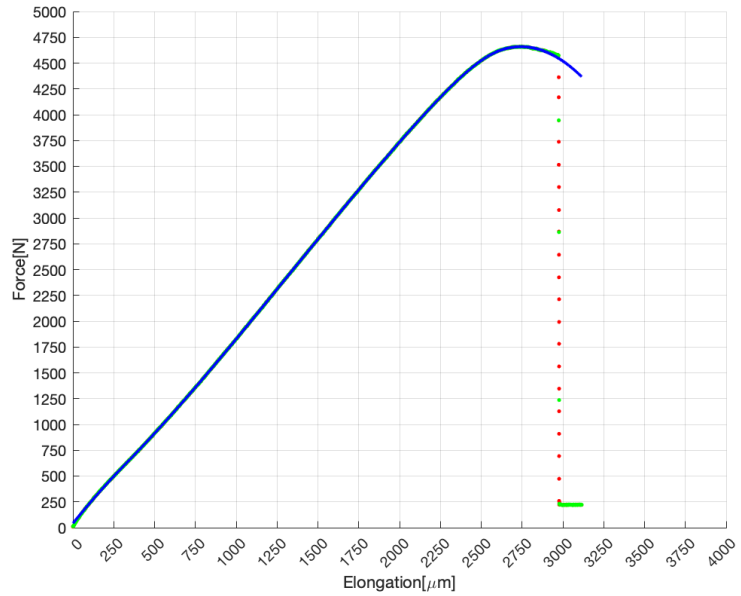


Figure A.71: Test 4.6 Force - Elongation curve

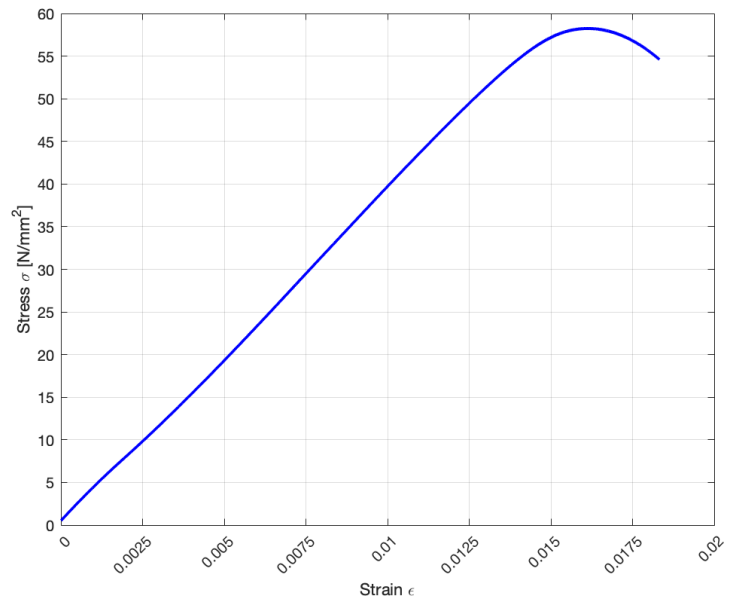


Figure A.72: Test 4.6 Stress - Strain curve

Print Duration [Hours]	Ultimate Tensile Stress [MPa]	Young's Modulus [MPa]	Cross Section Area [mm ²]	Print Orientation [°]
8	58.23	2746	80	45

Test 4.7



Figure A.73:
Test 4.7 Specimen

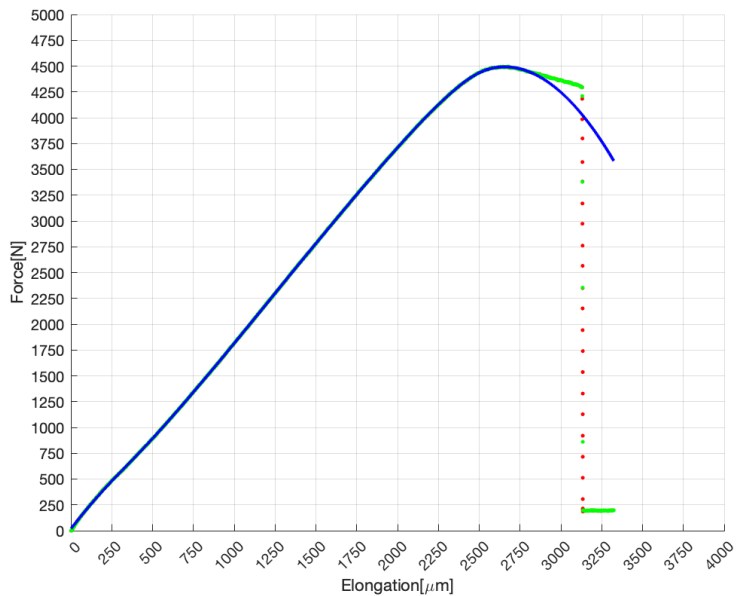


Figure A.74: Test 4.7 Force - Elongation curve

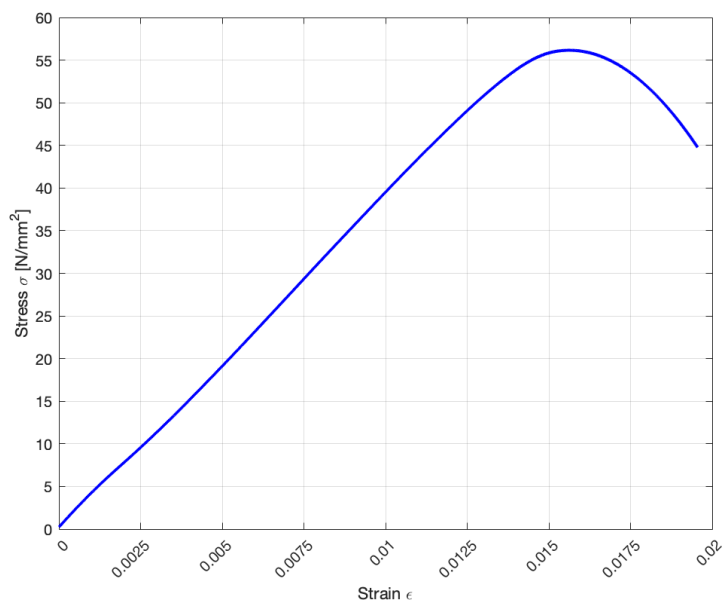


Figure A.75: Test 4.7 Stress - Strain curve

Print Duration [Hours]	Ultimate Tensile Stress [MPa]	Young's Modulus [MPa]	Cross Section Area [mm ²]	Print Orientation [°]
8	56.15	2744	80	45

Test 4.8



Figure A.76:
Test 4.8 Specimen

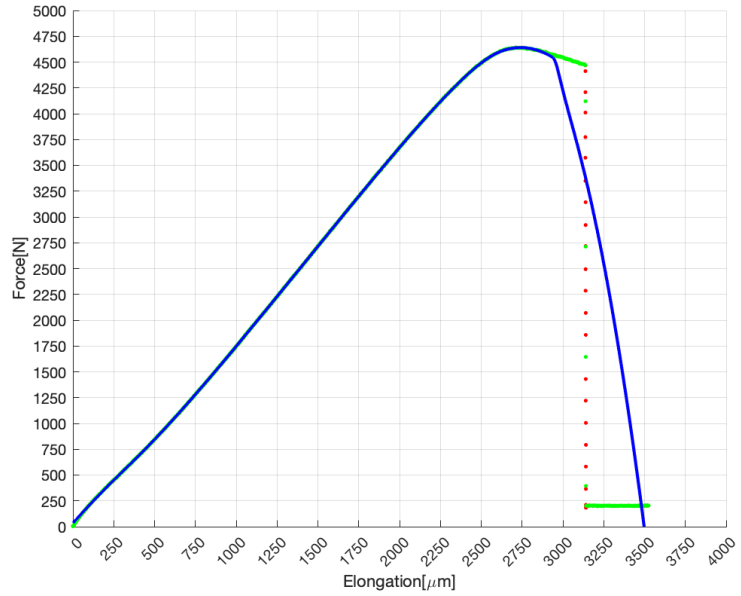


Figure A.77: Test 4.8 Force - Elongation curve

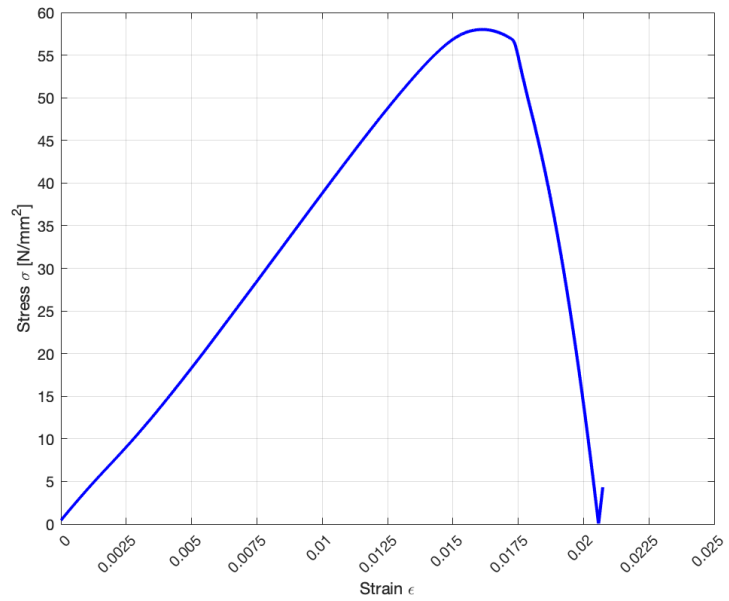


Figure A.78: Test 4.8 Stress - Strain curve

Print Duration [Hours]	Ultimate Tensile Stress [MPa]	Young's Modulus [MPa]	Cross Section Area [mm ²]	Print Orientation [°]
8	58.00	2762	80	45

Test 4.9



Figure A.79:
Test 4.9 Specimen

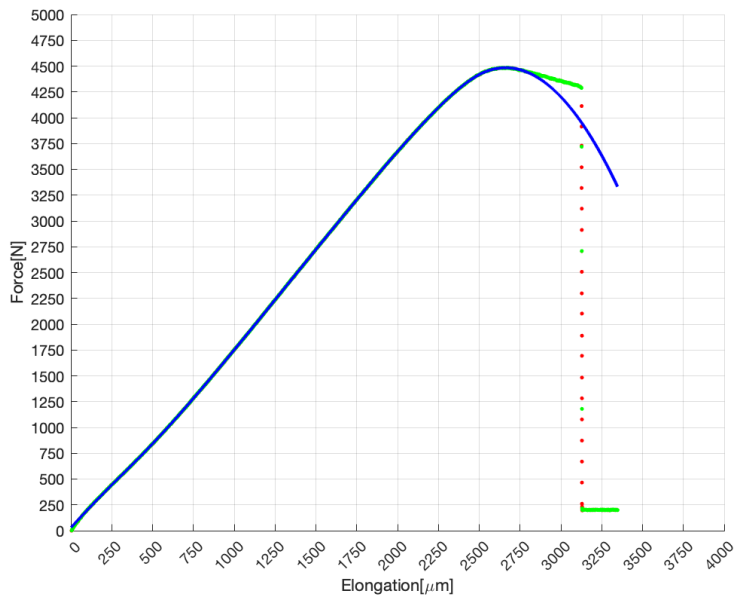


Figure A.80: Test 4.9 Force - Elongation curve

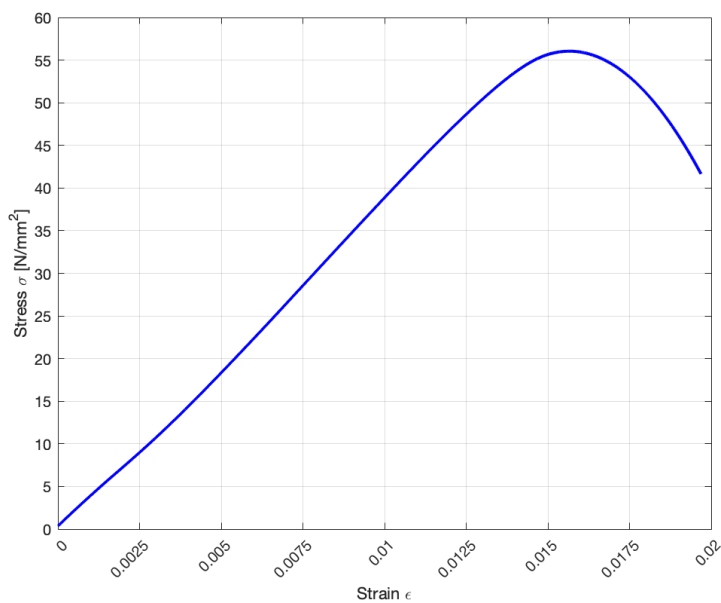


Figure A.81: Test 4.9 Stress - Strain curve

Print Duration [Hours]	Ultimate Tensile Stress [MPa]	Young's Modulus [MPa]	Cross Section Area [mm ²]	Print Orientation [°]
8	56.05	2760	80	45

Test 4.10



Figure A.82:
Test 4.10 Specimen

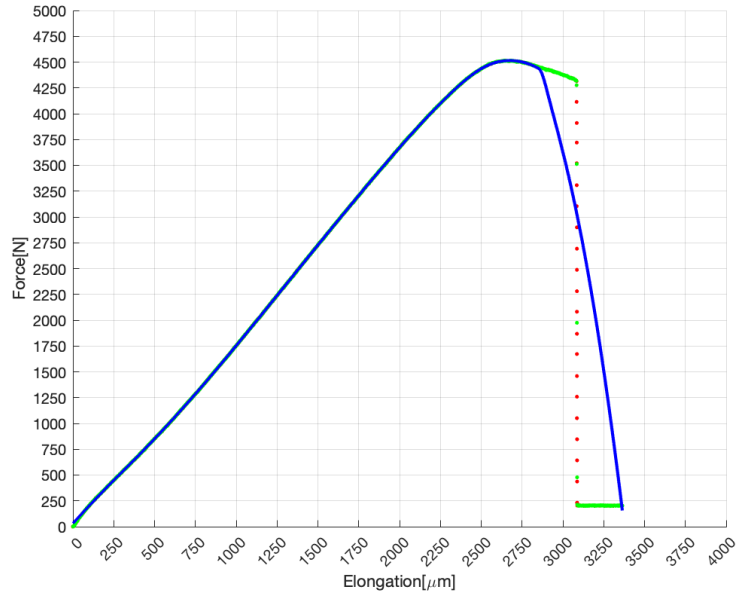


Figure A.83: Test 4.10 Force - Elongation curve

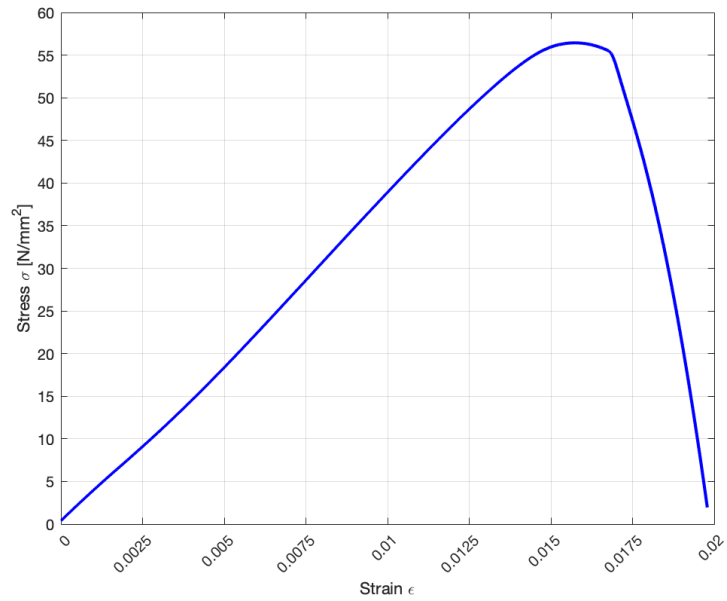


Figure A.84: Test 4.10 Stress - Strain curve

Print Duration [Hours]	Ultimate Tensile Stress [MPa]	Young's Modulus [MPa]	Cross Section Area [mm ²]	Print Orientation [°]
8	56.44	2768	80	45

A.2.3 Test 4.11 - Test 4.15, Printed at 90°

Test 4.11



Figure A.85:
Test 4.11 Specimen

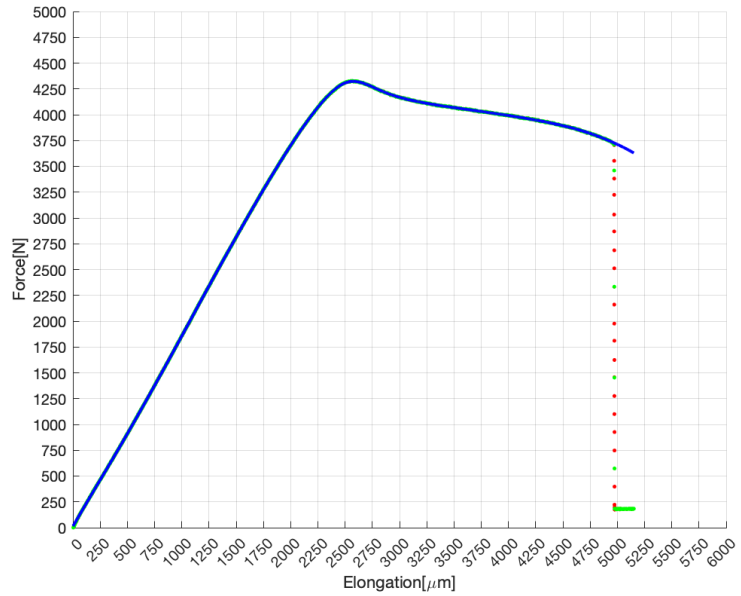


Figure A.86: Test 4.11 Force - Elongation curve

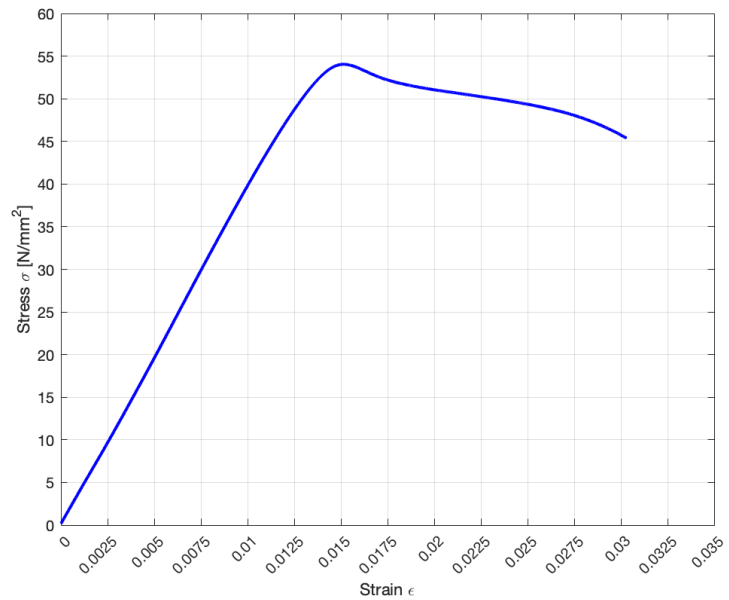


Figure A.87: Test 4.11 Stress - Strain curve

Print Duration [Hours]	Ultimate Tensile Stress [MPa]	Young's Modulus [MPa]	Cross Section Area [mm ²]	Print Orientation [°]
8	54.04	2732	80	90

Test 4.12



Figure A.88:
Test 4.12 Specimen

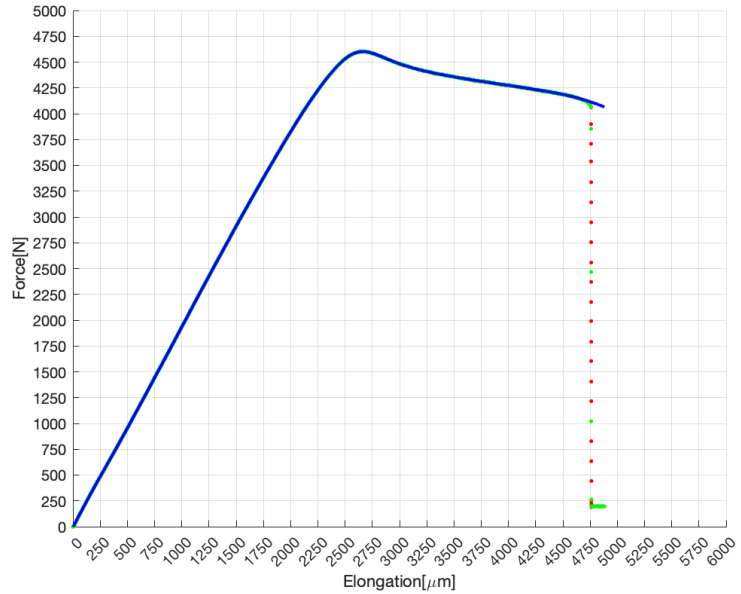


Figure A.89: Test 4.12 Force - Elongation curve

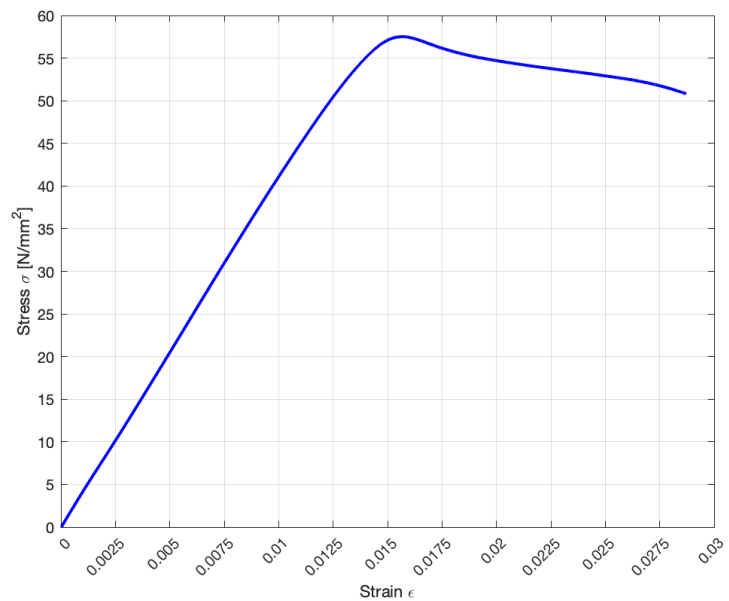


Figure A.90: Test 4.12 Stress - Strain curve

Print Duration [Hours]	Ultimate Tensile Stress [MPa]	Young's Modulus [MPa]	Cross Section Area [mm^2]	Print Orientation [$^\circ$]
8	57.51	2800	80	90

Test 4.13

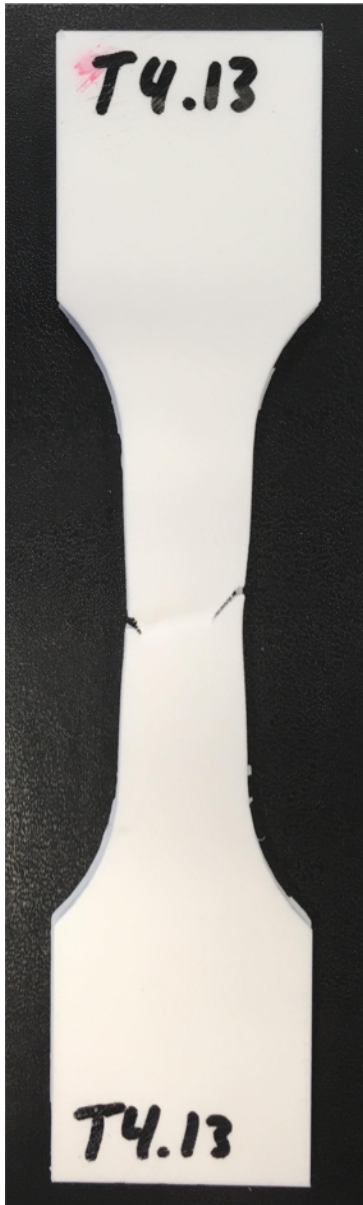


Figure A.91:
Test 4.13 Specimen

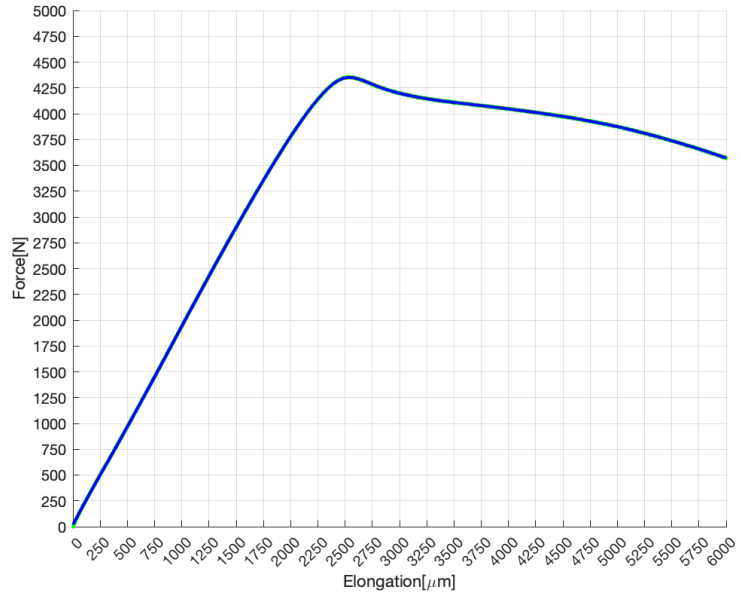


Figure A.92: Test 4.13 Force - Elongation curve

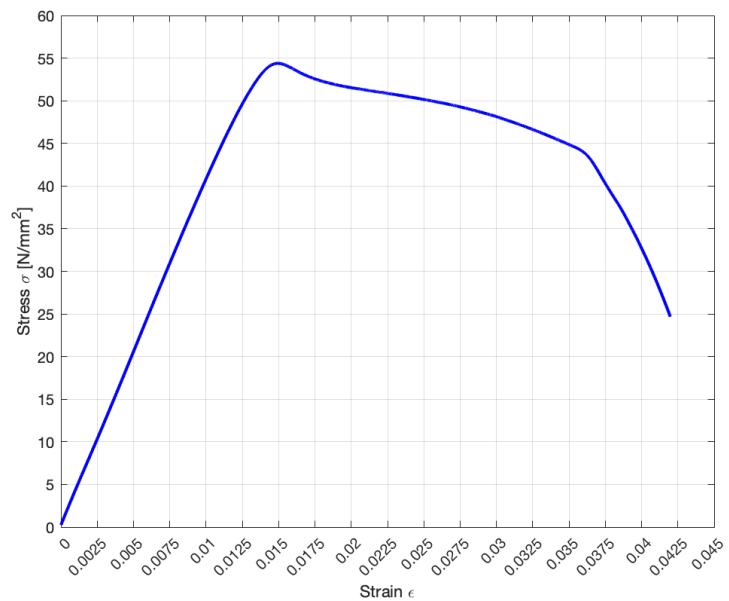


Figure A.93: Test 4.13 Stress - Strain curve

Print Duration [Hours]	Ultimate Tensile Stress [MPa]	Young's Modulus [MPa]	Cross Section Area [mm ²]	Print Orientation [°]
8	54.38	2768	80	90

Test 4.14



Figure A.94:
Test 4.14 Specimen

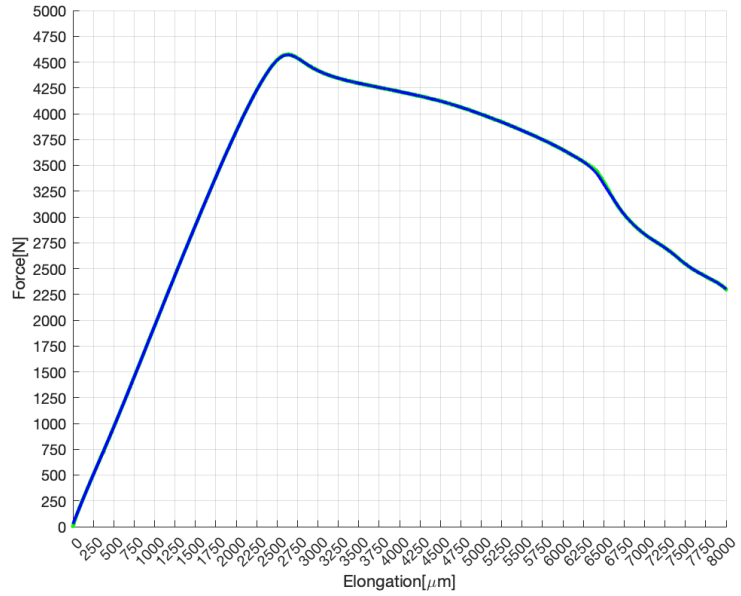


Figure A.95: Test 4.14 Force - Elongation curve

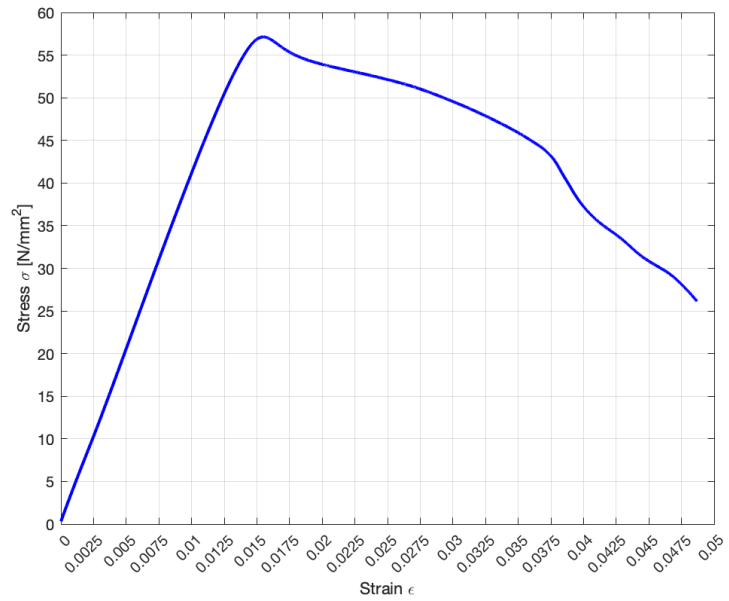


Figure A.96: Test 4.14 Stress - Strain curve

Print Duration [Hours]	Ultimate Tensile Stress [MPa]	Young's Modulus [MPa]	Cross Section Area [mm ²]	Print Orientation [°]
8	57.13	2798	80	90

Test 4.15



Figure A.97:
Test 4.15 Specimen

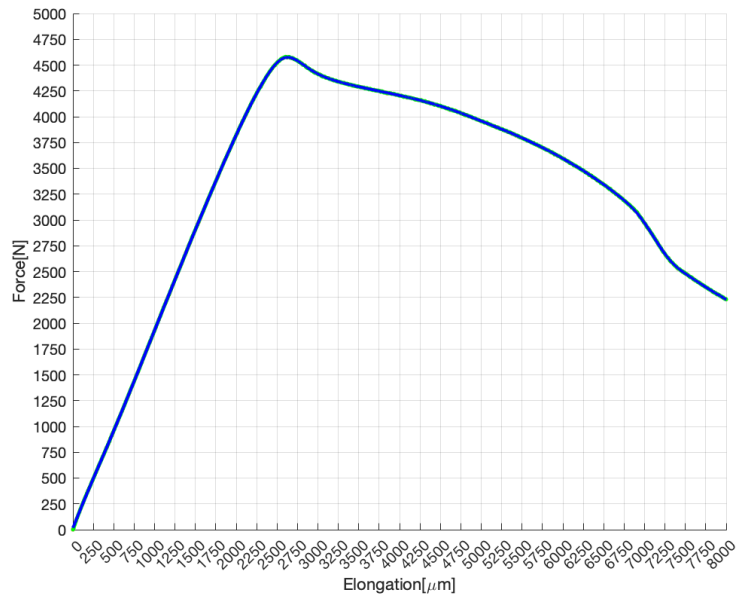


Figure A.98: Test 4.15 Force - Elongation curve

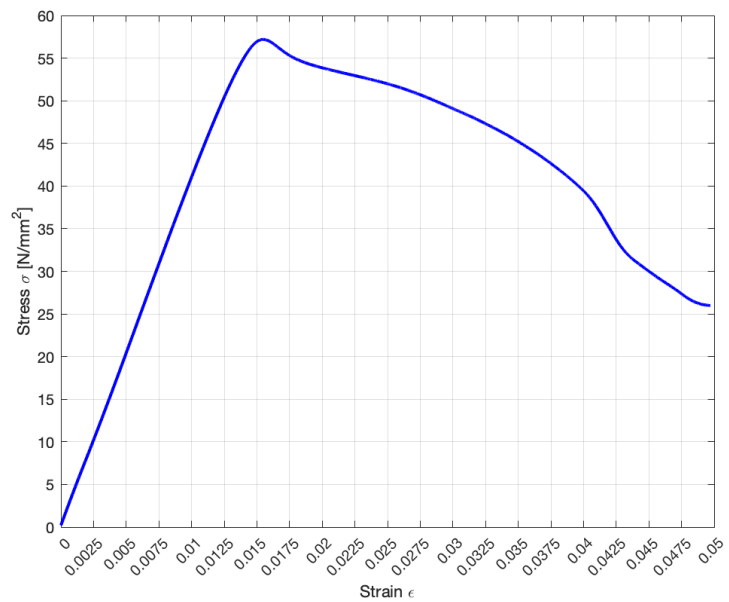


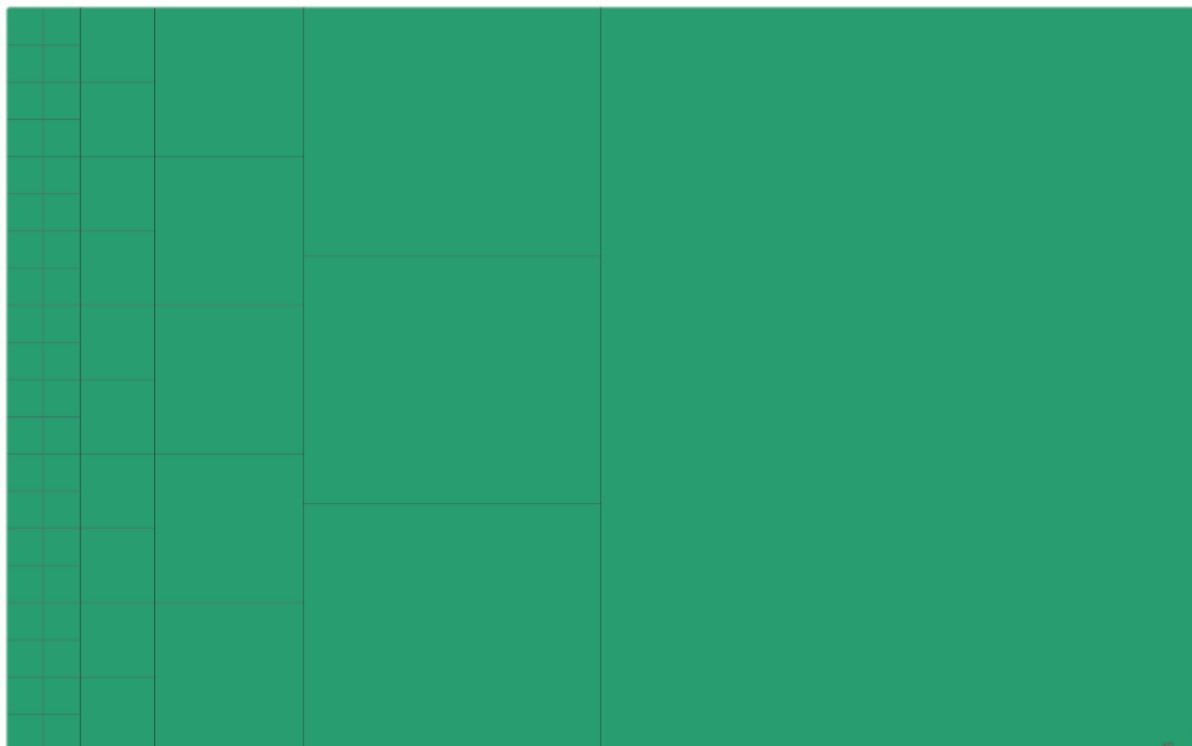
Figure A.99: Test 4.15 Stress - Strain curve

Print Duration [Hours]	Ultimate Tensile Stress [MPa]	Young's Modulus [MPa]	Cross Section Area [mm ²]	Print Orientation [°]
8	57.19	2790	80	90

Appendix B

Mesh Convergence Study

This section consist of pictures of the different mesh sizes that was tested in the mesh convergence study visualized in the figure below. They range from 0.5 - 8 mm in element size, and their deformation is visualized in Figure B.1 - B.5.



Mesh element size from 0.5 - 8mm

B.1 Mesh 0.5 mm element size

Deformation = $7.55721 \cdot 10^{-3}$ mm

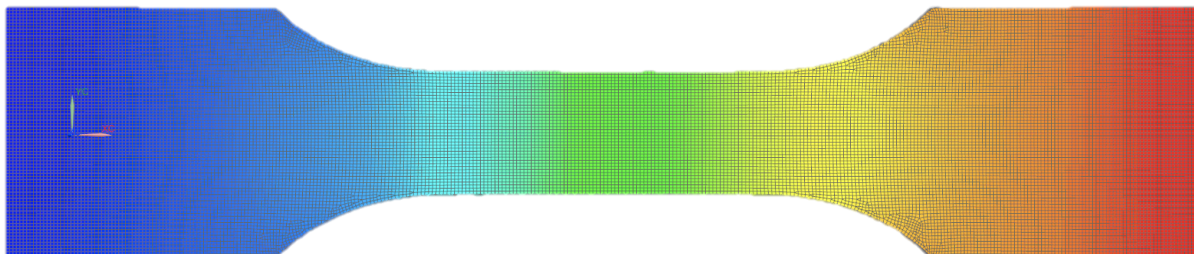


Figure B.1: 0.5 mm Element size

B.2 Mesh 1 mm element size

Deformation = $7.55611 \cdot 10^{-3}$ mm

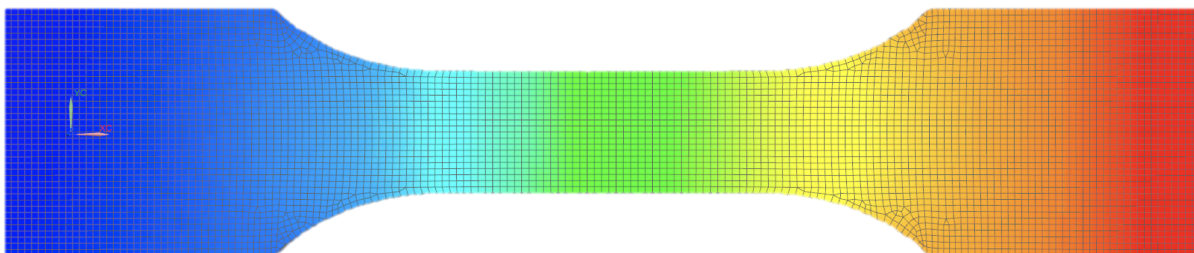


Figure B.2: 1 mm Element size

B.3 Mesh 2 mm element size

Deformation = $7.55239 \cdot 10^{-3}$ mm

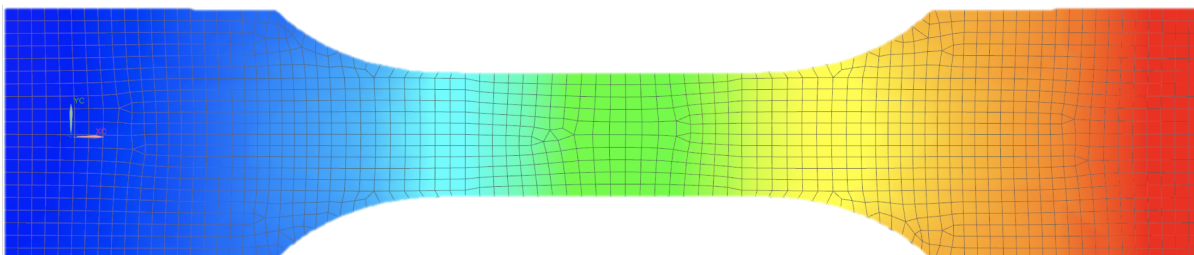


Figure B.3: 2 mm Element size

B.4 Mesh 4 mm element size

Deformation = $7.53669 \cdot 10^{-3}$ mm

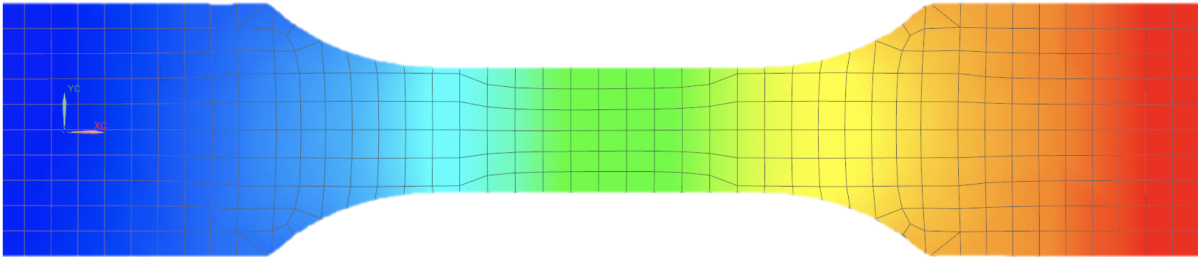


Figure B.4: 4 mm Element size

B.5 Mesh 8 mm element size

Deformation = $7.47606 \cdot 10^{-3}$ mm

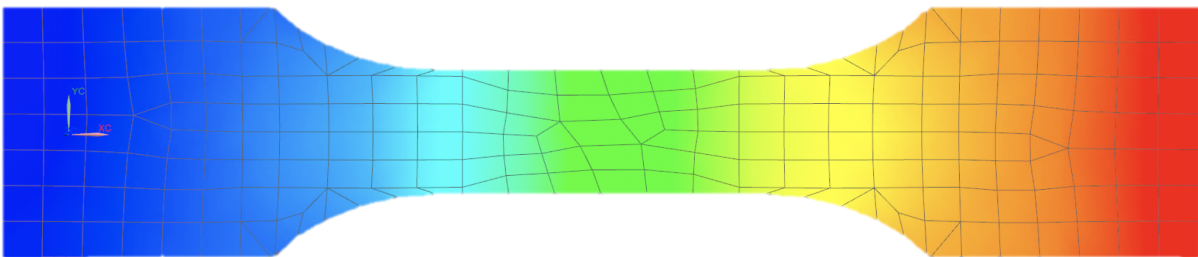


Figure B.5: 8 mm Element size

Appendix C

MATLAB Scripts

The MATLAB scripts are added in the appendix in order to show where the some of the numbers and plots are made and mentioned in this thesis. The scripts are commented where it is need, but some basic knowledge of MATLAB is needed to understand it all. Figure caption is added, referring to their respective code section.

C.1 Main Script, example T3.1

```
1 % extract xls to mat
2 clear all; close all;
3 if 1
4     fn = 'Test3.1.xlsx';
5
6     [num,txt,row] = xlsread(fn,1,'A:B');
7
8     force = num([4:end],1);
9     deform = num([4:end],2);
10
11     save('test31', 'deform', 'force')
12 end
13 data = load('test31');
14 %%%%%%%%%%%%%%%%%%%%%%%%%%%%%%%%%%%%%%%%%%%%%%%%%%%%%%%%%%%%%%%%%%%%%%%%%
15 deform_raw = data.deform;
16 force_raw = data.force;
17
18 deform = data.deform;
19 force = data.force;
20
21 % Remove leading entries with 0 deformation
22 ind = max(find(deform==0))+1;
23 force = force(ind:end);
24 deform = deform(ind:end);
25
26 % Compute mean value for multiple entries
27 nDeform = max(deform);
28 nVal = size(force,1);
29 deform_condensed = (1:nDeform)';
30 force_sum = zeros(nDeform,1);
31 for i=1:nVal
32     force_sum(deform(i)) = force_sum(deform(i))+force(i);
33 end
34 vals = accumarray(deform,1); % count deform values
35 force_condensed = force_sum./vals;
36
37 force = force_condensed;
38 deform = deform_condensed;
39
40 ind_width = 500; % number of indices to smooth over
41 span = deform(ind_width)-deform(1);
42 force_smooth = smooth(deform, force,span,'rloess');
43 indStart = 10;
44 [maxValue, maxIndex] = max(force);
45 indEnd = maxIndex;
```

```
46
47 deform_crop = deform(indStart:indEnd);
48 force_crop = force_smooth(indStart:indEnd);
49 force_coeff = fit(deform_crop,force_crop,'poly1')
50
51 %Figure of raw and smoothed data
52 figure(1)
53 hold on
54 plot(deform_raw, force_raw, '.r')
55 plot(deform_condensed,force_condensed, '.g')
56 plot(deform, force_smooth, '-b', 'linewidth',2)
57 xlim([0 4000])
58 ylim([0 2600])
59 xlabel('Elongation[\mum]')
60 ylabel('Force[N]')
61 xticks(0:500:8000);
62 yticks(0:200:3000);
63 grid on
64
65 % linear fit with matlab fitting
66 figure(2)
67 hold on
68 plot(force_coeff,deform_crop, force_crop)
69
70 % Histogram with kernel distribution
71 figure(3)
72 histogram = histfit(diff(force_crop), 100,'kernel');
73 % Finding the peak of the kernel distribution which will be used to
74 % determine the +/- confidence ratio in the diff(force_crop) graph.
75 [pks1,locs1] = findpeaks(histogram(2).YData);
76
77 max(pks1); %Highest Y value
78 finn= find(pks1 == max(pks1));
79 x_highest_peak = histogram(2).XData(locs1(finn));%X value based on highest
    Y value.
80
81 figure(4)
82 plot(histogram(2).XData, histogram(2).YData);
83 hold on
84 plot(x_highest_peak, max(pks1), 'o')
85
86
87 %Threshold range
88 peakpluss = x_highest_peak * 1.05;
89 peakminus = x_highest_peak * 0.95;
90
91 figure(5)
92 %Vertical line +5
```

APPENDIX C. MATLAB SCRIPTS

```
93 x_max=[0, 3000];
94 y_max=[peakpluss, peakpluss];
95 plot(x_max,y_max , 'm')
96 hold on
97 %Vertical line -5%
98 x_min=[0, 3000];
99 y_min=[peakminus, peakminus];
100 plot(x_min,y_min , 'r')
101 %Curve of force
102 plot(diff(force_crop), '-b')
103 legend('+5% of max', '-5% of max')
104 grid on
105
106
107 %Individual graph for the treshold range
108 %For loop to check if the blue line is above or under +/-% lines.
109 fc = diff(force_crop);
110 prev_fc = fc(1); % Value for diff(force_crop) for i-1, aka the previous one
111 .
112 for i=2:length(fc)
113     vall = fc(i); %Val 1 is the value for diff(force_crop) for index i.
114     if(prev_fc > peakpluss && vall < peakpluss)
115         plusskryss = i;
116     end
117     if(prev_fc > peakminus && vall < peakminus)
118         minuskryss = i;
119     end
120     prev_fc = vall;
121 end
122 figure(6)
123 plot(deform(plusskryss:minus_kryss), force_smooth(plusskryss:minus_kryss), '-b
124     ', 'linewidth', 2)
125 start = force_smooth(plusskryss);
126 slutt = force_smooth(minuskryss);
127 A = 40; %[mm] %Cross section area of test specimen
128 L = 170*1000; %[um] %Length of test specimen
129 E = ((slutt-start)/A)/((minuskryss-plusskryss)/L); %Not real Young's Modulus
130 , needs ratio
131 xlabel('Elongation[\mum]')
132 ylabel('Force[N]')
133 xticks(200:100:2000);
134 yticks(200:100:2000);
135 grid on
136 hold on
137 plot([plusskryss minuskryss], [start slutt], 'ro')
138
139
140 def = deform(plusskryss:minus_kryss)/L;
141 x1 = def(1);
```

```

138 x2 = def(end);
139 forc = force_smooth(plusskryss:minuskryss)/A;
140 y1 = forc(1);
141 y2 = forc(end);
142
143 stigning = (y2-y1)/(x2-x1);
144 x = [0:0.0001:0.03];
145 y = stigning*x-stigning*0.002;
146
147 %Stress - Strain Curve
148 figure(7)
149 plot(deform/L, abs(force_smooth/A), '-m', 'linewidth', 2)
150 hold on
151 %plot(x,y)
152 xlabel('Strain \epsilon', 'FontSize', 16)
153 ylabel('Stress \sigma [N/mm^2]', 'FontSize', 16)
154 xlim([0 0.02])
155 xticks(0:0.002:0.04);
156 yticks(0:5:60);
157 xtickangle(45)
158 ylim([0 60])
159 grid on
160
161 high = max(deform/L, force_smooth/A);
162 max(high)

```

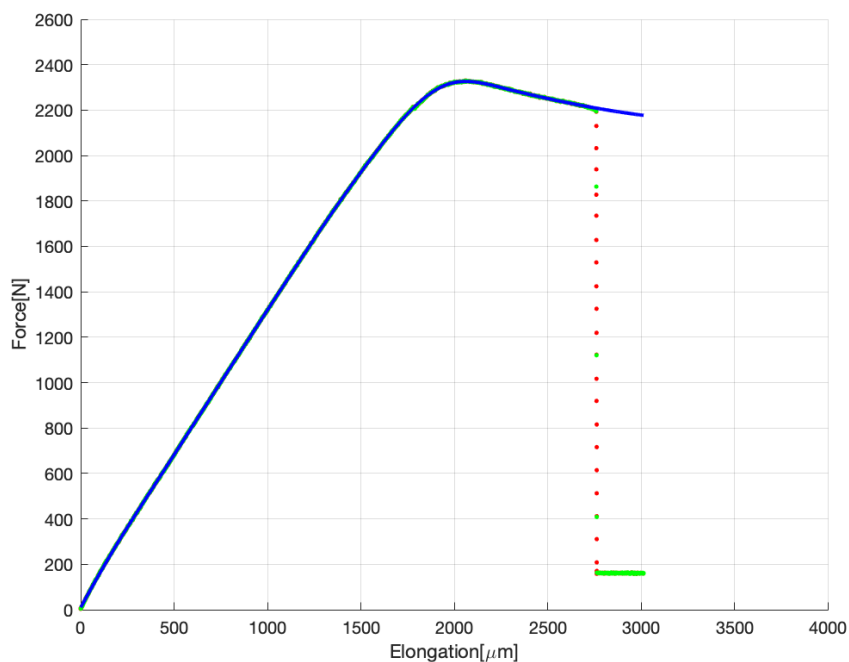


Figure C.1: Appendix C.1 - Figure 1

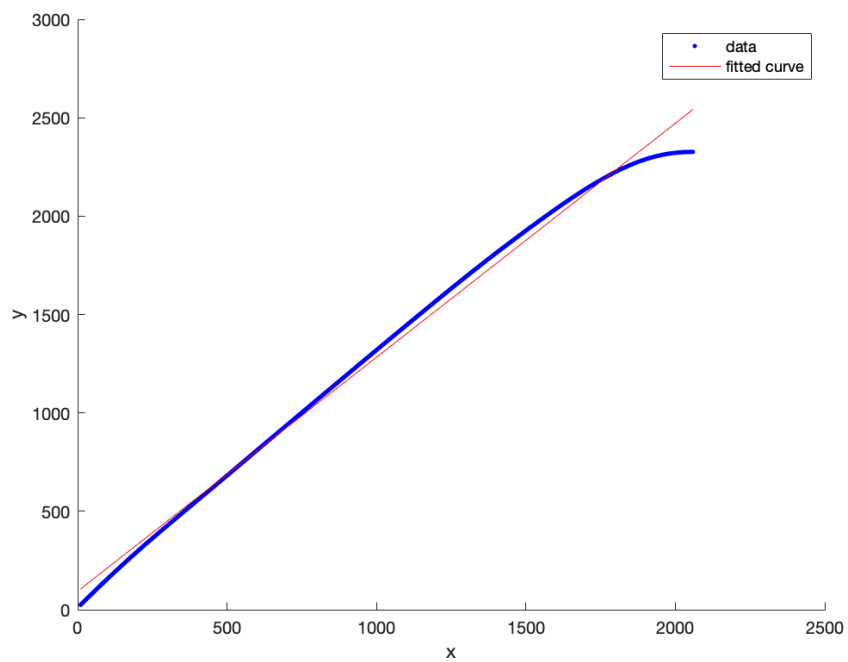


Figure C.2: Appendix C.1 - Figure 2

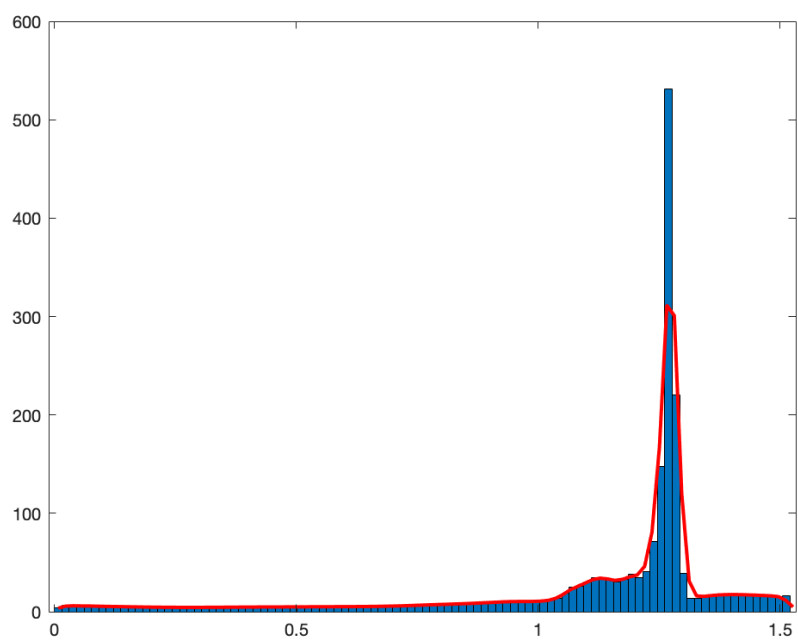


Figure C.3: Appendix C.1 - Figure 3

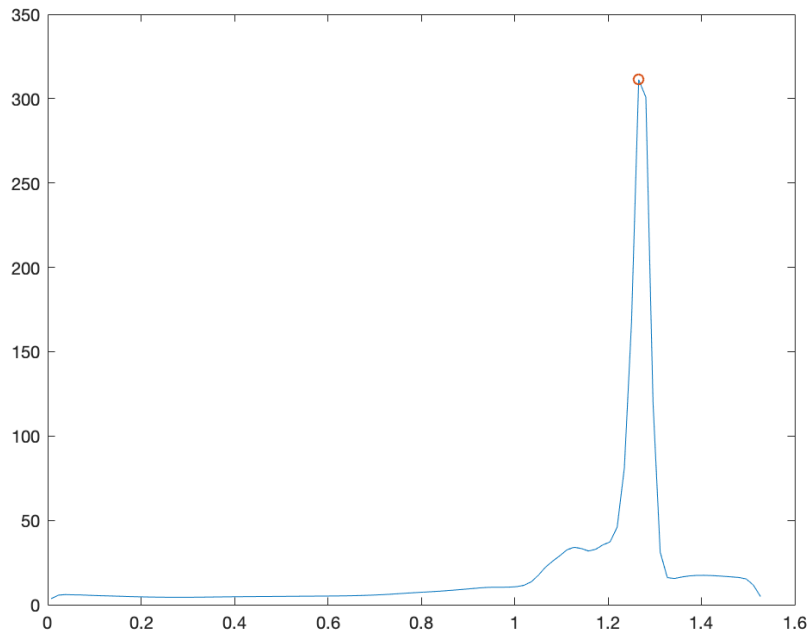


Figure C.4: Appendix C.1 - Figure 4

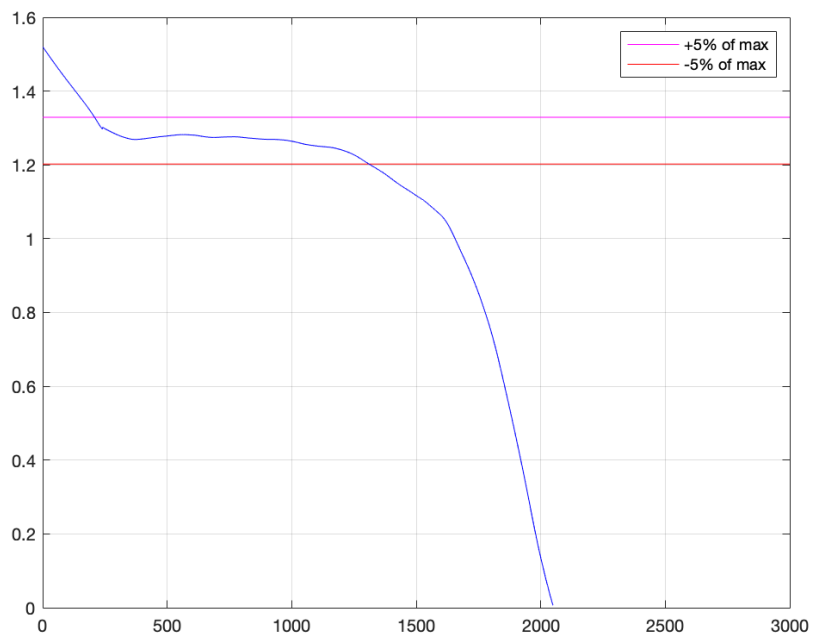


Figure C.5: Appendix C.1 - Figure 5

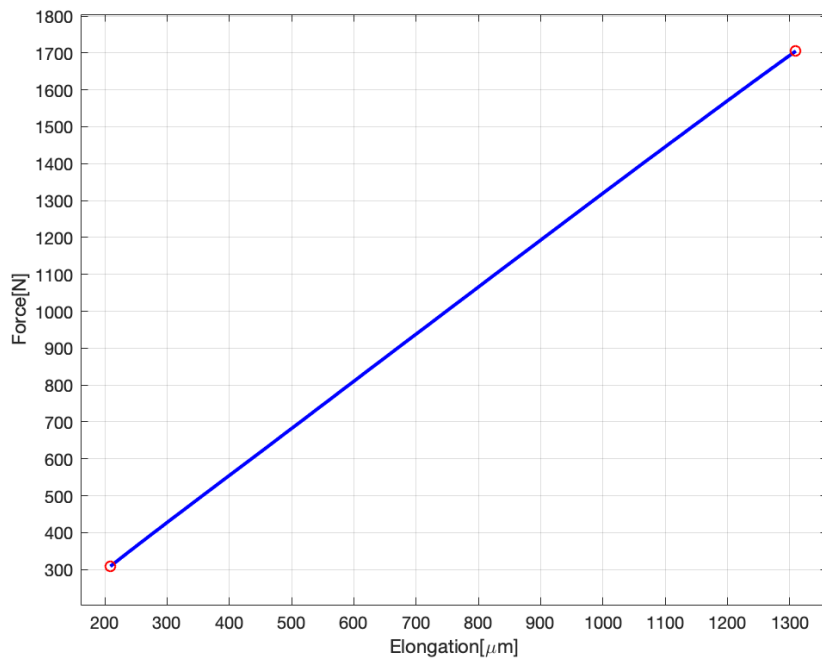


Figure C.6: Appendix C.1 - Figure 6

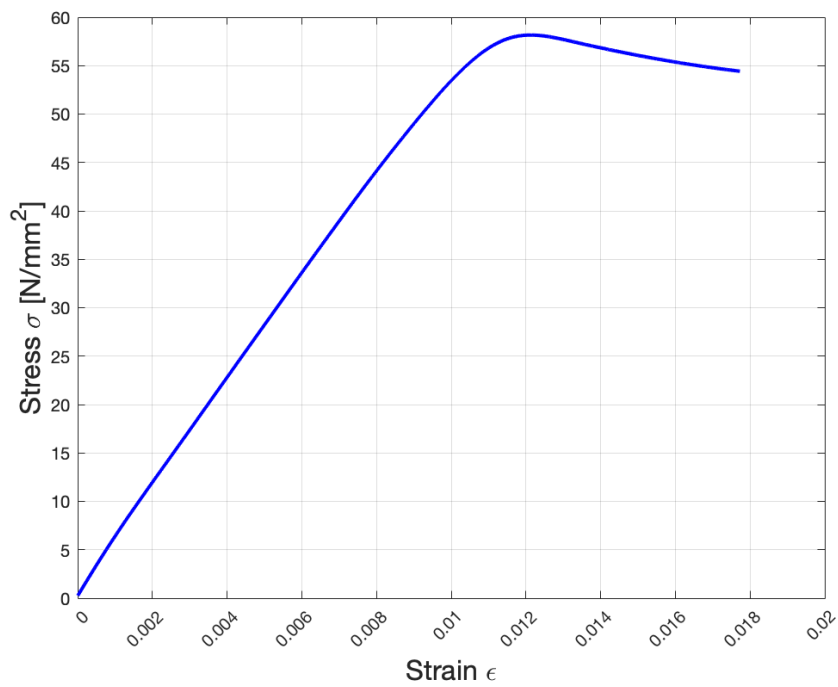


Figure C.7: Appendix C.1 - Figure 7

C.2 Initial Young's Modulus Comparison

```
1 clc, clear all, close all;
2 %Initial Young Modulus Plot
3 T2_1 = 5278;
4 T2_2 = 5140;
5 T2_3 = 5113;
6 T2_4 = 5345;
7 T2_5 = 5262;
8
9 T3_1 = 5391;
10 T3_2 = 5059;
11 T3_3 = 5213;
12 T3_4 = 5359;
13 T3_5 = 5130;
14
15 T3_6 = 0; % Failed
16 T3_7 = 5224;
17 T3_8 = 5097;
18 T3_9 = 5002;
19 T3_10 = 5166;
20 T3_11 = 5154;
21
22 T4_1 = 4282;
23 T4_2 = 4273;
24 T4_3 = 4190;
25 T4_4 = 3999;
26 T4_5 = 4136;
27
28 T4_6 = 4041;
29 T4_7 = 4039;
30 T4_8 = 4065;
31 T4_9 = 4061;
32 T4_10 = 4073;
33
34 T4_11 = 4021;
35 T4_12 = 4120;
36 T4_13 = 4073;
37 T4_14 = 4119;
38 T4_15 = 4106;
39
40 x = [1, 2, 3, 4, 5];
41 y = [T2_1, T2_2, T2_3, T2_4, T2_5];
42 x2 = [6, 7, 8, 9,10];
43 y2 = [T3_1, T3_2, T3_3, T3_4 T3_5];
44 x3 = [11, 12, 13, 14, 15, 16];
45 y3 = [T3_6, T3_7, T3_8, T3_9, T3_10, T3_11];
```

APPENDIX C. MATLAB SCRIPTS

```
46 x4 = [17, 18, 19, 20, 21];
47 y4 = [T4_1, T4_2, T4_3, T4_4, T4_5];
48 x5 = [22, 23, 24, 25, 26];
49 y5 = [T4_6, T4_7, T4_8, T4_9, T4_10];
50 x6 = [27, 28, 29, 30, 31];
51 y6 = [T4_11, T4_12, T4_13, T4_14, T4_15];
52
53 figure(1)
54 plot(x,y,'sq','linewidth',2)
55 hold on
56 plot(x2,y2,'sq','linewidth',2)
57 plot(x3,y3,'sq','linewidth',2)
58 plot(x4,y4,'sq','linewidth',2)
59 plot(x5,y5,'sq','linewidth',2)
60 plot(x6,y6,'sq','linewidth',2)
61 hold off
62 legend({'T2_1 - T2_5','T3_1 - T3_5','T3_6 - T3_11','T4_1 - T4_5','T4_6 -
        T4_10','T4_11 - T4_15'},'Location','southeast','Interpreter','none','
        FontSize',12)
63
64 ylim([0 5500]);
65 xlim([0 32]);
66 xticks(0:1:31);
67 yticks(0:200:5500);
68 grid on
69 xlabel('Test specimens')
70 ylabel('Youngs Modulus E [MPa]')
```

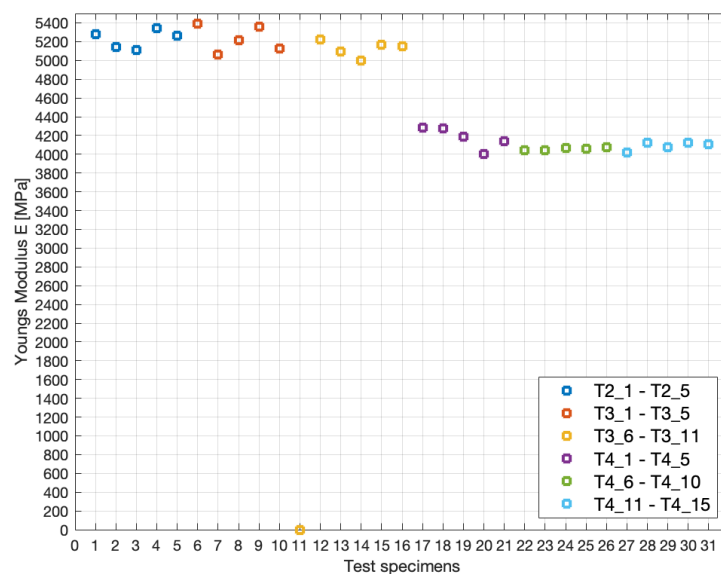


Figure C.8: Appendix C.2 - Figure 1

C.3 Young's Modulus Comparison

```
1 clc, clear all, close all;
2 %The scripts need to be run seperately, seperated with %%.
3 T2_1 = 2336;
4 T2_2 = 2275;
5 T2_3 = 2263;
6 T2_4 = 2366;
7 T2_5 = 2329;
8
9 T3_1 = 2386;
10 T3_2 = 2239;
11 T3_3 = 2307;
12 T3_4 = 2372;
13 T3_5 = 2271;
14
15 T3_6 = 0; % Failed
16 T3_7 = 2312;
17 T3_8 = 2256;
18 T3_9 = 2214;
19 T3_10 = 2286;
20 T3_11 = 2281;
21
22 T4_1 = 2910;
23 T4_2 = 2903;
24 T4_3 = 2847;
25 T4_4 = 2717;
26 T4_5 = 2810;
27
28 T4_6 = 2746;
29 T4_7 = 2744;
30 T4_8 = 2762;
31 T4_9 = 2760;
32 T4_10 = 2768;
33
34 T4_11 = 2732;
35 T4_12 = 2800;
36 T4_13 = 2768;
37 T4_14 = 2798;
38 T4_15 = 2790;
39
40 x = [1, 2, 3, 4, 5];
41 y = [T2_1, T2_2, T2_3, T2_4, T2_5];
42 x2 = [6, 7, 8, 9,10];
43 y2 = [T3_1, T3_2, T3_3, T3_4 T3_5];
44 x3 = [11, 12, 13, 14, 15, 16];
45 y3 = [T3_6, T3_7, T3_8, T3_9, T3_10, T3_11];
```

APPENDIX C. MATLAB SCRIPTS

```
46 x4 = [17, 18, 19, 20, 21];
47 y4 = [T4_1, T4_2, T4_3, T4_4, T4_5];
48 x5 = [22, 23, 24, 25, 26];
49 y5 = [T4_6, T4_7, T4_8, T4_9, T4_10];
50 x6 = [27, 28, 29, 30, 31];
51 y6 = [T4_11, T4_12, T4_13, T4_14, T4_15];
52
53 figure(1)
54 plot(x,y,'sq','linewidth',2)
55 hold on
56 plot(x2,y2,'sq','linewidth',2)
57 plot(x3,y3,'sq','linewidth',2)
58 plot(x4,y4,'sq','linewidth',2)
59 plot(x5,y5,'sq','linewidth',2)
60 plot(x6,y6,'sq','linewidth',2)
61 hold off
62 legend({'T2_1 - T2_5','T3_1 - T3_5','T3_6 - T3_11','T4_1 - T4_5','T4_6 -
        T4_10','T4_11 - T4_15'},'Location','southeast','Interpreter','none','
        FontSize',12)
63
64 ylim([0 3000]);
65 xlim([0 32]);
66 xticks(0:1:31);
67 yticks(0:100:3000);
68 grid on
69 xlabel('Test specimens')
70 ylabel('Youngs Modulus E [MPa]')
71
72
73 %% The individual 0, 45 and 90 degrees boxplots
74 figure(2)
75 zero = [T2_1, T2_2, T2_3, T2_4, T2_5];
76 fortyfive = [T3_1, T3_2, T3_3, T3_4 T3_5];
77 ninety = [T3_7, T3_8, T3_9, T3_10, T3_11];
78
79 zero2 = [T4_1, T4_2, T4_3, T4_4, T4_5];
80 fortyfive2 = [T4_6, T4_7, T4_8, T4_9 T4_10];
81 ninety2 = [T4_11, T4_12, T4_13, T4_14, T4_15];
82
83 First = [zero;fortyfive; ninety];
84 Second = [zero2;fortyfive2; ninety2];
85 First_Second = [First; Second]';
86
87 %Mean value
88 mzero = mean(zero);
89 mfortyfive = mean(fortyfive);
90 mninety = mean(ninety);
91 mzero2 = mean(zero2);
```

```

92 mfortyfive2 = mean(fortyfive2);
93 mninety2 = mean(ninety2);
94 samlet = [1 2 3 4 5 6; mzero mfortyfive mninety mzero2 mfortyfive2 mninety2
    ]';
95
96 boxplot(First_Second,'Labels',{'Printed at 0 deg','Printed at 45 deg', '
    Printed at 90 deg','Printed at 0 deg','Printed at 45 deg', 'Printed at
    90 deg'})
97 yticks(0:50:3000);
98 ylim([2100 3000]);
99 xtickangle(45)
100 ylabel('Youngs Modulus E [MPa]')
101 hold on
102 plot((samlet),'ko')
103 hold off
104 grid on

```

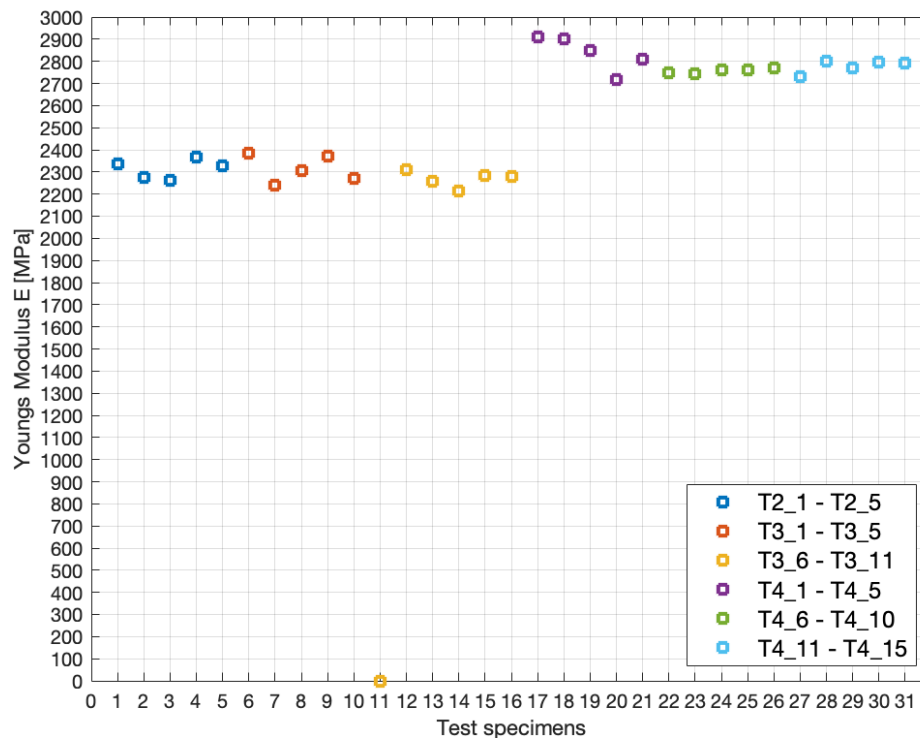


Figure C.9: Appendix C.3 - Figure 1

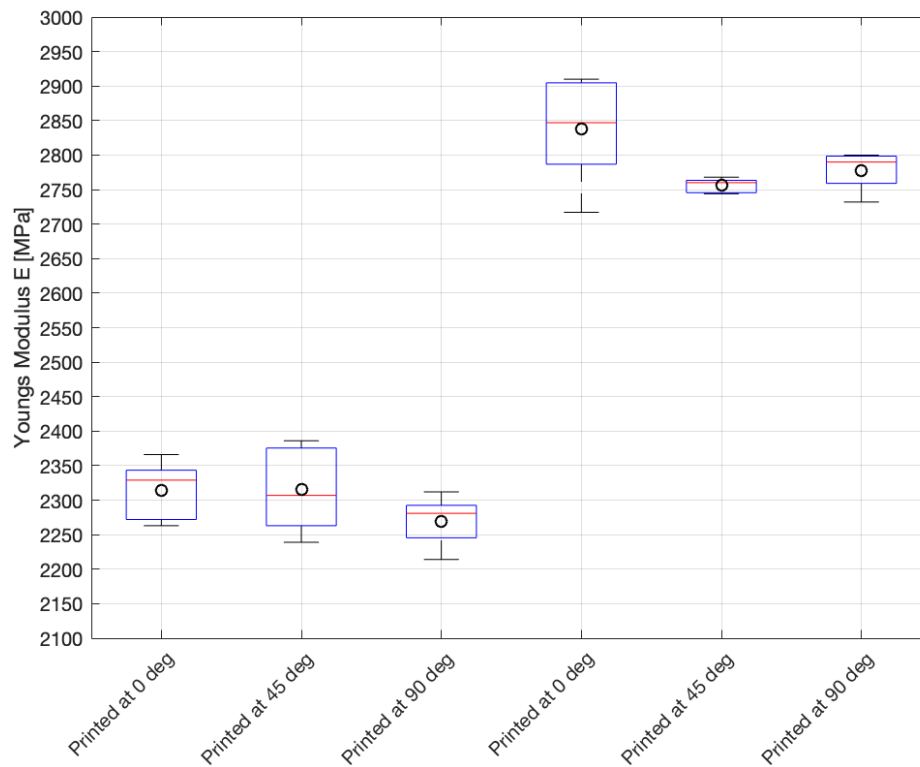


Figure C.10: Appendix C.3 - Figure 2

C.4 Mesh Convergence Study

```
1 %Mesh Convergence Study
2 clear all, close all;
3
4 x = [0.5 1 2 4 8];
5 y = [0.00755721 0.0075611 0.00755239 0.00753669 0.00747606];
6
7 plot(x,y, '-b')
8 hold on
9 plot(x,y, 'mo')
10 hold off
11 xticks(0:0.5:8);
12 xlim([0 8]);
13 ylim([0.0074 0.00757]);
14 xlabel('Mesh element size[mm]', 'FontSize', 16)
15 ylabel('Deformation[mm]', 'FontSize', 16)
16 grid on
```

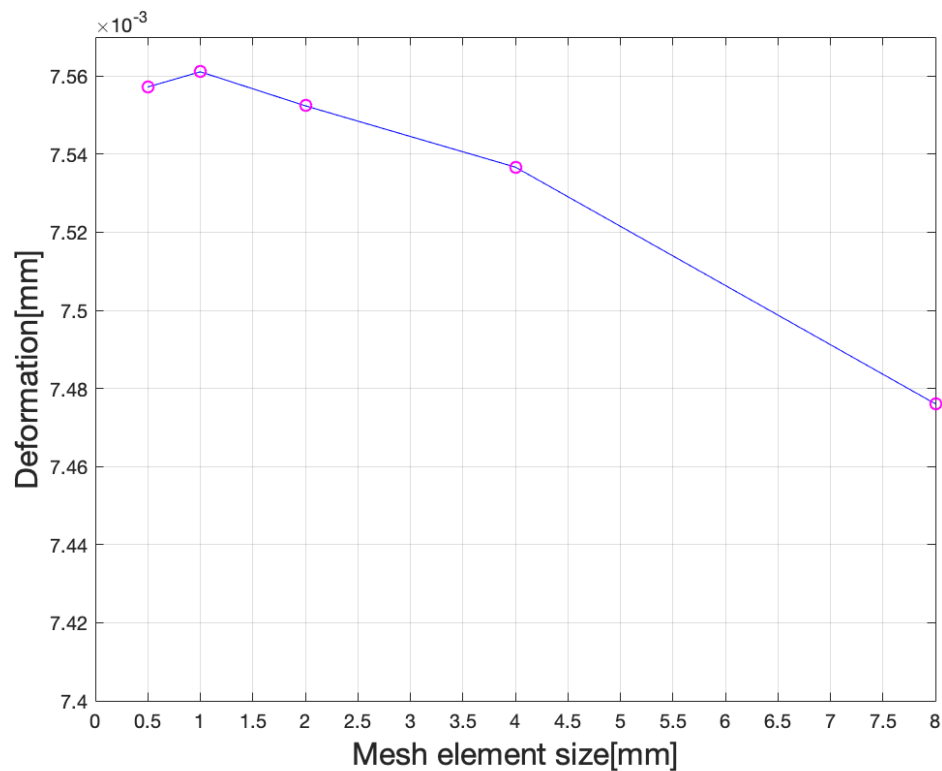


Figure C.11: Appendix C.4 - Figure 1

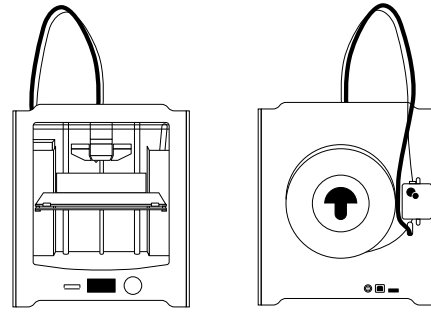
Appendix D

Datasheets

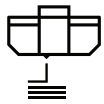
Datasheets for the physical equipment that have been used during this thesis are added here.

Ultimaker 2+

Specification sheet



The user-friendly Ultimaker 2+ combines high uptime with excellent print consistency. It's suitable for a limitless variety of applications, from functional prototypes to customized tools. The Ultimaker 2+ supports a wide range of materials and delivers powerful, first-class results with every print.



Quality you can rely on

Engineered to perform, Ultimaker 2+ features a heated build plate, a geared feeder, and efficient cooling. These make it particularly effective for printing bridging and accurate details – enabling you to create the consistent results you need.



Market-leading software

Trusted by over 2 million users, Ultimaker Cura software prepares your 3D model for printing. Free to download, it features the optimal preconfigured settings for Ultimaker printers and materials, so that you get the best results instantly.



Optimized, professional materials

The Ultimaker 2+ supports a wide range of materials. These are specially formulated and tested by our engineers to ensure repeatable, industrial-grade prints. You can also test other materials with Ultimaker's open filament system.



Here to help you succeed

The Ultimaker 2+ comes with a one-year warranty and lifetime support from our trained and certified global network of partners. And if you have a question, our online resources and community are there for you 24/7.

Ultimaker

Ultimaker 2+ specifications

Printer and printing properties	Technology	Fused filament fabrication (FFF)
	Print head	Single extrusion print head with swappable nozzles
	Build volume	XYZ: 223 x 223 x 205 mm
	Filament diameter	2.85 mm
	Layer resolution	0.25 mm nozzle: 150 - 60 micron 0.4 mm nozzle: 200 - 20 micron 0.6 mm nozzle: 400 - 20 micron 0.8 mm nozzle: 600 - 20 micron
	XYZ resolution	12.5, 12.5, 5 micron
	Print head travel speed	30 - 300 mm/s
	Build speed	0.25 mm nozzle: < 8 mm ³ /s 0.4 mm nozzle: < 16 mm ³ /s 0.6 mm nozzle: < 23 mm ³ /s 0.8 mm nozzle: < 24 mm ³ /s
	Build plate	Heated glass build plate
	Build plate temperature	20 - 100 °C
	Build plate leveling	Assisted leveling
	Build plate heat time	< 4 min (from 20 to 60 °C)
	Supported materials	Optimized for: PLA, ABS, Nylon, CPE, CPE+, PC, PP, TPU 95A (Also supports third-party materials)
	Nozzle diameter	0.25, 0.4, 0.6, and 0.8 mm nozzles (included)
	Nozzle temperature	180 - 260 °C
	Nozzle heat up time	~ 1 min
	Operating sound	50 dBA
Connectivity	Standalone 3D printing from SD card (included)	
Physical dimensions	Dimensions	342 x 357 x 388 mm 342 x 493 x 588 mm (with Bowden tubes and spool holder)
	Net weight	11.3 kg
	Shipping weight	18.5 kg
	Shipping box dimensions	390 x 400 x 565 mm
Power	Required input	100 - 240 VAC / 50 - 60 Hz
	Maximum output	221 W
Ambient conditions	Operating ambient temperature	15 - 32 °C
	Non-operating temperature	0 - 32 °C
Software	Supplied software	Ultimaker Cura, our free print preparation software
	Supported OS	MacOS, Windows, and Linux
	Plugin integration	SolidWorks, Siemens NX, Autodesk Inventor
	File types	Ultimaker Cura: STL, OBJ, X3D, 3MF, BMP, GIF, JPG, PNG Printable formats: GCODE
Warranty	Warranty period	12 months
	Technical support	Lifetime support from Ultimaker's global network of certified service partners

Quasar 200

200kN Advanced Universal Testing Machines

The 200 kN Quasar is the product of state of the art design, built to the highest quality levels and has many advanced technical features.

Programming tests and monitoring results can be controlled through our powerful and Intelligent Graphwork test software, which allows complete and accurate data management in accordance with European, North American and International Standards.

This instrument is suitable for use both in production lines where the operator has to be fast and efficient and can accurately control the test with the optional remote control unit and also laboratory environments where the advanced software lets users analyse the test data. Graphwork allows full control of processing, filing, managing, and transmitting data to the company network, database, and performs many other functions.

This Quasar frame has a flexible and modular construction. It can be equipped with various grips and fixtures, as well as extensometers, additional load cells, temperature chambers and many more accessories, for a wide range of applications (tensile, compression, flexure, etc.).

In addition, this user-friendly instrument can be fitted with additional load cells with lower capacities, providing the highest resolution and accuracy for micro-loads.

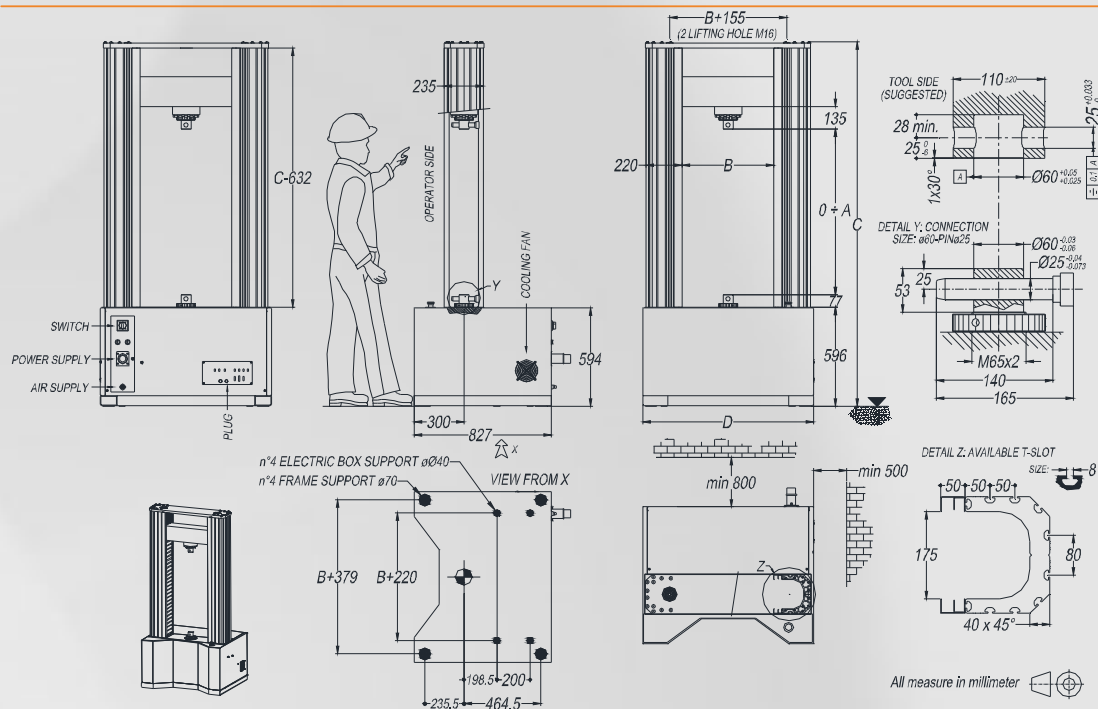
- Two-column rigid system with 200 kN maximum capacity
- Suitable for metals, plastics, composites and other materials
- Stylish design and advanced features
- One-Year Warranty
- Flexible and modular design for easy future expansion
- Key technical advantages include extremely high resolution of load and stroke readings, as well as minimum test speed of 0.0005mm/min, for the high performance and most accurate results
- Manufactured by an ISO 9001 certified company
- Excellent price-to-quality ratio



Universal testing machine Quasar 200 with special grip , "Micron Motor" extensometer, safety barrier and touch screen monitor



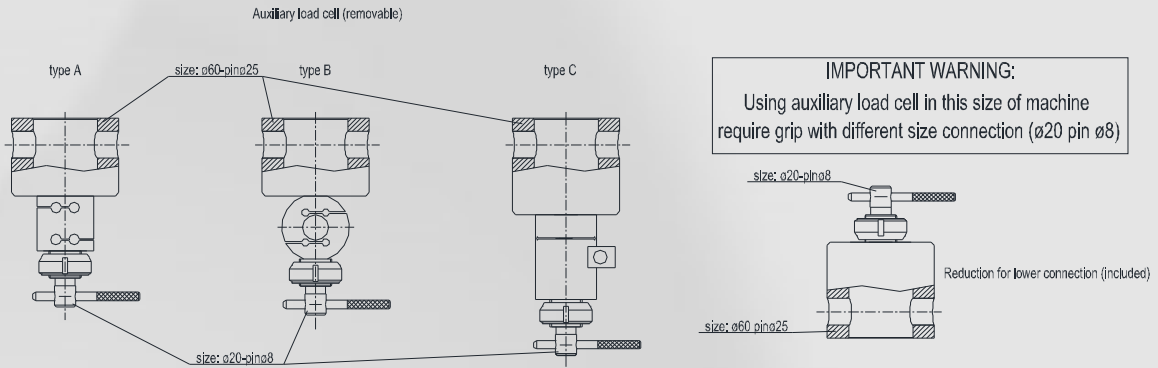
Ethernet connection



TECHNICAL SPECIFICATIONS:

ITEM	TQ01.07 ⁽¹⁰⁾	TQ01.07.01 ⁽¹⁰⁾	
Capacity of frame and max admissible load	200 kN (44,961 lbf)		
Load cell nominal size (tensile & compression)	250 kN ⁽¹⁾		
Max accidental overload ⁽¹¹⁾ / breaking load	375 kN / 750 kN ⁽¹⁾		
Standards met or exceeded	ISO 7500-1, ASTM E4, EN 10002-2, JIS B7721, GB/T 16825.1, DIN 51221, BS 1610 and other equivalent		
Load cell reading resolution	Over 3 million division (24 bit A/D converter)		
Frame stiffness ⁽²⁾	Average	250 kN/mm	
	Deformation max at full load	0.8 mm	
Stroke resolution	0.041 µm		
Speed at maximum load (in test)	0.0005 ÷ 500 mm/min.		
Idle speed	500 mm/min.		
Accuracy of positioning repeatability	0.02 mm (20 µm)		
Accuracy of the set crosshead speed	0.5% of setting speed ⁽³⁾		
Total stroke (Dimension A)	1,000 mm (39.37 in.)	1,500 mm (59.05 in.)	
Daylight between columns (Dimension B)	550 mm (21.65 in.)		
Testing area depth	Unlimited ⁽⁴⁾		
Power Supply	To be chosen: 220V±10% 50/60Hz or 120V±10% 50/60Hz (other on request) ⁽⁵⁾		
Power Rating	3,000 W		
Machine weight (without accessories)	730 Kg (1,610 lb)	850 Kg (1,875 lb)	
Finishing	Silver RAL 9006 / Black RAL 9011		
Ambient temperature	From +5 to +40 °C		
Air humidity (without condensing)	Max 80%		
Internal data sampling rate	1,000 Hz		
PC data transmission rate	500 Hz		
PC interface	Ethernet (A dedicated Ethernet port on PC is required)		
Dimension:	Height (Dimension C) ± 5 mm	2,198 mm (86.53 in.)	2,747 mm (108.15 in.)
	Width (Dimension D)	1,030 mm (40.55 in.)	
	Depth ⁽⁶⁾	827 mm (32.56 in.)	
Size when packed – approx ⁽⁷⁾	2,550x1,450 H1,350 mm		3,100x1,450 H1,350 mm
Noise level	< 72 db		
Suggested light local level	300 lux		

⁽¹⁾ Data of standard load cell. See below for other available auxiliary load cell
⁽²⁾ Including load cell. This value is evaluated in compression, without any type of grip
⁽³⁾ Average on 1 second or 0.01 mm of stroke (the longer in time) without or constant load.
⁽⁴⁾ Some type of extensometers or other devices may reduce this value
⁽⁵⁾ Some optional device need a compressed air line (5 bar) or different power supply
⁽⁶⁾ Frame dimension. Electrical connectors on the rear of the machine. See drawing
⁽⁷⁾ Machines are packed and travel in lying position



AVAILABLE AUXILIARY LOAD CELL: ⁽⁸⁾

ITEM	TQ03.04.01	TQ03.04.01.0A	TQ03.04.01.0B	TQ03.04.02	TQ03.04.03	TQ03.04.03.0A	TQ03.04.04	TQ03.04.05	TQ03.04.06	TQ03.04.07	TQ03.04.08	
Nominal size	10 N	20 N	50 N	100 N	250 N	500 N	1 kN	3 kN ⁽¹²⁾	5 kN	10 kN	25 kN	
Max accidental overload ⁽¹¹⁾ / breaking load	150% of nominal size / 300% of nominal size											
Stiffness ⁽⁹⁾	33 N/mm	67 N/mm	167 N/mm	333 N/mm	833 N/mm	2500 N/mm	5000 N/mm	15000N/mm	16500N/mm	33000N/mm	83500N/mm	
Average Deformation at full load	Max. 0.3 mm			Max. 0.2 mm				Max. 0.3 mm				
Type (see drawing)	A						B			C		
Kit for use as auxiliary cell (sold separately) ⁽¹³⁾	TQ03.05.02 (generic code, correct load cell must be specified)											

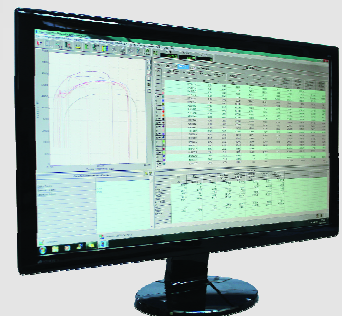
⁽⁸⁾ The main load cell is always a 250 kN size. No limit in number of auxiliary load cell to be used under the main one.
 All load cell can work in compression and tensile. If certification is required, every load cell (included main one) needs a different one.
⁽⁹⁾ Stiffness of the load cell only. The deformation under load is the sum frame + auxiliary cell
⁽¹⁰⁾ Standard 250kN load cell is included in the item of the frame machine
⁽¹¹⁾ A new calibration of the load cell may be necessary if "max accidental overload" is exceeded.
⁽¹²⁾ Max load of TQ03.04.05 load cell is software limited to 2.5 kN.
⁽¹³⁾ The kit include female and male connection, pin and locknut (as in draw). Every auxiliary load cell need 1 kit. Using auxiliary cell need grip with connection size ø20 pin ø8.

MAIN OPTIONAL:

	ITEM
Kevlar ball screw covers – (couple)	TQ11.02.03
Mobile pushbutton panel for machine control	TQ03.03
Silenced air compressor 0,75 Kw 1450 rpm 230V 50Hz 1A 98 litre/min	TQ03.08.04
Internal piping with solenoid valves for use pneumatic device by keypad – compressed air line required (min 5 bar) ⁽¹⁴⁾	Standard
Table for PC and printer only (width x depth x height mm 900 x 800 x 730) - grey	TQ03.07.03
Touch screen (~ 7 inch) colour monitor (to be use as keypad) ⁽¹⁵⁾⁽¹⁶⁾	TQ03.02.00
Calibration certificate class 1 in range 1%-100% of full load	TQ02.02.01
Calibration certificate class 0.5 in range 1%-100% of full load	TQ02.02.01.A
Extension of certification class 1 in range 0,2%-1% of full load (TQ02.02.01 or TQ02.02.01.A required)	TQ03.06.01
PC ⁽¹⁵⁾ multi-language	TQ03.01.03
Touch PC all-in-one with support on column ⁽¹⁵⁾⁽¹⁷⁾	TQ03.01.01.02
Colour printer A4	TQ03.01.02
USB Web cam ⁽¹⁵⁾ – the use of camera for recording test requires the special software module TQ02.01.04	TQ03.01.03
Electronic power supply stabilizer	TQ03.08.03
Integral barrier - Aluminium profile and mm thickness polycarbonate panels - Split opening front and rear door , with electric interlock ⁽¹⁸⁾	TQ11.01.02
Extra price for reinforced structure and panels in polycarbonate 8 mm thickness	TQ11.02.01
Analogic input channel (strain gage type) for longitudinal deformation	Standard
Analogic input channel (LVDT type) for longitudinal deformation	Standard
Second analogic input channel (strain gage type) for transversal deformation	TQ02.01.17
Second analogic input channel (LVDT type) for transversal deformation	Standard

⁽¹⁴⁾ Included filter+regulator+pressure indicator
⁽¹⁵⁾ Characteristic of electronic device are constantly changing, type of supplied item may change with technology
⁽¹⁶⁾ Item TQ03.03 and TQ03.02.00 may co-exist
⁽¹⁷⁾ not usable for some external special device (e.g. special extensometer, digital I/O)
⁽¹⁸⁾ Generic code. Dimension may change according installed device (e.g. special extensometer or grip)

NOTE: the machine needs a Windows® based PC and special software.





TQ03.01.01.0



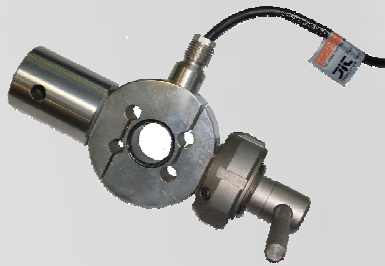
TQ03.03



TQ03.02.00



TQ08.11



TQ03.04.05 + TQ03.05.01



TQ03.07.03 + TQ03.01.03



TQ03.01.03



TQ03.08.04

Cesare Galdabini Spa, Via Giovanni XXIII, 183, 21010 Cardano al Campo (VA), Italy

Ph. ++39.0331.732.700
Fax. ++39.0331.730.650
Mail: info@galdabini.it
Web: www.galdabini.it

Specification are subject to change without prior notice

